UNIVERSITAT DE BARCELONA

Cortical network dynamics in physiological and pharmacologically induced brain states

Melodía Torao Angosto

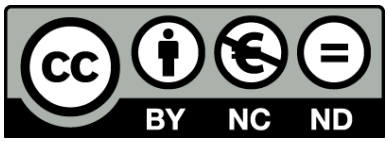

CORTICAL NETWORK DYNAMICS IN PHYSIOLOGICAL AND PHARMACOLOGICALLY INDUCED BRAIN STATES

Doctoral Thesis by
Melodía Torao Angosto

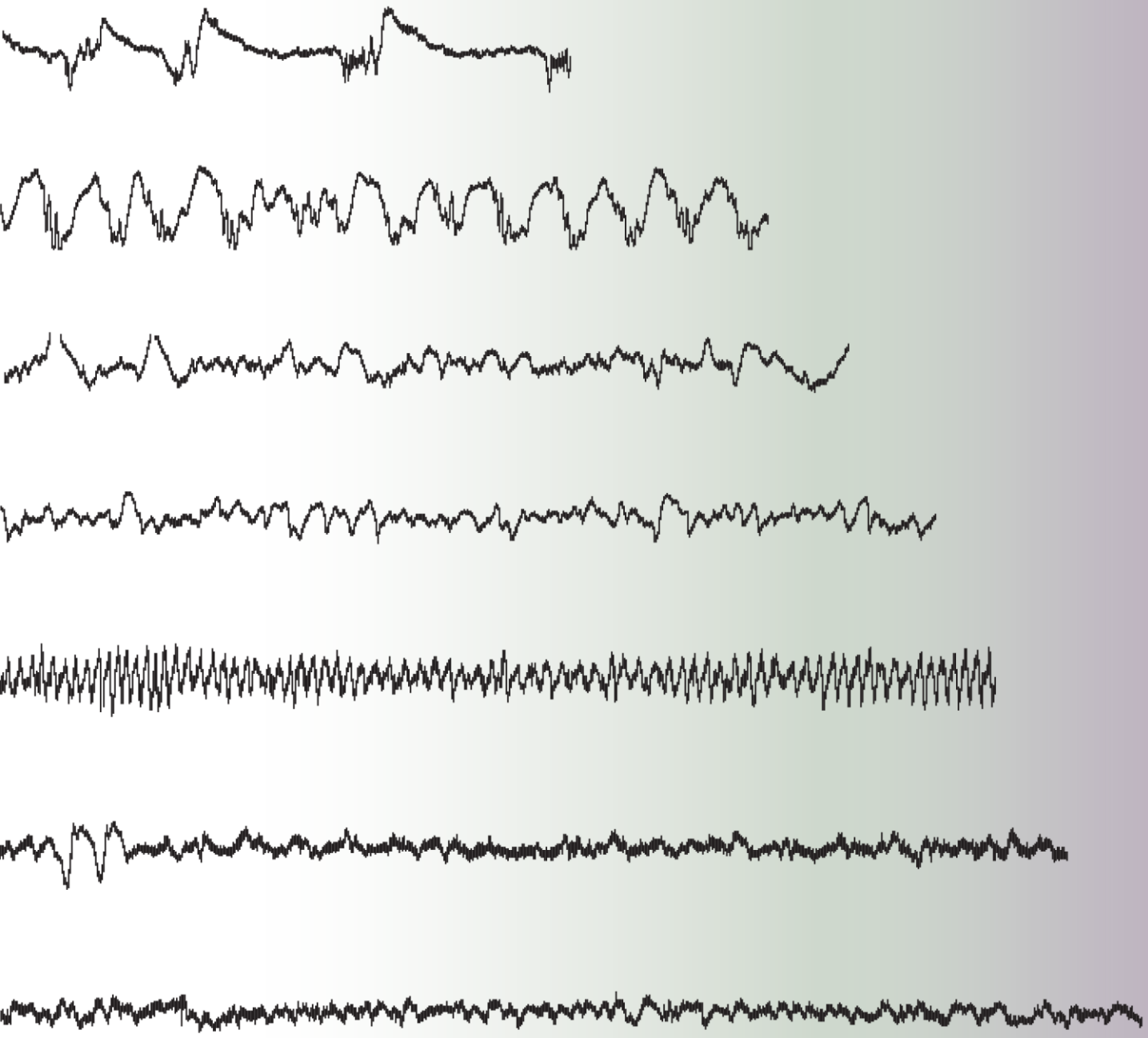

Supervisors:
Dr. María Victoria Sánchez Vives
Dr. Gemma Guillazo Blanch

2020

IDIBAPS
Institut D'Investigacions Biomèdiques August Pi i Sunyer

UNIVERSITAT DE BARCELONA

INSTITUT D'INVESTIGACIONS BIOMEDIQUES AUGUST PI I SUNYER
UNIVERSITY OF BARCELONA

THESIS FOR DOCTORAL DEGREE IN BIOMEDICINE

CORTICAL NETWORK DYNAMICS IN PHYSIOLOGICAL AND PHARMACOLOGICALLY INDUCED BRAIN STATES

Author:
Melodía Torao Angosto

Supervisors:
Dr. María V. Sánchez Vives
Dr. Gemma Guillazo Blanch

Area: *Clinical and Experimental Neuroscience*

Group: Systems Neuroscience

Research line: Neurophysiology and computation in cortical systems

Barcelona,

2020

A mis padres

"Yes. Sometimes we have to do the work even though we don't yet see a glimmer on the horizon that it's actually going to be possible."

— Angela Y. Davis

Abstract

Doctoral degree in Biomedicine

Cortical network dynamics in physiological and pharmacologically induced brain states

by **Melodía Torao Angosto**

The brain varies its state in accordance with the internal and external context, resulting into distinct patterns of activity and dynamics. The cerebral cortex and the interactions between cortical and subcortical areas, have a major role in the establishment and switching between different brain states.

In the present Thesis research work, we used multiple local field potentials, calcium imaging recordings and thalamic stimulation to explore different cortical dynamics at distinct brain states.

First, we investigated the physiological sleep-wake rhythms and spontaneous brain transitions. Secondly, we explored the transitions taking place over different levels of anesthesia, characterizing from a multiscale perspective, the cortical dynamics when transitioning from deep anesthesia to wakefulness. Finally, we investigated the impact of thalamic stimulation on the induction of brain transitions and found that it induces a transition from deep anesthesia to that equivalent to a higher arousal, a strategy that has been investigated for its clinical potential.

Melodía Torao Angosto was supported by a predoctoral fellowship from Spanish Ministry of Economy and Competitiveness (MINECO) (FPI, BES-2015-072806). This work was partially funded by the projects BFU2017-85048-Rfrom Spanish Ministry of Economy and Competitiveness (MINECO), European Union's Horizon 2020 research and innovation programme under grant agreement No 785907 (SGA2) and 945539 (SGA3) (Human Brain Project Flagship) to M.V.S.-V, PSI2014-52660-R to GG-B and by the CERCA Programme from the Government of Catalonia.

Acknowledgements

In the first place I would like to thank **Dr. Mavi Sánchez Vives** and **Dr. Gemma Guillazo Blanch**, the two women scientists who have given me the opportunity to do this thesis. Six years ago, Dr. Gemma Guillazo accepted me in her laboratory as a master student to later being accepted by Dr. Mavi Sánchez to join her lab. In the course of this studies I had the opportunity to learn from a multidisciplinary environment in neuroscience within their great teams. I'm grateful to have been able to work and learn from such empowering references for women in science.

One of the best things during this period were the people that I have encounter and learned from. I'm deeply grateful to **Belén** and **Nùria**, who have been not only my mentors, but also great friends/sisters with whom I share and indescribable connection and meaningful moments. With them I feel like I've started another chapter.

Thanks to **Almudena,** a friend that with her immense kindness has always helped me in any circumstance. I would like to thank **Bea** for being so extremely generous and unique, for sharing her extraordinary positivity and for the amazing parties!

I have been very fortunate to have worked with such understanding and helpful lab mates. Special thanks to **Vane** who has been an infinite source of guidance and support. Many thanks to all the computational team from which I have learned so much (and also have some fun) by unraveling the data: Lorena, Carlos, Alessandra, Marçal, Leo and Andrea. I particularly thank Andrea for his analysis. Special thanks to **Álvaro** and **Arnau**, a.k.a. "computational angels" for his persistent work and guidance. I'm also very happy for having founded *the dead band* with Álvaro which still has a lot to rock in the future.

My first years in the lab would not have been the same without my *bro* Mattia, Nahuel, Álex and Pol, talking about good music with **Mattia**, all having hilarious conversations at lunch, performing experiments while singing *the Backstreet Boys* and throwing parties at the slightest opportunity. I really miss that period.

These years were also marked by fulfilling long conversations with Miguel and Cristina as well as good moments during lunch, solving my doubts or just having a coffee in the entrance with Lorena, Julia and at a later stage with Miquel and his witty sense of humor. Thanks to Tony for taking care of our English!

Thanks to **Patricia**, I treasure our moments together and really appreciate the time you spent teaching me.

I would also like to thank **Brice Bathellier** and his team for give me the opportunity to do a short stay in his lab. It was a spectacular experience where I could see their methodology and perform their awesome techniques. Another special thing about that stay was meeting **Anton** and **Anthony,** to learn and perform experiments with them, cook, drink wine, go on the endless train and enjoy Paris.

It was also really nice when leaving the lab to have the opportunity of watching crappy TV shows and share a laugh with **Iván**, the best roommate anyone could wish for.

Thanks to **Claudia** and **Pedro** for helping me stay focused and to "keep my eyes on the prize".

Me gustaría agradecer a **Jesús**, que formó parte del inicio de esta aventura y fue un gran apoyo.

Quiero agradecer también a las niñas de baile, en especial a **Estel**, **Paz** y sobre todo a **Gina** que durante este tiempo me han escuchado (pacientemente) y me han hecho bailar, salir y despejarme en los momentos que más lo necesitaba. A **Jose** y **Ana** por cuidarme y hacerme sentir como una más de la familia.

Agradezco a mi **tita Ángeles** y mi **prima Saray** que, aunque mis estudios nos han mantenido estos últimos años la mayor parte del tiempo en la distancia, siempre han estado ahí cuando las he necesitado. A **Jose** y **Antonio** por ser los mejores amigos y hacerme sentir siempre arropada.

Y ante todo y sobre todo agradecer profundamente **a mis padres**, por apoyarme incondicionalmente en todos mis proyectos e intereses y animarme siempre a elegir mi camino.

Por supuesto gracias a **Marcos**, por su comprensión, su cuidado, sus ánimos y su amor durante esta dura etapa. No podría soñar con un mejor *team*.

Y por último agradezco a mi **Kira,** que me ha hecho compañía todos los días y noches mientras escribía la tesis y esperaba pacientemente a que le hiciese caso…

Thanks! ¡Gracias!

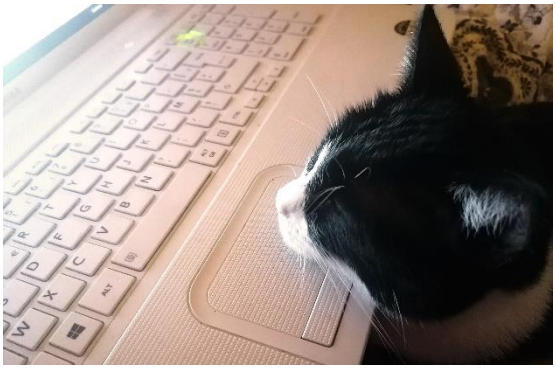

Figura 0. Ilustración de gata aburrida obstaculizando la escritura.

Contents

List of Figures

List of Abbreviations

A1	Primary Auditory Cortex
A2	Secondary Auditory Cortex
AAV	Adeno-Associated Virus
AP	Anteroposterior
ARAS	Ascending Reticular Activating System
CI	Calcium Imaging
CV	Coefficient of Variation
DV	Dorsoventral
ECoG	Electrocorticogram
EEG	Electroencephalogram
EMG	Electromyogram
fMRI	Functional Magnetic Resonance Imaging
FR	Firing Rate
GABA	γ- Aminobutyric Acid
GT	Ground Truth
K-Fold CV	K-Fold Cross Validation
LFP	Local Field Potential
M1	Primary Motor Cortex
ML	Mediolateral
MLR	Multi-Class Logistic Regression
MUA	Multi-Unit Activity
NMDA	N-Methyl-D- Aspartate
PF	Parafascicular Nucleus
PLV	Phase Locking Value
PrL	Prelimbic Cortex
PSD	Power Spectral Density
PtA	Parietal Association Cortex
REM	Rapid Eye Movement
ROI	Regions Of Interest
S1	Primary Somatosensory Cortex
SE	Standard Error
STD	Standard Deviation
SWS	Slow Wave Sleep
V1	Primary Visual Cortex

Chapter 1

Introduction

1.1. The states of the brain: many brains in one

The brain is dynamic. Congruent with behavioral changes, brain activity varies over time creating distinct patterns and dynamics according to different factors, such as physiological or pharmacologically induced origin, external or internal stimulation or the neural mechanisms involved. However, the specific mechanisms that drive the brain to stay or switch across all its possible states remain poorly understood. The neural activity produced in each brain state can be captured from multiple sources: from their electrical changes (electroencephalography (EEG), electrocorticography (ECoG), local field potential recording (LFP)) to its metabolic dynamics (functional magnetic resonance imaging (fMRI) and optical intrinsic signal imaging (CI)). All these types of data provide information from the spatial, temporal and frequency domains that are applied to measure different phenomena across multiple scales, allowing us to infer about the underlying brain network dynamics (e.g. synchrony, complexity or activation/deactivation). The cortex and its interactions have a major role in different brain states, hence studying the states within distributed cortical areas could provide very relevant data to the subject. Even with existing principles that allow the distinction between brain states as sleep, anesthetized or alert wakefulness, there is still a lack of concordance about their identification, categorization and stages subdivision. From this scenario, a further characterization of all the measurable elements that distinctively emerge in each brain state seems necessary in order to create a physiologically based common frame of reference that could also integrate cognition. This Thesis had the general objective of exploring from a multi-scale the characterization of physiological and pharmacologically induced brain states from distinct spontaneous and evoked cortical dynamics.

1.2. Brain states and transitions in the physiological sleep-wake cycle

1.2.1. The sleep-wake cycle

The sleep-wake cycle is a physiological process that follows an endogenous homeostasis and a circadian rhythm. Despite the large amount of time that we spend sleeping, there is not a clear consensus about its functional meaning. The highest point of agreement between studies seems to be its restorative function at multiple scales. For instance, sleep reduces caloric use (Krueger et al., 2016), reestablishes neuronal energy and promotes brain plasticity and connectivity (Crick and Mitchison, 1983; Krueger and Obál, 1993; Kavanau, 1994; Vyazovskiy et al., 2009; Inostroza and Born, 2013; Smith and Peters, 2011; Abel et al., 2013), and has an impact on cognition (Rosa et al., 1983; Benington and Heller, 1995).

During wakefulness, a progressive reduction in arousal occurs until the organism falls sleep. Within the sleep and awake cycle, different brain patterns succeed each other in a characteristic way. Wakefulness is characterized by a low-voltage and high-frequency electroencephalogram (EEG), an active electromyogram (EMG), as well as a high degree of consciousness (Horner and Peever, 2017). Sleep is characterized by inactivity of the organism, a certain degree of loss of consciousness and reduced behavioral responsiveness. During sleep, voluntary control and awareness of external stimuli is significantly reduced, although, an internal and subjective experience still exists and manifests itself in the form of dreams (Warltier, 2005). Sleep is divided into two main stages: slow wave sleep (SWS) and REM sleep. SWS entails the emergence of a slow oscillatory and synchronous activity pattern (0.5–4 Hz), alternating active periods of neural activity (Up states) with abrupt decreases of activity (Down states) (Steriade et al., 1993b; Steriade et al., 2001; Timofeev, et al., 2001). On the contrary, REM sleep is characterized by rapid eye movements, an awake-like brain activity pattern with low-amplitude and fast-frequency waves but accompanied by muscle atonia and the lowest reactivity to external stimuli (Saper et al., 2010, Dang-Vu, 2012).

From a neural scale, it is argued that entering into sleep is a continuum (Ogilvie, 2001), a gradual process where the neurons involved in the wake state have to change their firing mode and progressively turn off while the sleep-related neurons gradually turn on (Steriade et al., 1990; McCormick and Bal, 1997; Merica and Fortune, 2004). This gradual transition is also evident in the spectral elements that emerge locally (Nir et al., 2011) (e.g. slow, alpha, or delta waves and spindles) which co-exist at all sleep stages just varying in proportion (Merica and Fortune, 2004).

Sleep is initiated at a local level but there is always a transition to engage the whole brain (Krueger et al., 2013; 2016). According to Gervasoni et al., (2004) these transitions take place across multiple cortical and subcortical structures requiring transient oscillatory synchronization of synaptic inputs between all brain areas.

Although the transitions between the different stages of the sleep-wake cycle are gradual, in each state there is a particular predominance of neurotransmitters, areas involved, power and synchrony in different frequency bands, as well as the emergence of different patterns of spontaneous activity and distinct responses to internal and external stimuli (Livingstone and Hubel, 1981; Destexhe et al., 1999; Steriade et al., 2001; Massimini et al., 2005; Hennevin et al., 2007; Esser et al., 2009). The fluctuation of these features allows for the classification of the different stages of sleep.

1.2.2. Spectral profile of the sleep-wake cycle

Gamma waves are present in all states but are predominant in the spectral profile when the animal is awake and alert (Maloney et al., 1997; Gross and Gotman, 1999; McGinley et al., 2015). In fact, corticocortical coherence in the gamma band is used as a reliable neural correlate of wakefulness (Pal et al., 2016). However, wakefulness is not homogeneous. Variations in neural activity, information processing and behavioral state have led to the distinction of different sub-states based on features like the level of arousal, attention, awareness or the pattern of cortical activation. The most cited sub-states in the literature in decreasing order are alert wakefulness, relaxed wakefulness and drowsiness (Gervasoni et al., 2004; Buzsaki, 2006; Crochet and Petersen, 2006; Poulet and Petersen, 2008; Gentet et al., 2010; Niell and Stryker, 2010; Cohen and Maunsell, 2010, 2011; Vyazovskiy et al., 2011; Polack et al., 2013; Reimer et al., 2014; Vinck et al., 2015; McGinley et al., 2015).

Alpha waves (8-12 Hz) are maximal during alert wakefulness and gradually decrease their power as they go through relaxed wakefulness and drowsiness, where alpha power disappears (Tanaka et al., 1996). On the contrary, in this “drowsy” state the power in the theta range (4-7 Hz) increases. This power ratio of theta and alpha waves seems to constitute a robust feature to discriminate between alert and drowsy states of wakefulness (Tanaka et al., 1996). From the drowsy state, organisms naturally transition towards SWS, which is subdivided into stages of increasing synchronization of activity and depth of sleep. In humans we find a 4-stage subdivision while in animals like rodents 2 sub-stages; SWS-I and SWS-II (Oliver and Datta, 2019). A set of specific transient phenomena constitute the hallmarks of sleeping onset: vertex sharp waves (exclusively in humans), spindles and K-complexes (Fig. 1)

(Dement and Kleitman, 1957; Rechtschaffen and Kales, 1968; Tanaka et al., 1996; Iber et al., 2007). Spindles are transient patterns of sigma band (12-16 Hz approximately) and a minimum duration of 0.5 s while the K-complexes are composed of a sharp positive deflection followed by a larger negative one with a minimum duration of 0.5 s. K-complexes originate from frontal and temporal regions and mark the entrance into a deeper sleeping phase (Loomis et al., 1937; Agnew and Webb, 1972; Hori et al., 1994; De Gennaro et al., 2001; Jagannathan et al., 2018).

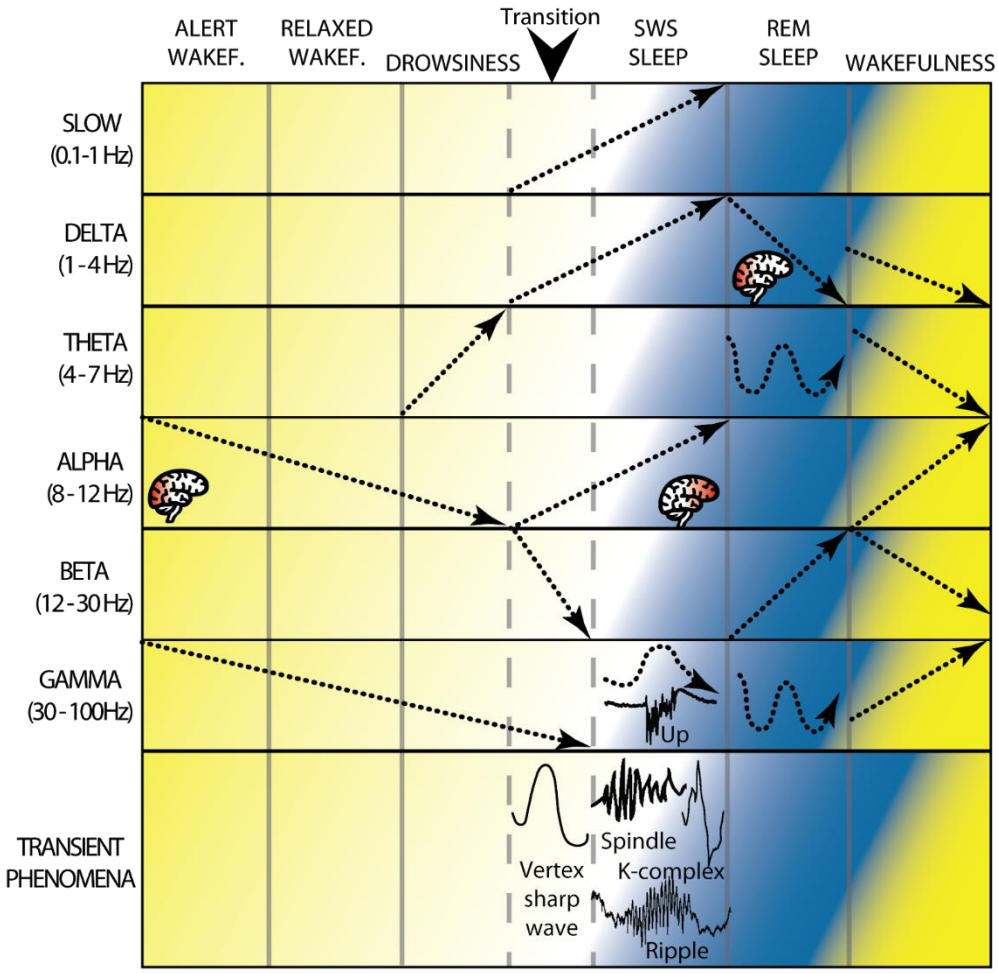

Figure 1. Illustration of the most representative spectral profile in each stage of the sleep-wake cycle based on the literature (original)
Arrows indicate the dynamics of each stage exhibited by frequency bands. These can be an increase, decrease or oscillation in power (marked by the orientation of the arrows), or in association with a discrete phenomenon (e.g. as in the case of the Up states in SWS). The red colored part of the brains indicates a topographical dominance of that rhythm in that stage: frontal or occipital.

Once the deepest stage of SWS (SWS-II in rodents) is reached, the activity in the beta band (12-30 Hz) decreases and the oscillation in the slow (<1 Hz) and the delta band (1-4 Hz) emerges prominently as a result of cortico-thalamo-cortical loops (Merica et al., 1991; 1992; Steriade and McCarley, 2005) their power being correlated with the depth of sleep (Sinha et

al., 1972; Feinberg and March, 1988). Gamma is present discontinuously, appearing in peaks in temporal association with the Up states of the slow oscillatory activity and ending with the onset of the Down state periods (Steriade et al., 1996; Grenier et al., 2001; Dickson et al., 2003; Compte et al., 2008; Mena-Segovia et al., 2008; Le Van Quyen et al., 2010).
During the SWS the alpha rhythm starts to progressively increase again (Fig. 1), but with topographical and functional differences. In wakefulness, both power and coherence of alpha waves predominate in occipital areas, but its emergence in SWS is produced in frontal areas (Hori et al., 1998; De Gennaro et al., 2001). Pivik and Harman (1995), argued that the alpha activity in SWS is associated with the global process of brain synchronization and unlinked from the existence of behavioral arousal, while the alpha rhythm in wakefulness instead, is correlated with the existence of an aroused state.

Facing the initiation of REM sleep, the high-amplitude waves from SWS are replaced by the low-amplitude REM waves which create a desynchronized pattern of activity, highly similar to that produced in wakefulness. An increase in the beta band in the range of 18–30 Hz, and a decrease of the delta band amplitude in the occipital cortex, seem to be the spectral trait that more faithfully reflects the establishment of the REM sleep period (Ursin and Sterman, 1981). Another prominent feature of REM sleep is the presence of a low-frequency theta (4–7 Hz) activity that is mainly generated in the hippocampus (Vanderwolf, 1969; Shiromani et al., 1992; Cantero et al., 2004). Gamma band is also present during REM sleep, but predominantly in the hippocampus and coupled with its robust theta oscillations (Montgomery et al., 2008).

Towards the spontaneous awakening from sleep, a global decline in the beta band occurs (Ferrara et al., 2006; Marzano et al., 2011). Likewise, the power in theta and delta bands begins to decrease, while power in the alpha band increases in the occipital orientation (Ogilvie and Simons, 1992;). According to these authors, this loss of power at low frequencies is due to the ending of the global hypersynchrony, characteristic of the sleeping stages. Spontaneous awakening can occur from the REM or SWS stages of sleep, leading to the sleep inertia period. This has been considered as an intermediate stage between sleep and awake, with remaining slow activity in theta and delta bands (1-9 Hz) and transient cognitive and behavioral impairments (Dinges et al, 1985, Ogilvie and Simons, 1992; Naitoh et al., 1993; Ferrara et al., 2006; Marzano et al., 2011; Vyazovskiy et al., 2014, Peter-Derex et al., 2015), although the precise dynamics of this awakening period are not yet clear.

These spectral differences are effective for categorizing between stages; nonetheless, they inform about local measures of the cortical dynamics not revealing anything about the interactions between different regions.

1.2.3. Variations in synchronization within the sleep-wake cycle

When two anatomically separated areas are connected and additionally have correlated activity in time, they are considered to be functionally related (Damoiseaux et al., 2006). This functional connectivity can be measured by means of their phase synchronization (or phase coherence) in different frequency bands. High levels of phase synchronization indicate a strong covariation of the neural oscillation; therefore, this index could give an insight of the strength into the functional connections between the analyzed areas (Uhlhaas et al., 2009; Bullock et al., 2009; Rieder et al., 2010; Cavelli et al., 2015; Pal et al., 2016). Many authors have proposed that the objective of this coordinated activity is to provide a precise temporal pattern for a large amount of neurons, allowing the performance of specific functions like processing and binding information, which is the substrate for mental operations, behavior and consciousness (Hebb, 1949; Buzsáki and Chrobak, 1995; Nicolelis et al., 1995; Singer, 1995; Engel and Singer, 2001; Varela et al., 2001; O'Connor et al., 2002; Fries, 2005; Damoiseaux et al., 2006; Ramachandran, 2015). For this reason, variations in synchronization are currently being widely investigated in order to find their correlated functional change.

Synchronization between two areas is influenced by different factors, like variations on the brain state or the distance separating the areas (von Stein and Sarnthein, 2000; Fries, 2005). Indeed, wakefulness and sleep show clearly distinct levels of phase synchronization of their oscillations (Gervasoni et al., 2004). During SWS, a global increase in synchronization at low frequencies is observed (Steriade et al., 1993; Achermann and Borbely, 1998a; Destexhe et al., 1999). On the other hand, during wakefulness oscillations occur at many frequency bands but synchronization is restricted among nearby regions, designated as local coupling (Steriade et al., 1996; Destexhe et al., 1999). Regarding the distance among areas as a factor in synchronization, an inverse relation between distance and frequency has been described; between distant regions the coupling in lower frequencies predominates, whilst among proximate areas synchronization in higher frequencies is enhanced (Achermann and Borbely, 1998a; Gross and Gotman, 1999; von Stein and Sarnthein, 2000).

In the literature, the gamma band is considered a key measure of inter-regional communication, but specific results across different studies are often contradictory, making its precise dynamics unclear. Synchronization in this band among cortical and subcortical areas is proposed as one possible mechanism through which the brain temporally joins multiple inputs to create a single perception, which is experienced by the subject at a conscious level (Gray and Singer, 1989; Llinás, 1991; Singer and Gray, 1995; Tassi and

Muzet, 2001; Hwang et al., 2019). Several authors described a variety of synchronization profiles of gamma through the sleep-wake cycle between cortical regions, finding the maximum values of gamma coherence during wakefulness; a decrease at an intermediate level during SWS to reach the minimum values during the periods of REM sleep (Castro et al., 2013; 2014; Cavelli et al., 2015; Pal et al., 2016). Otherwise, other authors agree in the attribution of the maximum synchronization value between cortical areas in the awake state, but they refer to a higher value in REM sleep, SWS being the state which exhibits the minimum coherence (Llinás and Ribary, 1993; Bragin, 1995; Maloney et al., 1997; Gross and Gotman, 1999) or even reported no differences at all in coherence between SWS and REM sleep (Cantero et al., 2004).

The interaction between both cortical and subcortical areas is crucial for the generation and maintenance of sleep, the switch among stages and the emergence of its different activity patterns. However, the interaction among regions that conform the cortical network seems to have a relevant role when there are variations in the arousal level. Thus, the study of the interaction between specific cortical regions can add relevant information about the underlying mechanisms of the cortical network within the sleep-wake cycle.

1.2.4. Neural responses to auditory stimulus in the sleep-wake cycle

During wakefulness the organism is active and self-aware. The brain is receptive and capable of monitoring internal and external stimuli which can trigger a neural cascade that ultimately leads to sensory perception and action. Therefore, whereas wakefulness can be described as a state for online processing of sensorimotor information, other stages of the sleep-wake cycle like the REM period can be considered as functionally isolated (Buzsaki, 1989; Chase and Morales, 1990; Stickgold et al., 2001; Dang-Vu, 2012). Only a few studies demonstrated behavioral reactivity to environmental stimuli during REM sleep. However, it has been shown that evoked potentials to multi-sensory stimuli during REM sleep are qualitative similar to those occurring during non-attentive wakefulness but differing in the areas involved (Bastuji and Garcia-Larrea, 1999; Portas, et al., 2000; Warltier et al., 2005; Wehrle et al., 2007).

Although there is a substantial absence of consciousness during SWS, several authors have claimed that a disconnection from the external world cannot be completely affirmed. SWS is an active state with discrete and synchronized neuronal activities from specific cerebral regions that reflect certain processing and give rise to distinct functional features (Portas et al. 2000; Destexhe et al. 2007; Dang-Vu et al., 2008). It has been hypothesized that reduced

awareness of environmental stimuli during sleep is necessary in order to prioritize the processing and consolidation of information acquired during the awake state (Fishbein, 1971; Smith et al., 1980; Buzsáki, 1989; Hennevin et al., 1995; Datta, 2000; Laureys et al., 2001; Stickgold et al., 2001, 2005; Ribeiro et al., 2004; Schabus et al., 2004; Clemens et al., 2006; Marshall et al., 2006). Both the spectral features and transient phenomena found in SWS are functionally relevant in this off-line processing, since they seem to modulate cortical function during this sleep stage (Hebb, 1949; Buzsáki, 1996; Dang-Vu et al., 2008). For instance, both spindles and Down state periods (produced by the hyperpolarization of thalamocortical cells) actively promote the disconnection of the cortex from the external inputs, helping in the maintenance of sleep (Elton et al., 1997; Cote et al., 2000; Massimini et al., 2003; Steriade and Timofeev, 2003), and conversely, K-complexes could appear as a pattern of cortical response to salient stimuli (Roth el al., 1956 ; Broughton, 1982), and therefore seem to be involved in the enhancement of the transmission of external information (Broughton, 1982; Muzet, 1990; Dang-Vu, 2012).

External sensory stimulation in SWS cannot not elicit a behavioral response but can originate diverse responses in brain activity (Livingstone and Hubel, 1981; Worgotter et al., 1998; Massimini et al., 2005). Specifically, it has been proven that auditory stimulation during SWS produces responses from several cortical regions, but the robust activation of primary auditory areas evidences the preservation of initial auditory processing (Peña, 1999; Portas et al., 2000; Cote, 2002; Issa and Wang, 2008; Strauss et al., 2015). However, further auditory processing seems altered in comparison to wakefulness, reflected in a lack of activation or response from secondary auditory regions and more broadly, from regions controlling the higher processing of sensory information required to achieve conscious perception (Portas et al., 2000; Nir et al., 2013). Strauss et al., (2015) attribute this effect to decreased long-range connectivity found in SWS. However, authors such as Issa and Wang (2008) state that there is a response in both primary and secondary auditory areas, thus excluding the lack of connectivity as a reason for the absence of further auditory processing.
There are contradictory results regarding state-dependent auditory cortical responses. Some results show no differences between cortical responses in any of the sleep-wake cycle stages (Hall and Borbely, 1970; ; Portas et al., 2000; Nir et al., 2013), while others show differences that can be either a decreased response during the sleep stages (Czisch et al., 2002) or an increase (Peña et al., 1999; Edeline et al., 2001). Within the regime of slow waves, a modulation between the phases of the wave (Up and Down states) has been described, modulation that is contingent on the intensity of the stimulation (Reig et al., 2015), suggesting a multifactorial interaction between brain states and amplitude of the responses.

There are diverse descriptions from multiple points of view, and it can be extracted that both the state and the pattern of brain activity have an active role in modulating the auditory cortical response. Thus, the investigation of these evoked responses within the sleep-wake cycle from a wider perspective that involves the interaction in the whole cortical network that is not only restricted to auditory areas, will contribute to a better understanding of this modulation.

1.3. Brain states and transitions in anesthetized states

1.3.1. The anesthetic-induced state of unconsciousness

Anesthesia is a pharmacologically induced state where the loss of consciousness is the main trait. Anesthetic substances act reversibly depressing the central nervous system, altering neuronal activity and brain metabolism, and disrupting functional connectivity (Imas et al., 2005; Peltier et al., 2005; Alkire et al., 2008; Barash, 2009; Schrouff et al., 2011; Boly et al., 2012; Mashour, 2013; Lee et al., 2013; Fagerholm et al., 2016; Gao et al., 2017; Hentschke et al., 2017). These substances have the capability of inducing unconsciousness along with other effects like, analgesia and movement suppression (Antognini and Carstens, 2002; Yang et al., 2009). They also cause a profound impairment in cognition, manifested in amnesia and hypnosis, which abolish awareness and impairs responsiveness to environmental stimuli (Campagna et al., 2003; Franks, 2008). Although the appearance of almost all these effects are common among anesthetics, there is considerable variability subject to the type of anesthetic or its dosage. It seems possible that unconsciousness can be reached through diverse mechanisms, evidenced for example, in the variety of different molecular targets that exist among anesthetics (Cariani, 2000; Rudolph and Antkowiak, 2004). Anesthesia and sleep share a loss of consciousness as well as other features like the slow oscillatory pattern of brain activity. This similarity seems supported by the reported existence of a significant overlap in neurotransmitters and circuitry suggesting that anesthetic substances affect the same systems involved on sleep (Nelson et al., 2002; Tung et al., 2004; Franks, 2008; Zecharia et al., 2009). However, the range of action of anesthesia also extends to wake-active areas from the ascending reticular activating system (ARAS) that sustain arousal and consciousness (French et al., 1953; Ma et al., 2002; Ma and Leung, 2006; Franks, 2008; Long et al., 2009; Leung et al., 2014) and they differ substantially in several parameters of their slow oscillatory dynamics (Akeju and Brown, 2017; Nghiem et al., 2020). This has led some authors to point out that beyond the similarities that they share, endogenous generated states and anesthetic induced states of unconsciousness are distinct (Warltier et al., 2005, Akeju and Brown, 2017). Nonetheless there exists a common agreement in the lack of comprehension of the precise mechanism by which anesthesia achieves its effects (Brown et al., 2010; Leung et al., 2014), and there is a complex interplay of variables that hinder a unitary description of the anesthetic-induced mechanisms of unconsciousness. In this context, the characterization about what occurs during the transition into the loss and recovery of consciousness at multiple levels can provide very relevant insight. And further, the interest of this characterization goes both ways: within the clinical practice, in order to

improve the anesthesia monitoring system based on the patients' brain states; and in neuroscience, to progress in the exploration and understanding of consciousness (Brown et al., 2011; Cimenser et al., 2011).

1.3.2. Neurophysiology of the anesthetic-induced state of unconsciousness

There has been a thorough search for the molecular basis of the anesthetic effect, among the repertoire of available anesthetics. Those that are explored more recurrently according to the literature are propofol (Ishizawa et al., 2016; Chennu, 2016; Pal et al., 2016; Lee et al., 2017; Paasonen et al., 2018), sevoflurane (Kim et al., 2016; Pal et al., 2016), isoflurane (Hamilton et al., 2017; Paasonen et al., 2018), ketamine (Lee et al., 2013; Blain-Moraes et al., 2014; Pal et al., 2015; Bonhomme et al., 2016; Li and Mashour, 2019), medetomidine (Grandjean et al., 2014; Paasonen et al., 2018) and mixtures of two or more anesthetic substances (Chander et al., 2014; Grandjean et al., 2014, Magnuson et al., 2014; Akeju et al., 2014).

The main molecular targets of action found are via the influence of the γ- aminobutyric acid type A ($GABA_A$), the N-methyl-D- aspartate (NMDA) receptors as well as two-pore K^+ channels, predominantly expressed in cortical neurons (Franks and Lieb, 1994; Franks, 2008). Almost all these cited substances affect these three targets, but the differences lie in the magnitude of action on each. Propofol and sevoflurane enhance GABAergic inhibitory transmission (Rudolph and Antkowiak, 2004; Bai et al., 1999; Brown et al., 2011; Chander et al., 2016) affecting the cortex, the thalamus, the brainstem nuclei from the ARAS and the spinal cord (French et al., 1953; Alkire et al., 1995; Fiset et al., 1999; Ramachandran, 2015). In these types of anesthetics, the emergence into consciousness seems to occur when the level of anesthetic substance decreases, and with it, a decrease in the level of GABAergic transmission. This allows the aminergic and cholinergic neurons from the ARAS to act and switch the activity of the brain and the organism to an aroused state, leading to the recovery of consciousness (Chander et al., 2014). Isoflurane among other volatile anesthetic agents, activate two-pore K^+ channels causing a general reduction in excitability (Franks and Lieb, 1988; Steinberg et al., 2015), but preeminently depresses the reticular formation that constitutes the ARAS (Rudolph and Antkowiak, 2004). Ketamine, in the other hand, is an atypical case, because it mainly antagonizes NMDA receptors, which mediate the slow components of synaptic transmission (Cull-Candy et al., 2001) and as a result produces a non-slow oscillatory brain activity pattern (Långsjö et al., 2005). Although ketamine in the literature is regularly grouped in the category of anesthetics, the administration of ketamine alone produces deep sedation, not surgical anesthesia (Garfield et al., 1972). According to its molecular mechanism, it seems to be preferably involved with analgesic effects, suggesting

that it would need to act on additional targets in order to cause an anesthetic induced state of unconsciousness (Franks, 2008). For this reason, in order to achieve an anesthetic effect, a combination of ketamine with medetomidine or xylazine is frequently used. These two substances are α-2-adrenoceptors agonists, so they act directly in these receptors located in the brainstem, where the ARAS is originated decreasing the release of norepinephrine and causing a general suppression of the central nervous system (Brown et al., 2010, 2011).

In terms of anatomy, the thalamus is the most frequently area reported to be inactive after the administration of most anesthetics (Veselis et al., 1997; Fiset et al., 1999; Alkire et al., 1998; 2000; Bonhomme et al., 2001; Kaisti et al., 2003; Belelli et al., 2005; Jia et al., 2005; Laitio et al., et al. 2007; Franks, 2008, Paasonen et al., 2018). Based on neuroimaging studies, this correlated inactivation observed across numerous anesthetics upon reaching unconsciousness, led Alkire et al. (2000) to formulate the thalamic switch hypothesis. In this hypothesis it is assumed that the thalamus functions as a an On-Off switch, therefore, its activation or deactivation either allows or prevents the emergence of consciousness. This is coherent, considering that it is the main hub that controls the flow of external sensory information to the cortex (Steriade et al., 1993), and that through this connection with cortical areas allows the processing and integration of information, critical for the conscious experience (Llinás et al., 1998; Van der Werf et al., 2002; Laureys and Tononi, 2009). As a consequence, the disruption produced of this thalamo-cortical connection by anesthesia, is considered by several authors a very reliable candidate to be the key feature causing the anesthetic induced state of unconsciousness (Angel, 1991; Fiset et al., 1999; Alkire et al., 2000; Hudetz et al., 2012; Guldenmund et al., 2013).

Given the large heterogeneity in the known neurochemical, neuroanatomical and neurophysiological functioning from distinct anesthetics, it seems necessary to characterize as many features as possible, during the moments of loss and recovery of consciousness in order to disentangle solely the mechanisms directly involved in the anesthetic induced state of unconsciousness. There are several descriptions from multiple levels in the search of a pattern that defines the anesthetic induced state of unconsciousness (Gugino et al., 2001; Breshears et al., 2010; Ching et al., 2010; Massimini et al., 2012; Purdon et al., 2013; Chander et al., 2014; Bettinardi et al., 2015; Mukamel et al., 2015; Ishizawa et al., 2016; Flores et al., 2017; Pavone et al., 2017; Lewis et al., 2018; Tort-Colet et al., 2019; Dasilva et al., 2020). However, there is still much unknown information, and the exploration of the activity from cortical networks involved in conscious perception within the spontaneous emergence from an anesthetic induced state of unconsciousness seems to contain relevant information.

1.3.3. Brain activity dynamics in anesthesia: the spatiotemporal and spectral profile.

Anesthesia induces a strongly marked slow oscillatory bistable activity pattern (<1 Hz or less) composed of "Up" states, periods of highly synchronized neuronal firing, that are followed by intervals of neuronal silence called "Down" states (Steriade et al., 1993; Sleigh et al., 1999; Tung et al., 2004; Ruiz-Mejías et al., 2011). As exposed in the previous chapter, this slow oscillatory pattern of activity is not exclusive to anesthetic states, being also present in the SWS stage of sleep, in altered conditions such as coma (Young, 2000) or in some varieties of epilepsies (Blumenfeld et al., 2004) and in brain slices (Sanchez-Vives and McCormick, 2000; Reig et al., 2006). The states and conditions in which this type of activity emerges implies certain degree of unconsciousness or physical isolation of the neural tissue, herby has been considered as a default activity pattern of the cortical network (Sanchez-Vives and Mattia, 2014, Sanchez-Vives et al., 2017).

Besides their differences in neuromodulation, the slow oscillation from sleep and anesthetized states could be considered as distinct types of regimes based also on dissimilarities in their temporal properties (Nghiem et al., 2020). Moreover, the anesthesia induced slow oscillation in general terms, tend to be less complex (Casali et al., 2013; Hudetz et al., 2015, 2016; Sarasso et al., 2015) and more regular than in natural sleep (Niedermeyer et al., 1999, Bruhn et al., 2000; Akeju and Brown, 2017). Nevertheless, it is worth mentioning that there are exceptions as ketamine, which despite producing an anesthetic induced state of unconsciousness, produces fast electroencephalographic activity that contrast with a slow oscillatory activity (Yamamura et al., 1981; Sakai et al., 1999; Maksimow et al., 2006).

In the transition from this anesthetized state to wakefulness several changes occur at multiple levels: from the global pattern of activity to dynamics in specific networks, brain regions or single neurons (Gervasoni et al., 2004). Following this multidimensionality, data of the neural activity during this anesthetic induced state has been collected from several sources (electrophysiology, macro and micro-scale functional imaging) allowing the measurement of different phenomena that provide information about brain dynamics across multiple scales. Beyond the contribution to the exploration of the underlying mechanisms pursuit by neuroscience, findings in the temporal and frequency dynamics form an anesthetic induced state of unconsciousness are also applied in the clinical field to monitor changes in the patient brain state under anesthesia (Gibbs et al., 1937; Kiersey et al., 1951; Tinker et al., 1977; Kearse et al., 1994; Billard et al., 1997; Rampil et al., 1998; John et al., 2001; John and Prichep, 2005).

The induction and deep stage of an anesthetic induced state of unconsciousness

During an anesthetic induced state of unconsciousness, several phenomena have been described that, due to their frequency of appearance, could be hallmarks of this state. One of these features is the variation in power in different frequency bands. Under anesthesia there is an increase of lower frequencies; slow (>1 Hz), delta (1-4 Hz) and the alpha (8-12 Hz) bands, against a decrease in the gamma band (30-500 Hz) (Lewis et al., 2012; Ní Mhuircheartaigh et al., 2013; Purdon et al., 2013; Warnaby et al., 2017). This emergence of slow rhythms is due to the switch in the firing of thalamic neurons that flip from tonic to burst mode (Steriade, 1996; Alkire et al., 1998; 2000) while the reduction of the gamma band seems to be related to the cortical suppression of activity, the principal source of this rhythm (Crone et al., 2001; Alkire et al., 2008). This power shift has been consistently reported to be highly remarkable during induction with GABAergic anesthetics (John et al., 2001; McCarthy et al., 2008; Breshears et al., 2010; Purdon et al., 2013; Lee et al., 2017; Prerau et al., 2017). Furthermore, the enhancement of delta activity is considered a typical feature of unconsciousness in both physiological and pharmacologically induced states, and it has been suggested as the trait that could potentially discriminate the state of transition into and out of unconsciousness (Vyazovskiy et al., 2009; Wang et al., 2014; Lee et al., 2017). On the other hand, oscillations in the alpha band are markers of the loss of perceptual awareness and responsiveness specifically in sleep (Dang-Vu et al., 2011; Supp et al., 2011, Purdon et al., 2013).

In the transition into an anesthetic induced state of unconsciousness changes also occur in the location of low-frequency bands predominance. When the anesthetic begins to exert its effect, delta and alpha activity migrates from the parietal to the frontal region (Gugino et al., 2001; Lee et al., 2013) leading to the emergence of a generalized phenomenon of anteriorization or "frontal predominance" (Hudson et al., 1983; Long et al., 1989; Gugino et al., 2001; John et al., 2001; Cimenser et al., 2011; Lee et al., 2013; Purdon et al., 2013; Ni Mhuircheartaigh et al., 2013; Vijayan et al., 2013). This contrast with what occurs in the transition to sleep, where the delta activity propagates inversely from frontal to parietal regions as a travelling wave (Massimini et al., 2004), suggesting that this could be a differential factor among a physiological or anesthetic induced state of unconsciousness. However, opposite effects are observed between delta and alpha on the synchrony of their oscillation as consciousness fades-out. Delta exhibits a general lack of coordinated activity, in contrast to an emergence of an alpha frontal hyper-synchronized activity, which is also originated by the thalamocortical synchrony (Feshchenko et al., 2004; Voss et al., 2006; Kreuzer et al., 2010; Cimenser et al., 2011; Purdon et al., 2013; Li et al., 2013; Akeju et al., 2014; Krzeminski et al., 2017). Hypersynchrony implies loss of specificity of each element

involved, hence in terms of brain activity, this could result in an inability to correctly integrate the information, critical process for consciousness (Tononi and Sporns, 2003; Fingelkurts et al., 2012; Mashour, 2004). Through complexity, a measure for the amount of information that is integrated within a neural system can be obtained (Tononi et al., 1998). From diverse studies mainly with GABAergic agents, it has also been inferred that the transition to unconsciousness is also marked by decrease in the complexity of the brain signals (Casali et al., 2013; Scott et al., 2014; Alonso et al., 2014; Hudetz et al., 2015, 2016; Sarasso et al., 2015; Schartner et al., 2015; Tajima et al., 2015; Solovey et al., 2015; Hudetz et al., 2016; Krzeminski et al., 2017; Li and Mashour, 2019). In contrast, the administration of other agents like ketamine, provokes the opposite pattern, with complex spatiotemporal dynamics and distinct alterations in connectivity (Liao et al., 2012; Scheidegger et al., 2012; Niesters et al., 2012; Sarasso et al., 2015; Bonhomme et al., 2016).

When consciousness is fading, anesthesia seems to rapidly disrupt the communication among connected brain regions, pointing to this as another possible cause that critically impairs the integration of conscious content (Alkire et al., 2008; Majeed et al., 2009; Pawela et al., 2009; Ferrarelli et al., 2010; Wilson et al., 2011; Mashour, 2013; Guldenmund et al., 2013; Magnuson et al., 2014; Muthukumaraswamy et al., 2015; Rivolta et al., 2015; Bonhomme et al., 2016; Zhurakovskaya et al., 2016; Lee et al., 2017; Mashour and Hudetz, 2017; Hashmi et al., 2017; Paasonen et al., 2018; Krzeminski et al., 2017; Pal et al., 2019). Alterations of frontoparietal axis connectivity has been recurrently described in the transition to unconsciousness (White and Alkire, 2003; Lee et al., 2009; 2011; 2013; Boveroux et al., 2010; Ku et al., 2011; Schrouff et al., 2011; Boly et al., 2012; Hudetz, 2012; Jordan et al., 2013; Amico et al., 2014; Blain-Moraes et al., 2014; Palanca et al., 2015; MacDonald et al., 2015; Bonhomme et al., 2016; Schroeder et al., 2016; Ranft et al., 2016; Sanders et al., 2018a; Li et al., 2019b) and in specific frequency bands, ranging from the slowest frequencies such as delta and alpha (Purdon et al., 2013; Chander et al., 2014; Blain-Moraes et al., 2014; Kim et al., 2016; Chennu, 2016; Lee et al., 2017), to higher ones like beta (Lee et al., 2017) and gamma (John, 2001; Imas et al., 2005; Pal et al., 2016, Li et al., 2017). The substantial amount of data from several perspectives linking frontoparietal connectivity with the loss of consciousness, has led to its proposal as a neural correlate of consciousness (Rees et al., 2002; Sarter et al., 2001; Naghavi and Nyberg, 2005; Di Perri et al., 2014).

The thalamocortical connection also experiences alterations during the transition to an anesthetized state, but the results are not homogeneous. In accordance with the thalamic switch hypothesis, several authors found a clear impairment in the thalamocortical connection (Alkire et al., 2000; Kochs et al., 2001; Hudetz et al., 2012; Guldenmund et al., 2013; reviewed: Hudetz and Mashour, 2016; Shin et al., 2016; Hamilton et al., 2017).

Contrarily, in other studies with GABAergic agents, a preservation of the thalamocortical connection has been found (Tu et al., 2011; Boly et al., 2012; Liu et al., 2013a; Guldenmund et al., 2013; Paasonen et al., 2018). This preservation is recurrent in the case of ketamine, where although the connection is altered, the transfer of information remains active (Schwender et al., 1993; Moghaddam et al., 1997; Långsjö et al., 2003; Lewis et al., 2012; Bonhomme et al., 2016; Schroeder et al., 2016) or even increased (Ferrer-Allado et al., 1973; Höflich et al., 2015). Therefore, sensory information can reach the cortex, but is profoundly distorted provoking alterations like feelings of dissociation, hallucinations and delirium (Garfield et al., 1972; Sleigh et al., 2014). Other anesthetics exhibit likewise other types of connectivity patterns. For instance, isoflurane provokes a pattern of widespread and low specific connectivity, while medetomidine preserves the connectivity among all cortical and subcortical specific functional networks (Kalthoff et al., 2013).

However, it is not only the type of agent that influences how connectivity is modulated or disrupted, functional connectivity is also very dose- dependent (Peltier et al., 2005; Kiviniemi et al., 2005; Lu et al., 2007; Pawela et al., 2009; Williams et al., 2010; Nasrallah et al., 2012; Liu et al., 2013a; Jonckers et al., 2014; Grandjean et al., 2014; Bettinardi et al., 2015; Barttfeld et al., 2015; Hudetz et al., 2015; Hamilton et al., 2017; Paasonen et al., 2018). Studies with ketamine and isoflurane illustrate this dose-dependency, showing an enhancement of the network synchrony at moderate doses, and completely disrupting this activity at higher concentrations (Maekawa et al., 1986; Lenz et al., 1998; Imas et al., 2005; Becker et al., 2012; Niesters et al., 2012; Driesen et al., 2013; Lissek et al., 2016).

The disruption of long-range connections during the anesthetic induced state of unconsciousness does not imply that all connections are interrupted. Lewis et al. (2012) showed that when the anesthetic exerts its effect, local networks do not alter, they remain intact but become functionally isolated in time and space. More specifically, Lee et al. (2017) reported an increase in the local connectivity of delta and beta bands in the parietal region within the transition to the anesthetic induced state of unconsciousness. One possibility is that anesthesia could be enhancing local connectivity, insufficient to achieve the functional integration of the information, critical for consciousness (Alkire et al., 2008; Tononi and Massimini, 2008; Tononi et al., 2016).

However, regardless of the network studied, the synchronization decrease in the gamma range is a prominent feature in the transition to the anesthetic induced state of unconsciousness and is also the first frequency to restore its synchrony during the recovery of consciousness (John, 2002; Mashour, 2006; Pal et al., 2016). Gamma is predominant in the awake state, when the subject is aware and alert (Maloney et al., 1997; Gross and Gotman, 1999;

McCormick et al., 2015), and is modified under diverse cognitive alterations (Ruiz-Mejías et al., 2016, Castano-Prat et al., 2019; Dasilva et al., 2020). It is the frequency band at which the binding of information occurs, allowing a unified and conscious experience for the subject (Rodriguez et al., 1999). Therefore, both the activity and synchrony in the gamma range has been repeatedly proposed as a correlate of consciousness (Engel and Singer, 2001; Merker, 2013, 2016). Although, gamma coherence with ketamine again follows a different dynamic, increasing when is injected at both subanesthetic (Rivolta et al., 2015; Shaw et al., 2015, Pal et al., 2015) and anesthetic doses (Lee et al., 2013; Li et al., 2019). Ketamine produces remarkable modulations of gamma in the cortex (Pinault, 2008; Kocsis, 2012; Schroeder et al., 2016) and subcortical regions (Leung, 1985; Hunt et al., 2006).

Another phenomenon described during the anesthetic induced state of unconsciousness is the interaction established between distinct frequency bands. Increases have been described in the coupling of the delta phase with the gamma power, as well as a stable anticorrelated phase of the theta-alpha and theta-gamma rhythms (Canolty, 2006; Breshears et al., 2010). Both theta and gamma bands have been permanently related to memory and further cognitive processes, while the interaction among them could be more involved with the cortico-hippocampal functional interplay (Buzsáki, 2002; Axmacher et al., 2010). Breshears et al. (2010) hypothesized that the persistence of an interaction between these rhythms throughout the anesthetic induced state of unconsciousness could explain the conservation of the memories acquired prior to the induction with anesthesia.

The fade-out from an anesthetic induced state of unconsciousness

Contradictory results have been described during the fade-out from an anesthetized state even using the same GABAergic anesthetics. Considering the data obtained from the induction as a point of reference, some authors have observed a reversal of the same induction dynamics in the progression towards consciousness (Breshears et al., 2010; Gugino et al., 2001; Lee et al., 2011; Lee et al., 2013; Purdon et al., 2013; Ni Mhuircheartaigh et al., 2013), while others found heterogeneity in the trajectories of this emergence (Chander et al., 2014).

This inverse dynamic is reflected in a decrease in power from delta and alpha activity over the frontal plane, followed by an increase in gamma frequencies as first signs of the emergence of consciousness (Gugino et al., 2001; Breshears et al., 2010; Purdon et al., 2013; Ni Mhuircheartaigh et al., 2013; Chander et al., 2014). Some authors also reported a decreased variability in the power of alpha, beta and gamma bands (Breshears et al., 2010) or even in all the frequency bands between cortical areas (Chander et al., 2014), a generalized stabilization of the oscillations, that could indicate the re-establishment of the long-range

connections. Within the emergence from the anesthetic induced state of unconsciousness, an increase in corticocortical connectivity specifically in both theta and high gamma bandwidths also occurs (Li et al., 2017). Also, in contrast to induction, a decrease in the coupling of the delta phase with the gamma power is produced, while the anticorrelated synchronization in the phase of theta-alpha and theta-gamma does not vary from induction and remains stable (Breshears et al., 2010).

The fade-out with other anesthetics shows some similarities with that described for the GABAergic agents, but there is not such an extent of literature. In isoflurane, for instance, the evolution from an anesthetized state does not seem gradual, finding discreet fluctuations in all frequencies produced in multiple steps (Hudson et al., 2014) With the mixture of ketamine and medetomidine, as with GABAergic agents, the emergence is marked by a generalized increase in the power of the gamma band. Conversely, an increase of alpha among functionally related cortical areas also occurs, contrary to the alteration in connectivity in this band correlated with the fading of consciousness found with GABAergic anesthetics (Bettinardi et al., 2015).

As exposed above, there seems to be a wide disparity in the spatiotemporal and spectral patterns found within the loss and recovery of consciousness dependent on the dose (Barttfeld et al., 2015; Hudetz et al., 2015; Lissek et al., 2016; Hamilton et al., 2017; Paasonen et al., 2018) or the nature of the anesthetic substances (Aouad and Nasr, 2005; Chen et al., 2010; Lepousé et al., 2006; Sikich and Lerman, 2004; Brown and Purdon, 2013). Considering this evidence, it seems necessary to obtain data from the induction and emergence from distinct anesthetics, with different techniques in order to elucidate if there is a consistency in the way that the brain regain its functionality that could lead to the underlying mechanisms and multiscale dynamics.

1.4. Thalamic stimulation during an anesthetized state

1.4.1. The thalamus

The thalamus is a brain region composed of two structures located in the center of both hemispheres. It originates in the diencephalon and is constituted by a mosaic of recognizable groups of cells called nuclei (Jones, 1985). This nuclear division is based on several parameters as: their cytoarchitecture (Morel et al., 1997), their function (Yuan et al., 2015) and their connections (Johansen-Berg et al., 2005a). All these nuclei are reciprocally interconnected by association fibers and linked to subcortical and specific cortical regions by projection fibers, the thalamocortical projections (Kumar et al., 2017; Jones, 1981; Van Buren and Borke, 1972) that do not establish local excitatory connections (Jones, 1981). Most of the thalamic nuclei contain exclusively glutamatergic excitatory neurons (Shi et al., 2017), but in those thalamic nuclei composed by inhibitory neurons, the inhibitory GABA neurotransmitter is predominant (Arcelli et al., 1997).

From a functional point of view, three basic types of thalamic nuclei can be differentiated: the relay, the association and the nonspecific thalamic nuclei.
The most widely studied function of the thalamus is as a sensory relay to the cortex. The group of the relay thalamic nuclei receive information from all the sensory systems, (except for olfactive information), and sends them to their corresponding primary cortical area. The medial and lateral geniculate nucleus receive respectively peripheral auditory and visual inputs tono and topographically organized, and they project that information to a specific part of the cortex preserving the original topography (Jones, 1991). These primary sensory nuclei have been fundamental for mapping and understanding a great part of the thalamic functioning.
Nevertheless, most of the thalamic nuclei do not receive substantial direct sensory inputs, therefore the sensory relay is not their unique function (Rovó et al., 2012). The thalamus also has a substantial number of association nuclei. The two largest thalamic regions of the mammalian brain belong to this functional group of nuclei; the pulvinar and mediodorsal nucleus, which receive their largest input directly from the cerebral cortex. Through this corticothalamic connectivity they play a relevant role in higher-order cognitive functions such as attention and consciousness (Jones, 2007; Sherman and Guillery, 2006), specially the mediodorsal nucleus due to its dense connections with frontal regions like prefrontal, anterior cingulate and premotor cortex (Goldman-Rakic and Porrino, 1985).

The nonspecific nuclei of the thalamus comprise two structures: the midline and intralaminar nuclei. Both macrostructures are located internally, in the medial dorsal part of the thalamus, embedded in the internal medullary lamina. In the midline formation, five different nuclei are distinguished: paratenial, paraventricular, intermediorsal, rhomboid and reuniens. In the intralaminar nuclei there is a first rostro-caudal division, and each orientation comprehend the distinct nuclei where the principals are: the central lateral, paracentral, central medial and parafascicular nucleus (PF).

The classification as "non-specific" nuclei were based on their spatially diffuse projections to large cortical territories (Lorente de No, 1938; Jones, 1998; Kuramoto et al., 2017) which resulted in a more global influence of the cortical activity, leading to that view of functional non-specificity. Evidence for this lack of specificity was also supported by the broad cortical recruiting effect observed after the electrical stimulation of several of these nuclei (Moruzzi and Magoun, 1949). Current anatomical reconstructions studies suggest that these nuclei could be clustered more precisely in terms of their patterns of connectivity (Van Der Werf et al., 2002) going against the old vision of their non-specificity.

1.4.2. The intralaminar nuclei of the thalamus and consciousness

The precise neuroanatomical support of consciousness has not yet been clearly identified (Alkire et al., 2008, Tononi and Laureys., 2008) but many data support the thalamus as a possible critical structure, and more specifically its nonspecific thalamocortical circuit, involving primarily the intralaminar nuclei (Bogen, 1995, Llinás and Ribary, 1998; 2001; Van der Werf et al., 2002).

These nuclei exhibit diffuse connections to the whole brain, particularly to prefrontal cortex and basal ganglia (Quiroz-Padilla et al., 2010; Edlow et al., 2012). They intervene in the regulation of wakefulness through the extensive monosynaptic inputs that they receive from different brainstem nuclei from the mesencephalic reticular formation (Llinás et al., 2002). The reticular formation is a diffuse network of neurons constituting the ascending reticular activating system (ARAS). The ARAS is a system constituted by a network of nerve fibers ascending from the brainstem and projecting to the cortex through both thalamic and extrathalamic pathways. The thalamic pathway is composed mainly by cholinergic and glutamatergic neurons and is directly involved in the regulation of arousal and the active and desynchronized cortical activity pattern. The extrathalamic pathway contains the hypothalamus and basal forebrain acting as relays and using amines as neurotransmitters.

Through this pathway the regulation of the circadian sleep-wake cycle is produced with the involvement of the hypothalamus (Edlow et al., 2012).

Cortical activation predisposes the organism to receive and process external and internal information, boosting alertness and attention, and is a fundamental requirement for consciousness. It has been found that very small lesions in the intralaminar thalamus cause a loss of consciousness (Bogen, 1995; Schiff and Plum, 2000) and its inhibition during epileptic seizures causes the emergence of slow oscillatory cortical activity as in a state of deep sleep or coma (Blumenfeld, 2012). Studies on patients with disorders of consciousness have reported reductions in functional connectivity restricted to the cortico-thalamo-cortical networks from the intralaminar nuclei (Laureys et al., 1999; 2000a; 2000b; Cauda et al., 2009; Boly et al., 2009; Zhou et al., 2011). The opposite dynamic has been found during the recovery of consciousness, an increase in neural connectivity between the intralaminar thalamus and the anterior frontal cortex (Jang et al., 2016). Also, studies and clinical trials involving different types of stimulation within the systems comprising the ARAS repeatedly reported EEG activation and wakefulness (Moruzzi and Magoun, 1949; Brown et al., 2012). In particular, the pharmacological or electrical stimulation of different intralaminar nuclei has proved to be capable of restoring consciousness in anesthetized animals (Alkire et al., 2007; Redinbaugh *et al.*, 2020), after epileptic seizures (Kundishora et al., 2017) or even in patients with disorders of consciousness stimulating electrically the centromedian (Cohadon et al., 1985) or parafascicular nucleus (Tsubokawa et al., 1990; Schiff et al., 2007; Yamamoto el al., 2010).

A variety of physiological effects have been described after the electrical stimulation of nuclei involved in the ARAS, especially from the nonspecific thalamocortical circuit. Widespread responses in the cortex have been reported after an electrical stimulation (Morison and Dempsey, 1942; Jasper, 1949; Hanbury et al., 1954). In some cases, the stimulation has elicited an enhancement of cortico-cortical synchrony (Redinbaugh et al., 2020), specifically in the gamma range (Munk et al., 1996; Herculano-Houzel et al., 1999) which is considered as a relevant rhythm for conscious perception (Gray and Singer 1989; Srinivasan et al., 1999; Meador et al., 2002; Doesburg et al., 2005; Nakatani et al., 2005; Palva et al., 2005; Hwang et al., 2019). On the other hand, cortical desynchronization is the most reported change in the activity pattern after a thalamic electrical stimulation, observed when the stimulation is delivered during the postictal slow wave state (Kundishora et al., 2017), a state of quiet wakefulness (Poulet et al., 2012) or anesthesia (Moruzzi and Magoun, 1949). In summary, intralaminar nuclei lesions result in loss of consciousness and slow oscillatory cortical activity while several types of stimulation cause enhancement of behavioral arousal and a desynchronized cortical activity pattern.

Neuroanatomical and empirical results support the possible central role of the intralaminar nuclei in consciousness, mainly due to its role as an information integrator between several systems specialized in sensory information (sensory and motor specific thalamic nuclei), high order information (prefrontal cortex) and arousal (ARAS) (Mumford, 1991).

1.4.3. Electrical stimulation of the intralaminar parafascicular nucleus of the thalamus to restore consciousness

The centromedian-parafascicular complex in humans and primates, and the PF in rodents (Jones, 1985; Macchi and Bentivoglio, 1986; Groenewegen and Berendse, 1994) is considered the main intralaminar nucleus located in its caudal part. As a part of the intralaminar thalamus, the PF is related to several functional systems. However, numerous studies lesioning and stimulating specifically this nucleus, have highlighted its involvement in higher order functions, like learning, memory, attention, cognition and consciousness (Delacour 1969; Kinomura et al., 1996; Vale-Martínez et al., 1999; Guillazo-Blanch et al., 1999; Minamimoto and Kimura, 2002; Raeva, 2006; Quiroz-Padilla, M. F., et al, 2006, 2007; Minamimoto et al. 2009; Bradfield et al., 2013). The modulation of the activity of the PF nucleus has demonstrated to have prominent effects on cognition, specifically its lesion has revealed a critical role in the acquisition phase of learning and its stimulation a facilitation of the memory in a behavioral task (Guillazo-Blanch et al., 1999; Quiroz-Padilla et al., 2006). These cognitive effects are supported anatomically by its large and specific connection with the prefrontal cortex and the dorsal striatum (Marini and Pianca, 1996; Quiroz-Padilla et al., 2010; Bradfield et al., 2013), and points to a convergence in the mechanisms of consciousness, memory, learning and cognition.

The physiological effects found from the experimental stimulation of the PF nucleus, are the same observed with the stimulation in other intralaminar nuclei (1.4.2): cortical desynchronization in the case of high-frequency stimulation and an increment in cortical responses as well as an increase in neuronal recruitment with low-frequency stimulation (Jasper et al., 1955; Weinberger et al., 1965; Sasaki et al., 1970).

Based in these experimental results, the electrical stimulation of the PF is being applied in clinical trials on patients with disorders of consciousness in order to restore cognitive functions and consciousness (Schiff et al., 2007; Gummadavelli et al., 2015). In the context of altered consciousness, the stimulation provokes a broad activation of the forebrain, brainstem and spinal cord systems causing fluctuations in arousal reflected in the

manifestation of conscious behaviors (Pfaff, 2005; Schiff et al., 2007). The electroencephalogram of this patients after the stimulation frequently exhibits activity shifts to a higher-frequency content and a more asynchronous pattern. Nevertheless, the outcomes of the PF stimulation are heterogeneous. Chudy et al. (2012) found in all the patients a pronounced arousal behavioral effect restricted to the duration of the electrical stimulation in the PF nucleus without further effects. On the other hand, Cohadon and Richer (1993) observed the recovery of some degree of consciousness only in half of the stimulated patients. The most paradigmatic cases have been observed by Yamamoto et al. (2005) and Schiff et al. (2007), both obtaining the complete recovery of consciousness of their patients (capable to interact and communicate).

Mann et al. (2017) postulated that the improvements in behavioral outcomes observed with chronic electrical deep brain stimulation are probably a combination of physiological changes that also improve network dynamics between brain regions. However, the specific mechanism underlying brain circuit modulation by chronic electrical deep brain stimulation of certain nuclei is still unknown (Yamamoto et al., 2010)

Chapter 2

Objectives

2.1. Brain states and transitions in the physiological sleep-wake cycle

Regarding the objectives from this part of the Thesis work focused in the sleep-wake cycle, these were:

1. To explore the specific spectral profile and cortical network dynamics that characterizes the distinct stages of the sleep-wake cycle.
2. To use the distinctive features found from each stage of the sleep in the experiments to develop an algorithm for automatic detection of the sleep-wake stages.
3. To test the experimental design of a protocol for the delivery of distinct auditory stimuli with multi-cortical site recordings in the chronic animal during its physiological sleep-wake cycle.

2.2. Brain states and transitions in anesthetized states

Considering the lack of a unitary description of the brain dynamics during distinct levels of anesthesia and within the loss and recovery of the consciousness, the objectives of this part of the Thesis work were organized as follow:

1. To explore the specific spectral profile and cortical network dynamics that characterize the different stages of an anesthetic state of unconsciousness.

2. To find a method to accurately classify the distinct emergent patterns of activity during an anesthetized state of unconsciousness.

3. To investigate the multiscale cortical activity dynamics of neural populations from single-neuron scale during the states of wakefulness and anesthesia.

2.3. Thalamic stimulation during an anesthetized state

The involvement of the intralaminar PF nucleus in consciousness, and its potential to restore it using electrical stimulation in a state of unconsciousness, has been reported in clinical trials, together with a wide variety of effects. Nevertheless, there are still few experimental studies exploring the physiological mechanisms mediating these outcomes. Considering these findings, the objectives from this part of the Thesis work was:

1. To explore the evoked changes in the cortical dynamics produced by the electrical stimulation of the thalamic parafascicular nucleus on an anesthetized brain state to better understand the involved underlying mechanisms.

Chapter 3

Methods

3.1. Brain states and transitions in the physiological sleep-wake cycle

3.1.1. Experimental procedure: Recording the cortical activity during the sleep-wake cycle in the freely moving rat

Subjects

In this experimental protocol, 6 male Lister-Hooded rats (250-450 grs., 6-10 months old) were used. Until the day of the surgery the animals were placed in polysulfone cages (48,2 cm x 26,7 cm x 21 cm with a floor area of 940 cm^2), preferentially in pairs from the same breed, with access to food and water ad libitum. All the procedures with animals were carried out in accordance with Spanish regulatory laws (BOE-A-2013-1337), which comply with the European Union guidelines on protection of vertebrates used for experimentation (2010/63/EU). All experiments were supervised and approved by the Animal Experimentation Ethics Committee of the Universitat de Barcelona (287/17 P3).

Surgery for the chronic placement of the electrodes

To obtain LFP recordings in the freely moving rat from their sleep-wake cycles, we performed surgeries to chronically implant the electrodes.

For the chronic implants we made a fixed microdrive consisting in a case blank connector with crimping contacts (Molex, USA) (Fig. 3) to attach the inserted electrodes. The recording electrodes were handmade twisting stainless steel insulated wires of 100 µm (California Fine Wire Co, California, USA) obtaining two separate tips for each electrode. For the recording of the EMG from the neck muscle, a single electrode was made with a 125 µm Tungsten insulated wire (Advent Research Materials Ltd, Oxford, England).

To perform the implantation surgery, first, the rat was placed in an induction chamber at 100% oxygen for 10 min for habituation and the prevention of apnea. The initial exposure to the isoflurane was performed at the highest concentration (5%) for 5 min (0.6 L/min, 1 bar). Afterwards the concentration was lowered to 3% for 1 min. Immediately after, the rat was mounted in the stereotaxic apparatus (Kopf Instruments, Tujunga, CA, USA) with an adapted anesthesia delivering mask (Kopf Instruments, Tujunga, CA, USA) to maintain the administration of isoflurane (2%) mixed with oxygen during the surgery. The depth of surgical anesthesia was checked regularly by the absence of reflexes. Before the performance of the incision, atropine was injected subcutaneously (0.05 mg/kg) to prevent respiratory secretions, 0.6 ml. of saline solution (0.9%) for hydration and 10 mg/kg intraperitoneal of methylprednisolone (Urbason) to prevent inflammation. The rectal temperature was monitored and maintained at 37 °C during the procedure through a probe and an electric blanket (RWD Life Science Co., Ltd).
After exposing the skull, 5 to 6 holes were made for anchoring screws. One of the posterior screws acted as ground by means of a soldered wire. The craniotomies for the electrode insertion were made in all subjects in 4 functionally relevant and distributed cortical coordinates from the left hemisphere: Prelimbic cortex (PrL) located at 3.7 mm anteroposterior from bregma (AP), 0.8 mm mediolateral (ML), -2.7 mm dorsoventral (DV), primary motor cortex (M1) (0.4 mm AP, 1 mm ML, and -1.2 mm DV), primary somatosensory cortex (S1) (-3.14 mm AP, 5 mm ML, -1.2 mm DV) and the primary visual cortex (V1) (-7.3 mm AP, 2.2 mm ML, -0.6 mm DV). The stereotaxic coordinates were obtained from the Paxinos and Watson (2007) rat atlas. The PrL and V1 was recorded from the 6 animals, M1 in 5 and S1 in 3 of them.

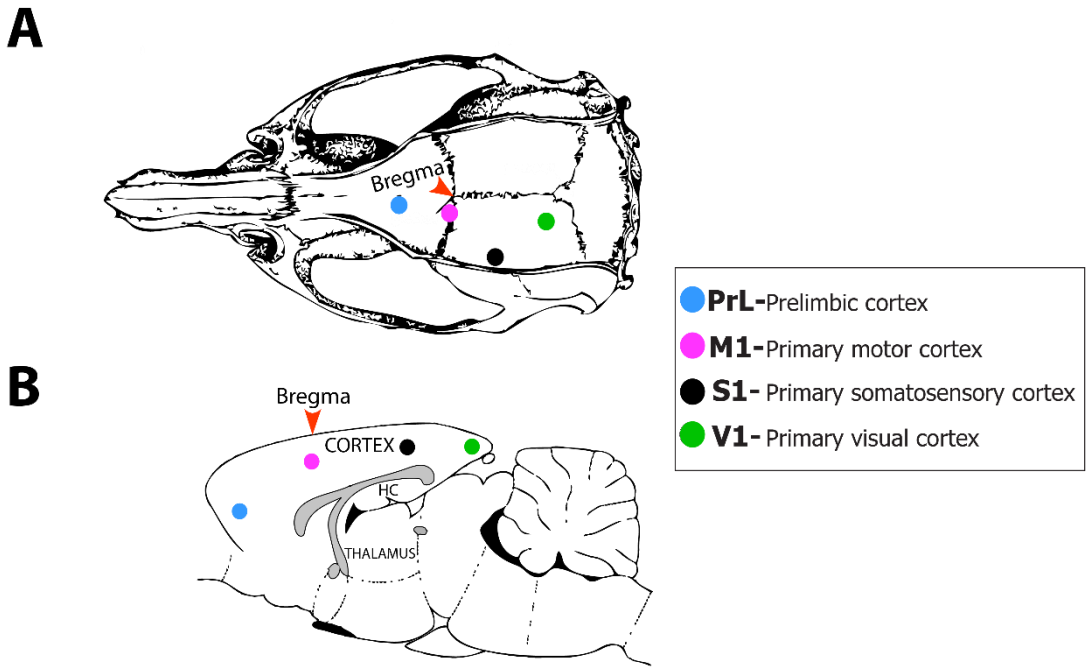

Figure 2. Map of the recorded areas from different planes.
(A) Dorsal view of the rat skull with the anteroposterior and medial localization of the electrodes marked with circles in the different (color coded). **(B)** Sagittal plane of the rat brain showing the depth of the electrodes in each of its location (color coded). *Figure adapted from Paxinos and Watson, 2007.*

After the placement of the electrodes, these were fixed to the skull with a first application of glue (Loctite 406, Henkel, Germany) and then a second layer of glass ionomer luting cement (Medicaline, Geestland, Germany). Afterward, the electrodes were welded to the contacts of the case blank connector and in the last step of the surgery the case was attached to the skull with glass ionomer luting cement. Buprenorphine (0.06 mg/kg) and Enrofloxacin (25 mg/kg) were administered for a minimum of 5 days after surgery for analgesia and the prevention and treatment of possible infections. After the post-surgical treatment period, 5 days of handling and habituation to the recording chamber were performed in order to minimize stress and abrupt movements of the animal during the experimental sessions.

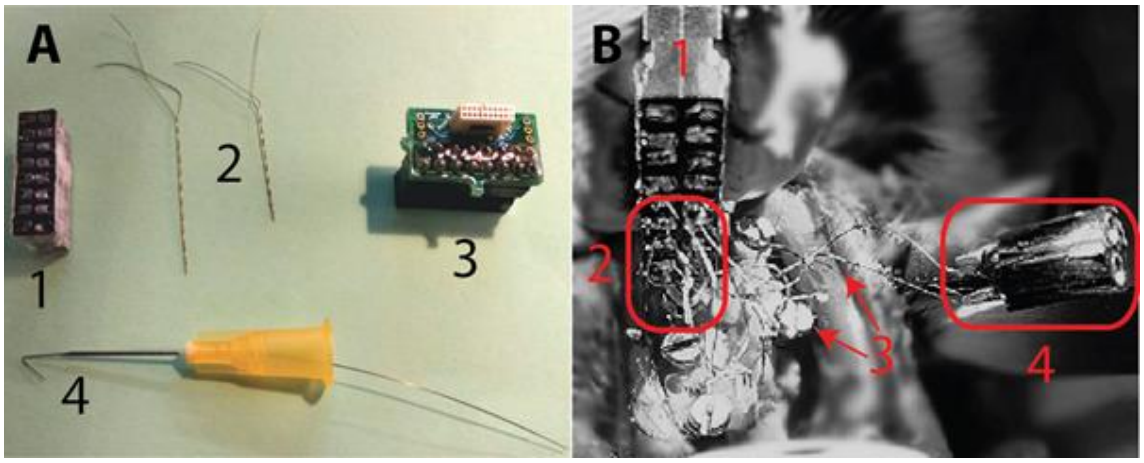

Figure 3. Materials for chronic implants and its placement process
(A) 1. Case blank connector with tinned contacts. 2. Twisted bipolar electrodes. 3. Case connector to the headstage adapter (custom-made in IMB-CNM (CSIC)). 4. EMG wire mounted in a 26G hypodermic needle to insert in the neck muscle. **(B)** Picture of the step of welding the electrodes to the case blank connector in the implant surgery. 1. Case blank connector. 2. Tips of the implanted recording electrodes welded to the connector contacts. 3. Tips of the implanted stimulation electrodes (top arrow) and anchoring screws (left arrow). 4. Case connector for stimulation.

Recording protocol

After the post-surgical recovery period, the rats were recorded daily for several hours during their natural sleep-wake cycle of sleep for a minimum of 3 days.
To record the LFP from the implanted electrodes in the freely moving rat, the subject was first connected to the headstage micro preamplifier (Multi Channel Systems, Germany) by means of a custom-made adapter (IMB-CNM (CSIC)) to the implanted case (Fig. 3A-1). Then, the animal was placed in a plastic recording cage (57x39x42 cm), while was videotaped and recorded. Recordings were acquired, digitized at 10 KHz using a data acquisition interface and Spike 2 software (Cambridge Electronic Design, UK).
The data analysis was performed with the software MATLAB (The MathWorks Inc., Natick, MA) and Spike 2.

3.1.2. *Pilot study.* Experimental procedure: Recording the cortical activity and delivery of auditory stimulation during the sleep-wake cycle in the freely moving rat

Derived from the experimental work performed in the characterization of cortical dynamics in physiological states within this Thesis, further objectives were proposed. We also aimed to explore cortical responses to auditory stimulation in the distinct stages of the sleep-wake cycle. For this purpose, we designed an experimental protocol for the delivery of auditory

stimulation while recording cortical activity during the sleep-wake cycle and we tested this protocol in one subject. For this subject we performed the surgery for the implantation of the electrodes, using the same coordinates as before to reach PrL, M1 and V1 regions (3.1.1). In addition we also placed electrodes in the primary auditory cortex (A1) (-4.3 mm AP, 6.6 mm ML, -1.9 mm DV), the secondary auditory cortex (A2) (-3.14 mm AP, 6.1 mm AP, -3 DV) and the parietal association cortex (PtA) (-4 mm AP, 3 mm ML, -0.9 mm DV). We attached a pair of aluminum earphones holders to the implant as in Abolafia et al. (2011; 2013) for the sound delivery.

Recording protocol

After the recovering period, we performed baseline recordings of the natural sleep-wake cycle in the freely moving animal for a minimum of three days. We used these baseline recordings to calculate specific parameters from the signal of this subject, required for the training and configuration of an online algorithm of stage detection (4.1.2). Then, we proceeded to the recording and the sound delivery during each stage of the sleep-wake cycle.
The recoding was performed in the plastic recording cage placed inside a double wooden box (80x80 cm and 60x60 cm). The two wooden boxes were separated by 6 cm thick foam for acoustic isolation, and the level of isolation was tested with a sound level meter (Labmatrix Manufacturing LLP, India), finding a maximum level of environmental noise of 35 dB.
We delivered tones of three different frequencies: 4 kHz and 8 kHz as pure tones and white noise with 110 ms of total duration considering a 5 ms rise/fall cosine ramps. Each type of stimuli could appear at 45 dB or 60 dB of intensity. The sounds were presented randomly for the frequency, intensity and time conditions, with an interstimuli interval ranging from 1 to 5 s. The randomization for the presentation time was subject to an exponential distribution in order to minimize the animal expectancy, with 2 s mean truncated to values smaller than 1 s and larger than 5 s.
The auditory stimulation was delivered using a pair of earphones (ER-6i Isolator, Etymotic Research, USA) mounted in the implanted earphone holders, ensuring the direct arrival of the sound to the animal.
During the recording, the algorithm detected in which state the animal was and delivered the distinct conditions of the stimuli balanced between the three stages.

The algorithm for online detection was implemented in the software MATLAB (The MathWorks Inc., Natick, MA) and the creation and delivery of sounds were performed with the software Spike 2 (Cambridge Electronic Design), the data acquisition interface (Cambridge Electronic Design) to convert the digital signal to analog and an attenuator to further control the properties of the sound (Cambridge Electronic Design).

3.1.3. Data analysis

Manual classification of the sleep-wake stages

We performed a manual classification of the three main stages of the sleep-wake cycle: awake, SWS and REM. The classification was made offline, by visual inspection of the electrophysiological features from the recordings. The criteria for the classification was based on the validated scale for sleep scoring (Iber et al., 2007). Following this scale, we examined the amplitude, frequency, the presence of slow components and transient phenomena in the raw signal in addition to the amplitude of the EMG signal and the postural and behavioural changes observed in the video recording.

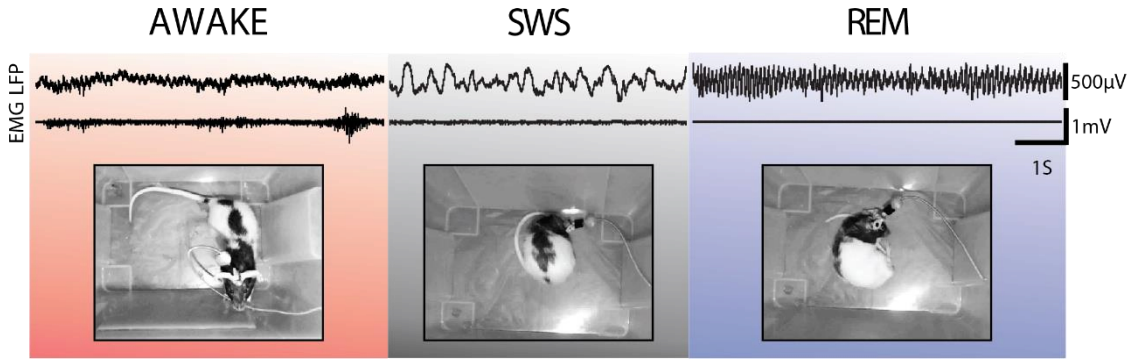

Figure 4. Example of the traits exhibited in the three main detected stages from the experimental recordings
Raw LFP signal and EMG signal (top) and captions from the video tracking (bottom) showing respectively a representative activity, muscular tonicity, behaviors and posture from each stage.

For the manual classification of the different stages, in addition to the features from the cortical signals, the context of both brain activity and behaviour must be considered.
The LFP traits exhibited in the awake state were characterized by a low amplitude and asynchronous signal. The animal could be still causing variations of voltage in the EMG due to the presence of muscular tone, or could be in motion, in which case the activity was evidenced in the EMG and the video. This awake pattern of activity could potentially appear at any time during the cycle, even suddenly interrupting the REM (Fig. 5A) or SWS sleep (Fig. 5B). Also, if the animal performed an accommodation movement during the SWS with no recovery of active behaviors, the awake activity emerged simultaneously with a short-lasted muscular movement for reenter to SWS a few seconds later, what is considered a microarousal (Fig. 5C).

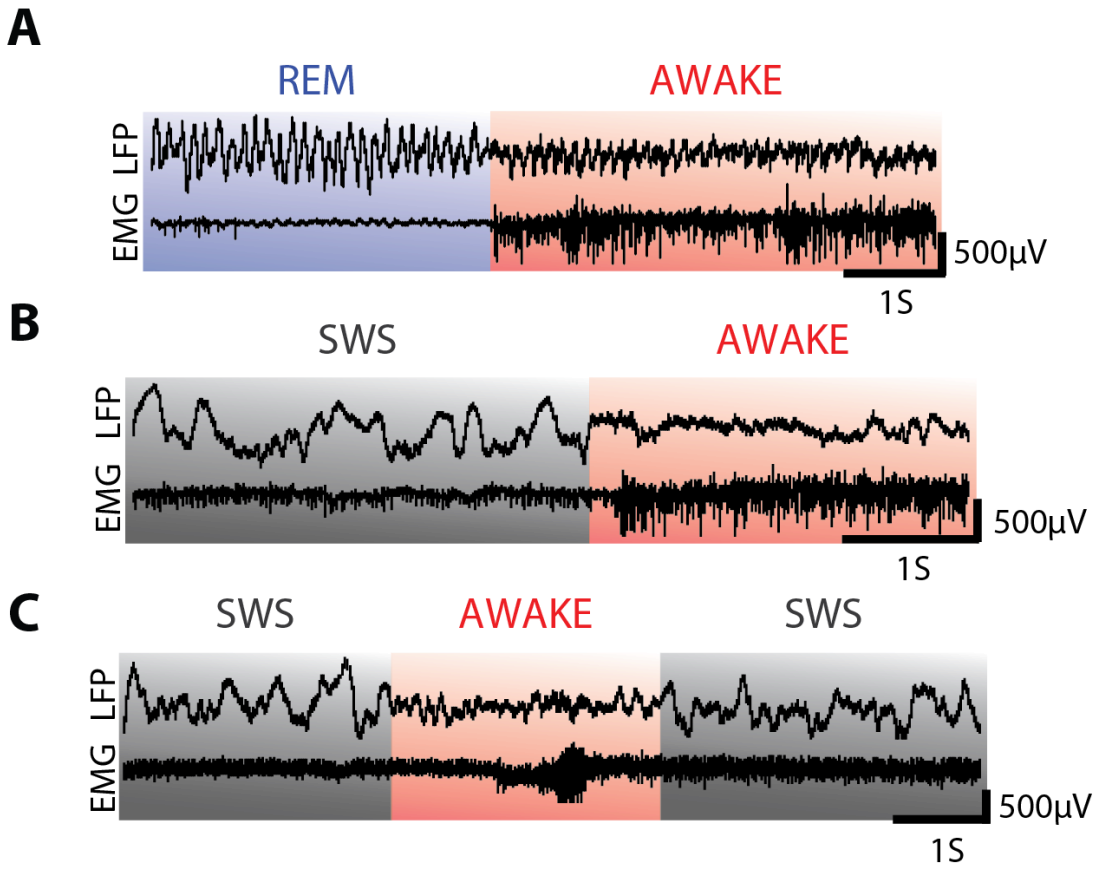

Figure 5. Emergence of the awake activity pattern from different sleep stages
Raw LFP signal (top) and EMG signal (bottom) **(A)** From REM sleep **(B)** From SWS **(C)** Microarousal due to a short postural movement.

In the course of the SWS an oscillatory pattern could be observed. The signal had a highest amplitude, compared to the signal in the awake and REM sleep stages, and the Up and Down states were discernible. The EMG could exhibit slight variations of voltage, because the animal still preserved a certain muscular tone, but to a lesser degree than when the animal was considered awake. This slow oscillatory pattern generally appeared with a transition from the awake or the REM sleep. The SWS traits emerged mixed with the awake or REM activity morphing to the Up and Down states.

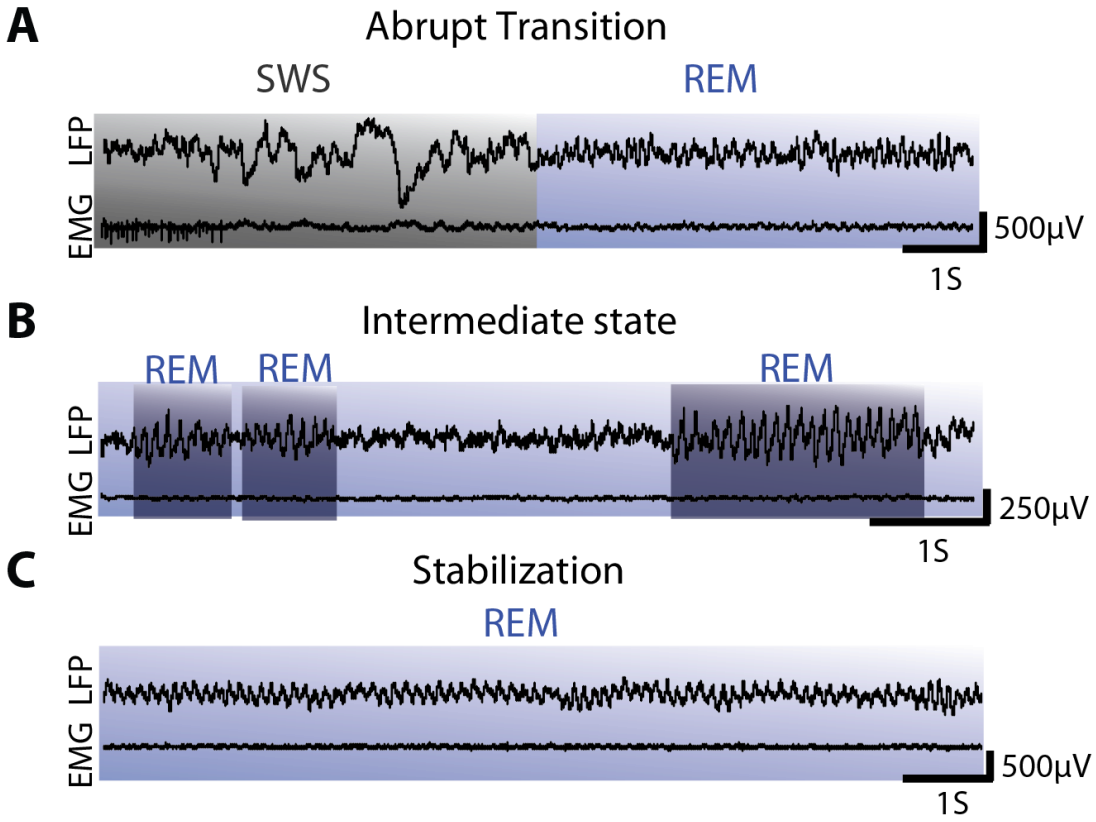

Figure 6. REM phases
Raw LFP signal (top) and EMG signal (bottom). **(A)** Abrupt transition from SWS **(B)** Intermediate state in the transition to the establishment of REM sleep. Spindles marked in in darker blue **(C)** Stabilization of the signal in a more synchronous pattern.

When the animal was in REM sleep, the signal exhibited a low amplitude and more synchronous pattern than in the awake state. REM sleep can only appear after a period of SWS, and the transition from SWS to REM could be sudden (Fig. 6A), but after a few seconds of initial REM activity, the so-called "intermediate state" appeared (Fig. 6B) (Gottesmann, 1973; Sánchez-López et al., 2018), where large-amplitude sleep spindles emerged in frontal cortices. After the transition, the signal stabilized in a regular REM pattern that remained until the end of the stage (Fig. 6C). Compared with the SWS, REM is relatively short in rats, not usually lasting more than 5 min continuously, could appear several times in the same uninterrupted period of sleep.

Power spectral density

We first extracted the power of the spectral content exhibited by each recorded cortical area in every stage. In order to reduce the overall computational cost, each signal, with an original sampling frequency of 10 kHz, was downsampled to a final sampling frequency of 500 Hz.

The power spectra were computed by means of a wavelet analysis using the Matlab's *Wavelet analysis toolbox* in periods of 60 s with a 1 s shift.

Synchronization: Phase Locking Value

To have an insight of the cortical network dynamics within the different stages of the sleep-wake cycle, we examined the interaction among the distinct cortical regions. For this, we computed the Phase Locking Value (PLV) for all the frequency bands, within the signals of all combinations of area pairs using again the Matlab's *Wavelet analysis toolbox* in periods of 60 s with a 1 s shift.

The PLV, is the absolute value of the mean phase difference between two signals expressed as a complex unit-length vector (Lachaux et al., 1999; Mormann et al., 2000). Applied to our case, each area is considered like an independent oscillator.

$$PLV_{i,j} = \frac{1}{T}\left|\sum_{t=1}^{T} e^{-i(\varphi i^{(t)} - \varphi j^{(t)})}\right|$$

In the above equation *i* and *j* represent the different areas to compare. PLV can take a value between 0 to 1, 0 being the case where no phase synchrony exists between both signals and 1 reflecting that both signals are fully phase-synchronized. This value is considered as a measure of trial-to-trial variability in the relative phases of two signals, providing an insight into the synchronization among the two specific compared areas (Aydore et al., 2012).

Sleep-wake stages offline classification

Considering our manual classification of the distinct stages as the ground truth, we applied a classificator based on a multi-class logistic regression (MLR) in order to evaluate the accuracy shown by distinct activity-related measurements from the dynamics of the cortical network to differentiate between the three stages of the cycle. This classification method provided the probability of the brain of being in one specific stage (awake, SWS or REM sleep) given this set of neuronal activity-related measurements considered as the independent variables. For this case we used 48 predictor variables, which were the PLV values across the 6 pairs of cortical areas (PrL-M1, S1-V1, M1-S1, M1-V1, PrL-S1 and PrL-V1) and 8 frequency bands (slow (0.1-1 Hz), delta (1-4 Hz), theta (4-7 Hz), alpha (8-12 Hz), beta (12-30 Hz), low gamma (30-60 Hz), medium gamma (60-150 Hz) and high gamma (150-300 Hz)).
MLR uses a linear combination of the predictors *f(k,i)* to quantify the aforementioned probabilities that, given observation *i* of the independent variables the brain is in state *k*.

$$f(k,i) = \beta_{0,k} + \beta_{1,k}x_{1,i} + \beta_{2,k}x_{2,i} + \beta_{3,k}x_{3,i}$$

This function *f* equates the log-odds of the probability *P(k|i)* of being in state k, that is $\log\left(\frac{P(k|i)}{1-P(k|i)}\right)$= *f(k,i)*. The β are known as the regression coefficients. We found a set of β coefficients that define the three boundaries (awake-SWS, awake-REM and SWS-REM) that separate the three stages by training the classifier with 80% of the manually classified states for each animal individually. The training set was balanced across stages by using the same number of samples of the awake and SWS as that of REM data, because REM occurs more sporadically. Then, the MLR was tested on the remaining 20% of the data. This process was cross-validated using an iterative procedure by means of a gradient-descent optimization algorithm that maximizes the likelihood. A z-score normalization of the β coefficients were performed for each animal individually.

We first used this classifier to obtain the PLV values that characterize the three stages in each pair of cortical areas. However, we also applied this classifier to find optimal ratios of power spectral density (PSD) and EMG that allowed an instant classification of the stages, to further develop an algorithm for the automatic online detection of the sleep-wake stages.

Statistics

When a comparison between multiple independent variables was required in the data analysis in order to examine the existence of an interaction, a three-way-ANOVA was applied. For the rest of comparisons, a Wilcoxon sign-rank test was used depending on the distribution of the data.

The data analysis to study the cortical dynamics in the different stages of the sleep-wake cycle were performed by Dr. Belén de Sancristóbal from our laboratory and the Universitat Pompeu Fabra, Spain.

3.2. Brain states and transitions in anesthetized states

3.2.1. Experimental procedure for electrophysiological recordings: Recording the cortical activity during the loss and recovery of consciousness with ketamine and medetomidine anesthesia

Subjects and surgery for the placement of the chronic implant

For these experiments 4 male Lister-Hooded rats (250-450 grs., 6-10 months old) were implanted and recorded, but one of the animals was excluded from the analysis due to the presence of epileptic activity. Therefore 3 animals with a total of 5 recording sessions of the induction and fade-out with the anesthetic mixture were included in the analysis. The same housing protocol previously described in (3.1.1) was followed until the day for chronic implant surgery. All experiments were carried out in accordance with Spanish regulatory laws (BOE-A-2013-1337), which comply with the European Union guidelines and were supervised and approved by the Animal Experimentation Ethics Committee of the Universitat de Barcelona (287/17 P3).

Both the electrodes and the surgical procedure for its chronic implantation was the same as in (3.1.1). As in previous experiments, not all the animals had the same implanted and recorded areas. The 3 analyzed animals had electrodes placed in PrL cortex (3.7 mm AP, 0.8 mm ML, -2.7 mm DV) and in V1 (7.3 mm AP, 2.2 mm ML, -0.6 mm DV) while two of the subjects had electrodes additionally in M1 (0.4 mm AP, 1 mm ML, and -1.2 mm DV) and S1 (-3.14 mm AP, 5 mm ML, -1.2 mm DV).

Anesthesia and recording protocol

These set of experiments consisted in the intraperitoneal administration of the anesthetic mixture of ketamine/medetomidine and the recording of the cortical activity from the injection (induction), during the slow oscillatory period of deep anesthesia until the complete fade-out of the anesthetic effect, where consciousness was recovered. The same materials, software and set-up from the experiments in the sleep-wake cycle were used to obtain the LFP recordings from the implanted animals (3.1.1). We first injected subcutaneously 0.6 ml. of saline solution (0.9%) for hydration followed by atropine (0.05 mg/kg) to prevent respiratory secretions throughout the anesthetized period. The rectal temperature was monitored and maintained at 37°C during the recording by means of a probe and an electric blanket. We administered three different doses of anesthesia: One considered as light (20 mg/kg of ketamine and 0.15 mg/kg of medetomidine), and other two doses considered as

deep (40 mg/kg of ketamine and 0.3 mg/kg of medetomidine and 60 mg/kg of ketamine and 0.5 mg/kg of medetomidine), keeping the ratio of 0.75% of medetomidine per unit of ketamine. We analyzed as deep two different doses because we considered that the dynamics of the activity were equivalent. In one animal we injected the light concentration on three different days and for the remaining two subjects, each one received just one type of dose from the deep concentration. Immediately after the anesthesia administration, the rat was placed in a plastic cage and connected to the headstage, recording the fast induction of anesthesia, until the loss of consciousness is achieved. The fade out from the anesthesia was considered complete, and the recovery of consciousness was assumed, based in the observations of voluntary displacement movements, reflected in the video and EMG and considered a reliable sign of wakefulness.

The data analysis was performed with the software MATLAB, Python (PSF) and Spike 2.

3.2.2. Experimental procedure for calcium imaging recordings: Recording the cortical neuronal activity during the loss and recovery of consciousness with isoflurane

This experimental part was performed in the context of an international short-term research stay in the Bathellier Laboratory (UNIC-CNRS, Paris, France). The implant and imaging recording were performed on C57Bl6J male and female mice between 8–16 weeks old. A total of 16 mice were injected and implanted with the surgical procedure, of which 6 subjects were suitable for imaging and 3 subjects met the criteria for the analysis. All procedures followed the European Union guidelines and were approved by the French Ethical Committee (authorization 00275.01).

Neural activity involves movements of calcium ions that can be recorded, allowing the tracking of specific neural populations. GCaMP6 is a genetically modified calcium indicator that can be injected in the brain through a virus and is expressed in specific neurons providing them with fluorescence (Chen et al., 2013). Changes in fluorescence from each neuron can be recorded through two-photon laser scanning microscopy.

At least 3 weeks before the calcium imaging recordings, we performed a surgery to inject the adeno-associated virus (AAV) expressing GCaMP6s (Vector Core, Philadelphia, PA) and implant a glass window as in Ceballo et al. (2019). For the surgery the animal was first anesthetized with a mixture of ketamine and medetomidine and placed in the stereotaxic apparatus. The condition of deep anesthesia was checked regularly by the absence of reflexes

before the incision. After exposing the skull, the masseter muscle was removed, and the jawbone peak was filed to have a clear access to A1. A craniotomy of approximately 5 mm was performed in A1 for the injection of the virus. We administered 150 nL of a 30-time dilution of the virus in 3 to 4 consecutive spots in the cortex. The craniotomy was covered with a glass window, and a metal post was placed above to restrain the animal during the image recording. The implant was sealed with cyanolite glue and dental adhesive (Superbond C&B, Sun Medical co. Japan).

A few days before imaging, the animals were daily habituated to the head-post and rewarded with jelly, so that they could be still in the moment of the head-fixed awake recording.

After checking with ultraviolet light that the GCaMP6s was expressed, we started the imaging recording with a two-photon laser microscope (Femtonics, Budapest, Hungary) equipped with an 8 kHz resonant scanner combined with a pulsed laser (MaiTai-DS, SpectraPhysics, Santa Clara, CA) tuned at 900 nm. Images were acquired at 31.5 Hz in blocks of 5 min for each recording.

After a first baseline recording in wakefulness, we delivered the isoflurane at a concentration of 1.6% recording the transition into the anesthetized state. After some recordings at 1.6% of isoflurane, the anesthetic was switched off at the beginning of the last recording, capturing the fade-out and the recovery of consciousness. We were able to record simultaneously among 150-250 cells for each animal in 1x1 mm fields of view.

The calcium imaging recordings were performed with the supervision of Dr. Anton Filipchuck (CNRS).

3.2.3. Electrophysiological data analysis

Classification of stages and activity patterns at different anesthesia levels

Manual classification of anesthesia functional stages and activity patterns of the induction

It was observed that subsequent to the injection of the anesthetic mixture, the cortical activity of the animal underwent across a sequence of distinguishable changes between patterns of activity within a relatively short period of time, which typically ranged from 5 to 10 min. This period from the anesthetic injection until the establishment of a regular slow oscillatory activity was defined as the anesthetic induction stage. Then, the signal from this anesthetic

induction period was manually classified into the two main observed activity patterns: awake-like and slow oscillation. The criteria for this division was based in the visually observable changes from the raw signal, such as the amplitude, frequency and length of the oscillatory activity.

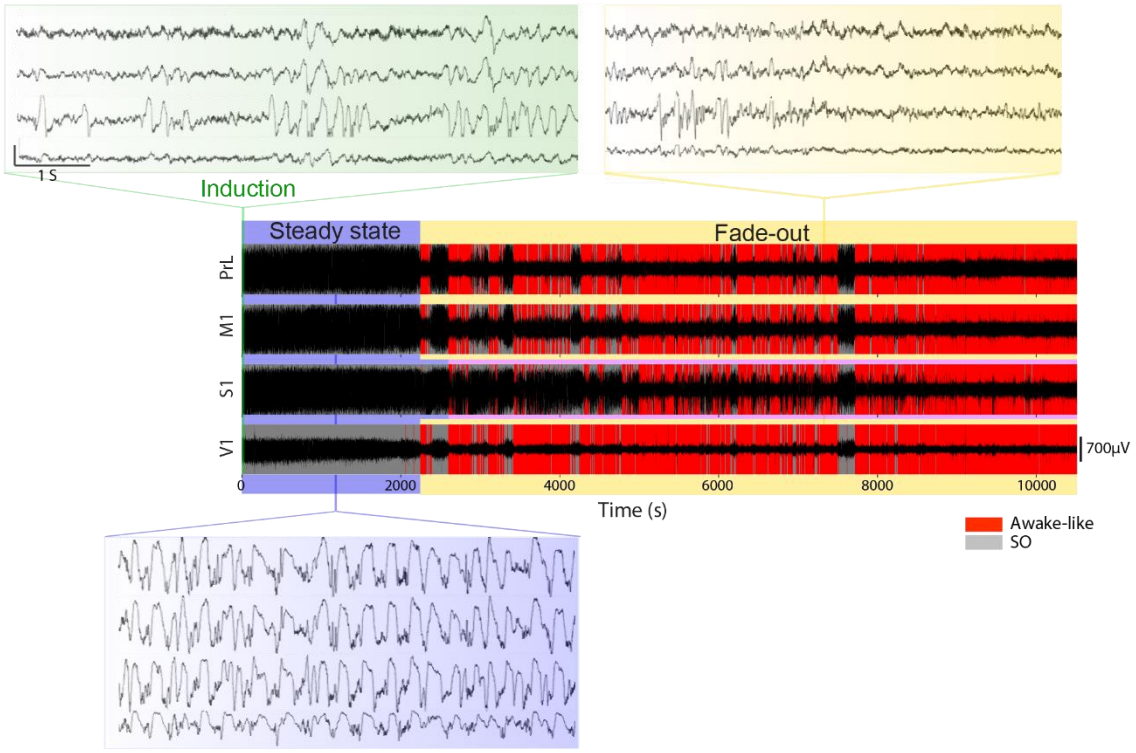

Figure 7. Illustration of the pattern of activity detection and functional stages division
Color-coded labeling of the two patterns of activity (awake-like and SO= slow oscillation) and each functional stage (Induction, steady stage and fade-out) on the raw recording of a subject's experimental session. Colored panels show examples of representative activity during each stage in all the cortical recorded areas.

Through several experiments we noticed recurrence in the pattern of temporal appearance of the two types of activity not only restricted to the induction period. Since there is not a solid definition for a division into functional stages in a general state of anesthesia, we classified those periods manually also based in observables changes in activity dynamics. The manual division performed resulted in three functional stages that contained the two main patterns of activity: induction, steady stage and fade-out.

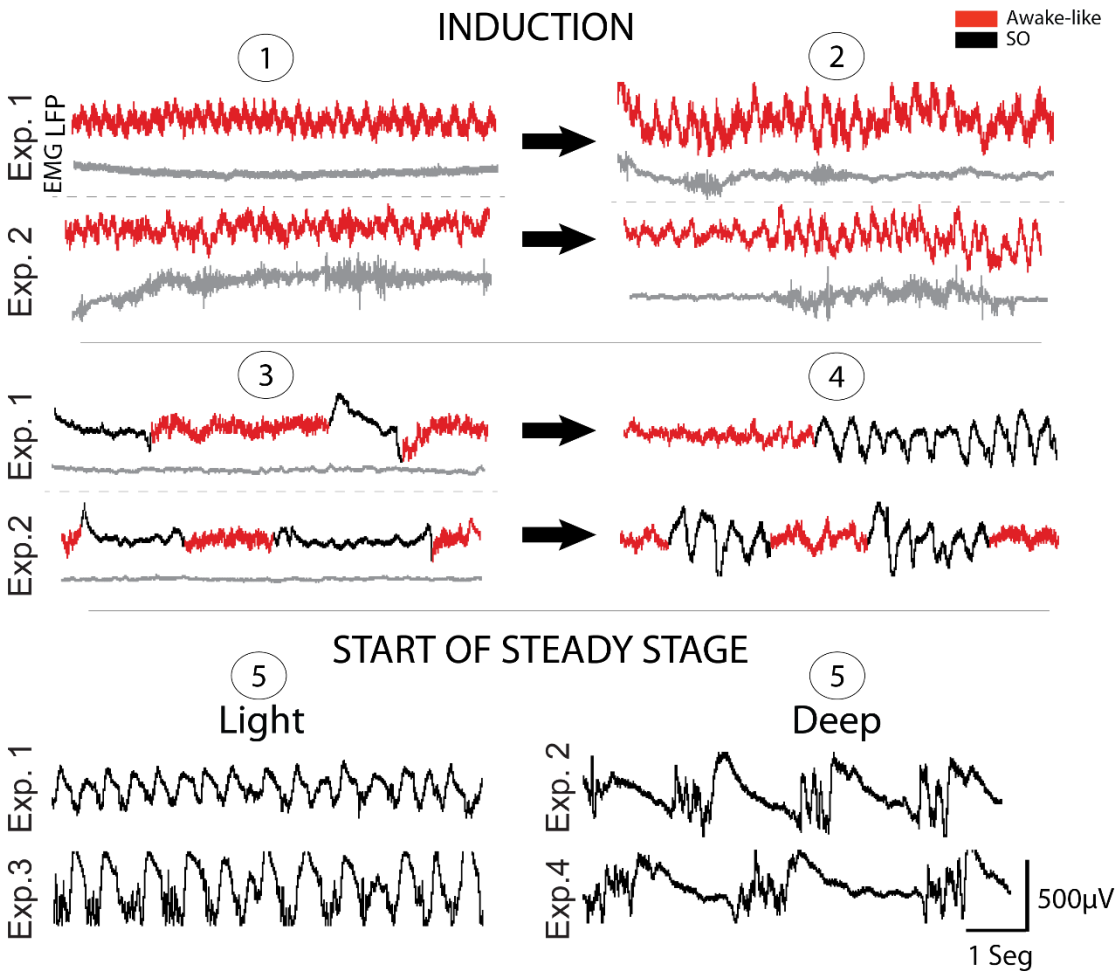

Figure 8. Examples of representative activity during the anesthetic induction
Raw LFP and EMG signal (grey trace) showing, respectively, characteristic features of the signal and muscular tonicity in different subjects. Numbers depict the temporal appearance of each type of activity.

When the slow oscillatory activity lasted more than 10 min uninterruptedly, this period was defined as the steady stage, regardless of whether the oscillation regime was derived from a deep or light depth of anesthetic dose (Fig. 8-5). The steady stage could last among 30 to 75 min and was considered finalized once appeared the first awake-like period of activity. The completion of this stage implied the start of the fade-out stage; a transitional period marked by the emergence of awake-like periods of activity within the slow oscillation as a result of the anesthetic effect fading-out. This fluctuation in the appearance of types of activity patterns was also observed during the induction and previously described during the emergence of anesthesia by Tort-Colet et al. (2019). This fade-out lasted from 4 to 5 hours until wakefulness was reached.

Considering these observations, we aimed to explore if the cortical dynamics identified in the activity during the short lapse of the induction was representative of those dynamics that emerged when the anesthesia was fading-out.

Supervised classification of the activity patterns from the fade-out

From the manually classified awake-like and slow oscillatory activity patterns from the induction considered as the ground truth (GT), an MLR classifier was applied to build a logistic regression model. The predictors of the model were based in the spectral content of the awake-like and slow oscillatory activity patterns from each of the predefined frequency bands. By computing the same spectral features for the remaining unclassified signal of the fade-out, the model was able to classify these data into awake-like or slow oscillatory activity with a given probability. Therefore, this model was a powerful tool for comparing the dynamics from the distinct stages following a unified classification criterion among stages.

In order to reduce the overall computational cost, raw signals were downsampled from 10 kHz to 1kHz. Then, the PSD from the fade-out signal for each activity pattern and channel was computed in non-overlapping 2 s time windows by applying Welch's method with a Hanning window of equal length (Welch, 1967).

The MLR classificator to use with these spectral features followed the same principles as in (3.1.3). MLR provides the predicted class (awake-like or slow oscillation) and the probability of a sample of being correctly classified. In this case, 8 frequency bands were the predictors to build the model (slow (0.1-1 Hz), delta (1-4 Hz), theta (4-7 Hz), alpha (8-12 Hz), beta (12-30 Hz), low gamma (30-60 Hz), medium gamma (60-150 Hz) and high gamma (150-300 Hz)).

The predictor variables incorporated into the model were defined as the average power spectra in the time window, in dB units within the 8 described frequency band ranges. With these predictors and the output (GT), an MLR classifier was applied to the GT data in order to build a model to classify the unlabeled data from the fade-out among the two defined activity patterns (slow oscillation and awake-like). Python's *scikit-learn* package was used to design a pipeline, first, z-score normalizing the predictor variables and then applying the classifier. In order to test the accuracy of the model, a K-Fold Cross Validation (K-Fold CV) (k = 5) was performed. K-Fold CV splitted the data in k folds, and among all folds, one was selected as the test set and the remaining folds as the training set. All training sets were balanced by using the same proportion of samples for each activity pattern. The training set built the model and the test set was used for testing it, obtaining the model's accuracy. In this case the accuracy was defined as a confusion matrix. The confusion matrix allowed us to

know the percentage of points that belonged to a specific class and have really been classified as that class (percentage of Predicted value vs True value). If the accuracy level was high (more than 80%), the fitted model was applied to predict the unlabeled data from the fade-out. The predictions for all recorded areas were obtained and further analysis of cortical dynamics were then performed.

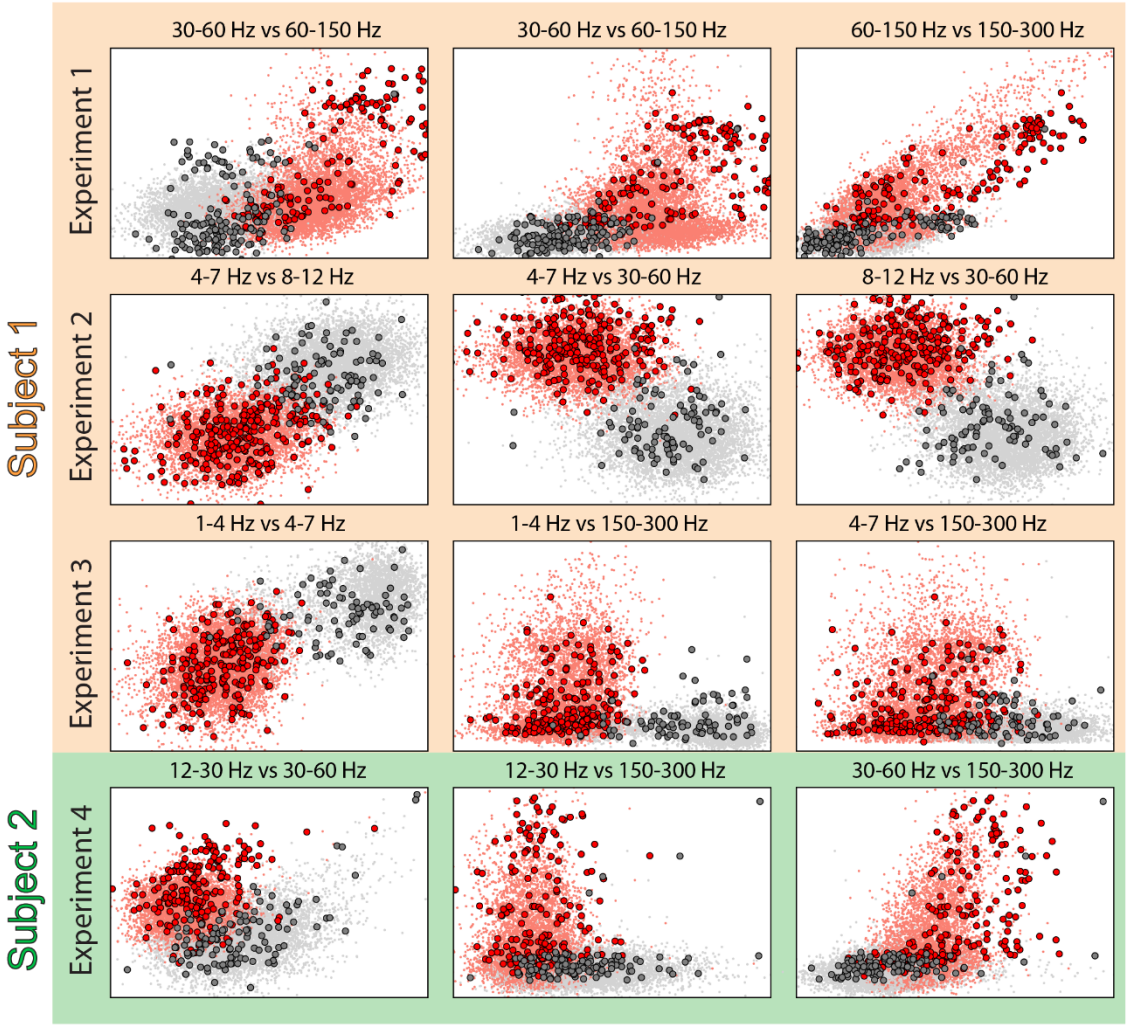

Figure 9. Spatial representation of the frequency ratios that best classify among activity patterns
The estimation of the most effective frequencies separating activity patterns was obtained from the 3 highest absolute β regression coefficients for each model (experimental session). Here, 4 experimental sessions from 2 different subjects are illustrated. Each point is represented in the frequency pairs space together with its label classification. Solid dots correspond to data from the induction (ground truth data used to build the model) and the transparent background dots to the labelled data from the fade-out. The convergence in spatial clustering can be observed.

Synchronization: Phase Locking Value

To further explore the cortical dynamics among stages of the anesthetized state, the synchronization was estimated by computing the PLV for all the aforementioned frequency

bands. The same equation as in (3.1.3) was applied. For this data, signals were first band-pass filtered and the phase of the analytic part of the signal was obtained using the Hilbert transform *(scipy.signal.hilbert)* and angle function from *numpy package*. Then, the PLV was obtained in time windows of 2 s for every pair of channels and each frequency band.

Statistics

In order to explore the relevance of the variables (activity pattern, frequency band and cortical area) used to classify stages of an anesthetized state, we build a linear regression model for each experimental session:

$$Z_{log(PSD)} = \beta_0 + \beta_1 \cdot Frequency + \beta_2 \cdot Area_{PrL} + \beta_3 \cdot Area_{M1} + \beta_4 \cdot Area_{S1} + \beta_5 \cdot Activity\ pattern$$

β being the predictor coefficients. With this model, we could input values for the independent variables obtaining a value for the outcome variable, in this case a prediction for the PSD values. Applying a linear regression model to the data is equivalent to performing an ANOVA, but it allows us to input continuous independent variables and not just to be restricted using categorical variables as in ANOVA. The obtained estimates for each predictor coefficient in conjunction with their confidence intervals indicated if a predictor can reliably predict the outcome variable (being statistically significant). The predictor is considered statistically significant when the range: predictor estimated value ± SE · 2 does not contain 0.

3.2.4. Calcium imaging data analysis

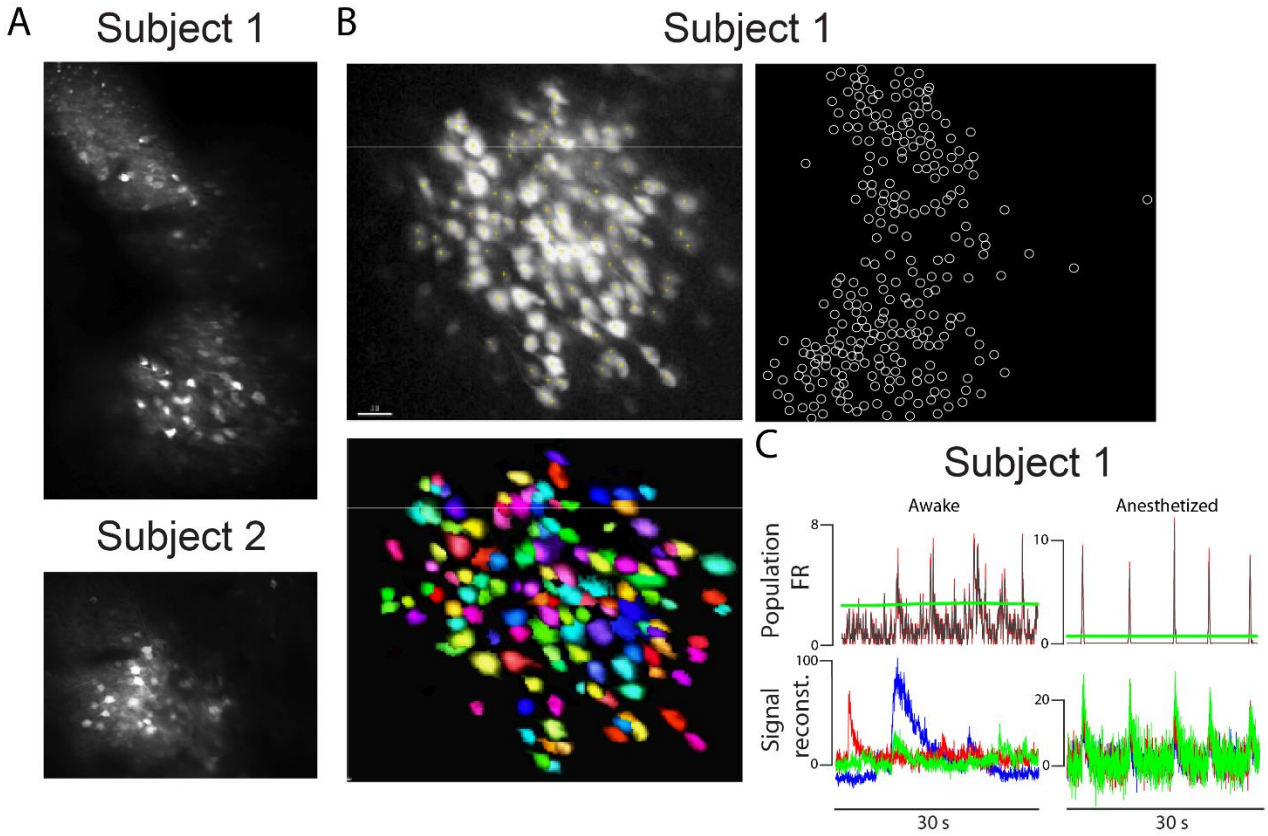

Figure 10. Examples of calcium imaging recording and data preprocessing
(A) Example of the cortical field in a frame from the recording in 2 different subjects. It can be observed the neurons expressing GCaMP6 and brighter, the ones firing in that moment. (B) Identification of the ROIs. (Top, left) Zoom to the image showing the STD of the activity from the whole experiment (Bottom, left) Selected ROIs by the clustering algorithm from the image above (Top, right) All identified ROIs from the recorded cortical field (C) Raw calcium traces from the MLSspike algorithm (Deneux et al, 2016) (bottom) and population firing rate (top) from awake (left) and anesthetized (right) recordings.

First, the data was preprocessed in order to correct motion artifacts, subtract the neuropil contamination and select the single neurons as Regions Of Interest (ROI). The ROI detection was made with a semi-automated hierarchical clustering algorithm based on pixel covariance over time developed by Deneux et al. (2010). The signal within the selected ROI was extracted to reconstruct time series based in the change in fluorescence (ΔF/F0). The identification of the spikes was estimated from the raw calcium traces using *MLSspike* algorithm (Deneux et al., 2016).

Detection and quantification of Up and Down states during wakefulness and anesthesia

In these CI recordings during wakefulness we observed synchronous events very similar to the Up states that we detected during anesthesia. In order to compare the resemblance among both synchronous events from distinct brain states, we first singled out these periods of activity from the awake recordings by means of a detection algorithm. Up and Down states were assumed as the two conditions to detect, defined by the population firing rate (FR). The FR was calculated using a sliding window approach as the number of spikes generated by the recorded neurons in a time window of 70 frames shifted by 50 frames. A Gaussian mixture model was fitted to the FR time series in order to estimate the two states (Up and Down states). We fitted both a single Gaussian model and a model composed by two Gaussians and selected the one fitting best our held data. We split the data using a K-Fold CV with k=6, estimated models parameters on the training set and evaluated the BIC score on the test set. The selected model was the one with lower BIC value. In the following we use DeltaBIC = BIC_1 – BIC_2, where BIC_x is the average BIC score for the model with x components. Values of |DeltaBIC| larger than 10 are usually considered as highly supportive.

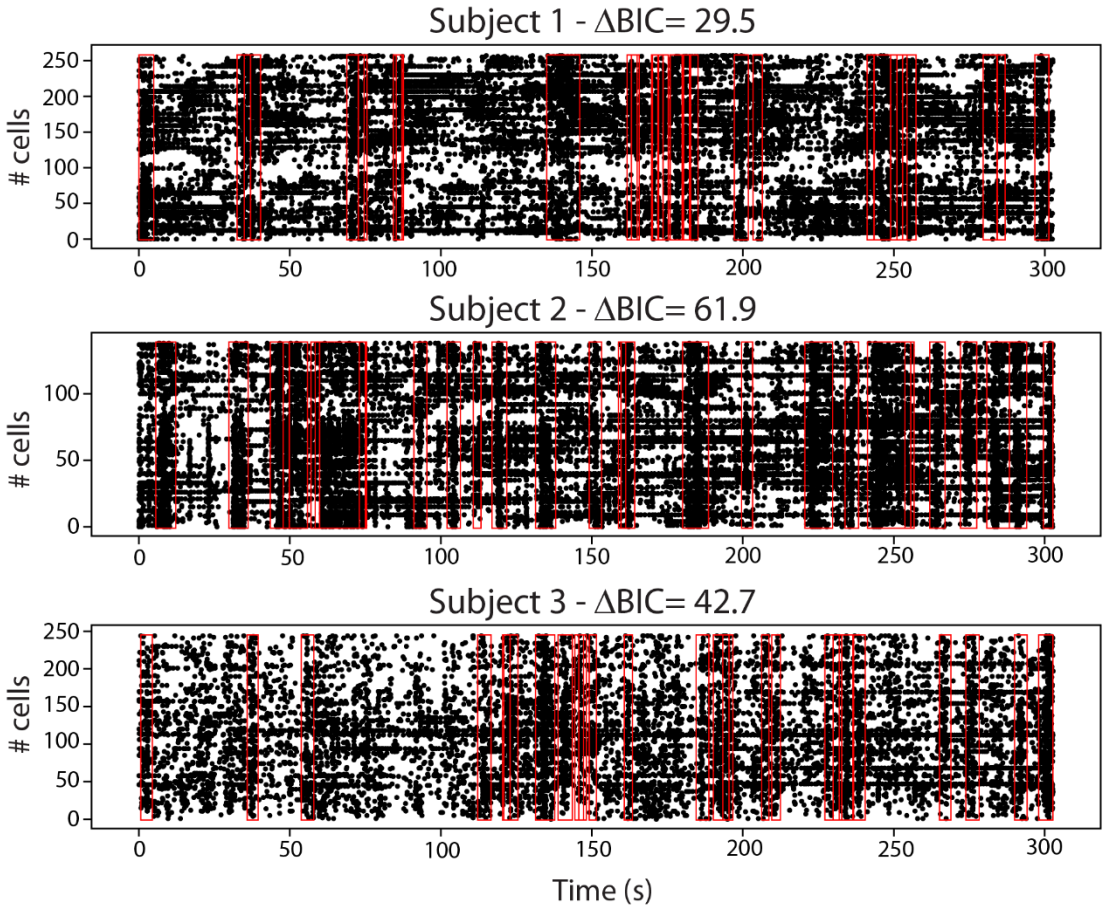

Figure 11. Up detection on the neural population activity

Red lines mark the events selected as Up states in the raster plot. Each dot corresponds to a spike onset.

The threshold for the detection of a two-component model (Fig. 11) was fixed at $\mu_{c0} + 2\sigma_{c0}$,where σ_{c0} is the standard deviation of the component with the smallest mean.

From the detected Up and Down states in all the recordings from the 3 subjects, we estimated the FR (from the number of spikes produced by each neuron), the Up and Down state duration and the size of the Up state as the number of neurons that fire in each UP state.

Statistics

In order to explore the association among the FR and Up states size parameters, we estimated a linear model as: $x_{FU}^{s} = w_0^s + w_1 x_{SU}^{s} + \eta^s$ where x_{FU} and x_{SU} were the firing rate and size of UP events respectively and superscript s $\in$ indicated the brain state (awake or anesthetized).

The data analysis to study the cortical dynamics in the loss and recovery of consciousness in anesthesia with electrophysiology were performed by Arnau Manasanch Berengué and with calcium imaging by Dr. Andrea Insabato from our laboratory while part of the data preprocessing was performed by Dr. Anton Filipchuck (CNRS).

3.3. Thalamic stimulation during an anesthetized state

3.3.1. Experimental procedure: Electrical stimulation of the parafascicular nucleus and recording the cortical activity in anesthetized rats

Subjects

For these experiments 20 Lister-Hooded and Wistar male rats (250-450 grs., 6-10 months old) were stimulated and recorded. In 8 of them we successfully targeted the parafascicular nucleus and achieved the anatomical inclusion criteria for further analysis. The same protocol for care and housing than in previous described experiments was followed (3.1.1). All the procedures with animals were carried out in accordance with Spanish regulatory laws (BOE-A-2013-1337), which comply with the European Union guidelines on protection of vertebrates used for experimentation (2010/63/EU). All experiments were supervised and approved by the Animal Experimentation Ethics Committee of the Universitat de Barcelona (286/17 P2).

Surgery for the recording "in vivo"

In order to obtain the LFP recordings with the animal anesthetized with isoflurane, we first performed surgery to introduce the electrodes in the target areas. We followed the same procedure as in (3.1.1). For these experiments, 3 craniotomies were opened in one of the hemispheres. These were placed in: the PrL (3.7 mm AP, 0.8 mm ML, and -2.7 mm DV), the PF nucleus (-4.3 mm AP , 1.2 mm ML and -5.3 mm DV) and in V1 (-7.3 mm AP ,2.2 mm ML and -1.5 mm DV) (Paxinos and Watson, 2005). Then, we inserted single sharpened tungsten electrodes of < 1 MΩ impedance and a tip diameter of 2-3µm (WPI, Sarasota, FL) in PrL and V1. For the electrical stimulation of the PF nucleus, we inserted a bipolar tungsten electrode of the same characteristics but with a tip separation of 500 µm. Then, the experimental protocol was performed.

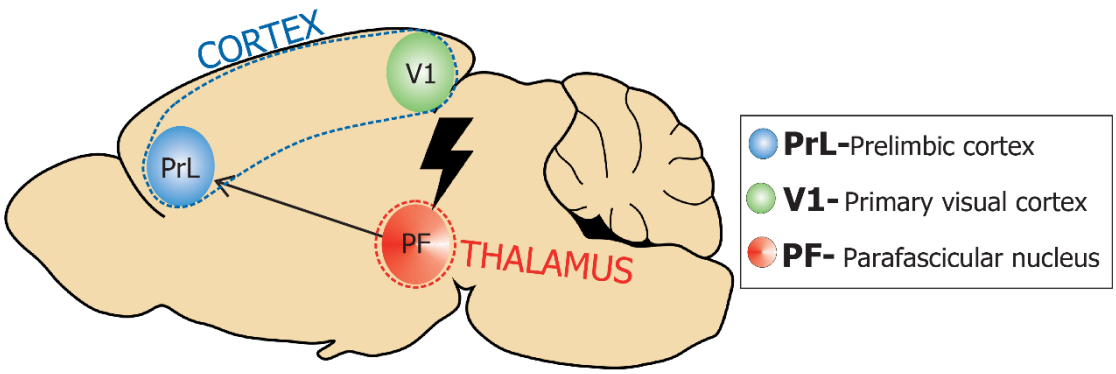

Figure 12. Recorded and stimulated areas
Illustration of the location and anatomical connection (black arrow) of the recorded areas and the stimulated nucleus (black ray) in the experiments in vivo.

After the experiments were completed, with the animal deeply anesthetized we administered an overdose of intraperitoneal sodium pentobarbital to perform a transcardiac perfusion. The brain was removed for anatomical reconstruction of the electrode placement by histology and magnetic resonance.

Recording and stimulation protocol

In this experimental protocol, the animal was anesthetized with isoflurane and then, stimulated and recorded *in vivo*. The recording was made in 2 distinct cortical areas; PrL and V1. The PrL cortex in rodents is the analogous area of the prefrontal cortex in primates (Bedwell et al., 2014; 2017) and is likewise innervated by the PF nucleus as previously described (1.4.3). On the contrary, V1 is not directly connected with the PF nucleus and is distant from the PrL area, thus it was recorded as a control area.

After a minimum of 30 min of baseline recording, the electrical stimulation was delivered by means of a A-360 stimulus isolation unit (WPI Sarasota, FL) during 120 s at 60 µA of intensity. The entire protocol consisted in square pulse trains with a train frequency of 50 Hz and train duration of 500 ms. Each train was composed of 25 pulses of 0.5 ms. duration each and 20 ms. of interval inter-pulses. The selection of the stimulation parameters was based on those reported to elicit behavioral arousal effects and cognitive improvements (Moruzzi and Magoun, 1949; Cohadon and Richer, 1993; Tsubokawa et al., 1990; Vale-Martínez et al., 1999; Guillazo-Blanch et al., 1999; Sos-Hinojosa, et al., 2003; Lin et al., 2007; Andero et al., 2007; Yamamoto et al., 2010; Cervera-Ferri et al., 2016; Redinbaugh et al., 2020). A post-stimulation recording was made for a minimum of 30 min to track long-lasting post-stimulation effects.

For the acquisition and analysis of the recordings we used the same sampling frequency, equipment and software as in previous experiments (3.1).

3.3.2. Data analysis

The data from the 30 min before and after the electrical stimulation of the PF nucleus were analyzed in order to obtain a quantification of the changes in the activity in its target (PrL) and control area (V1). As mentioned before, those areas are not equally connected with the PF and they differ in function, therefore distinct responses were expected. To assess these changes, we estimated and compared spectral dynamics, synchronization and several parameters from the slow oscillation after and before the PF stimulation.
The spectral components of the recorded signals were obtained by means of a PSD analysis (3.1.3) using the built-in Matlab's function *pwelch* with a Hanning sliding window of 1 s length with a 0.5 s overlap. In addition, wavelet-based spectrograms were also computed to obtain the spectral representation in the time domain. We measured phase synchronization between areas by computing the PLV for each of the specific frequency bands using the same procedure and parameters as in (3.1.3). Regarding the parameters from the slow oscillation, we computed the FR for the entire signal and for the Up states, the duration of both Up and Down states and the variance coefficient of the slow oscillation (CV). The CV gives a measure of the variability for all detected events from the slow oscillation.

Parameters of the slow oscillatory activity

Firing rate

The FR is defined as the number of spikes generated by a set of neurons firing in a finite period. Power changes in the Fourier components at high frequencies of the LFP provides an estimation of the population FR (Mattia and Del Giudice, 2002). The power change in the Fourier components were estimated at high frequencies (>200 Hz) giving as a result the multi-unit activity of the signal

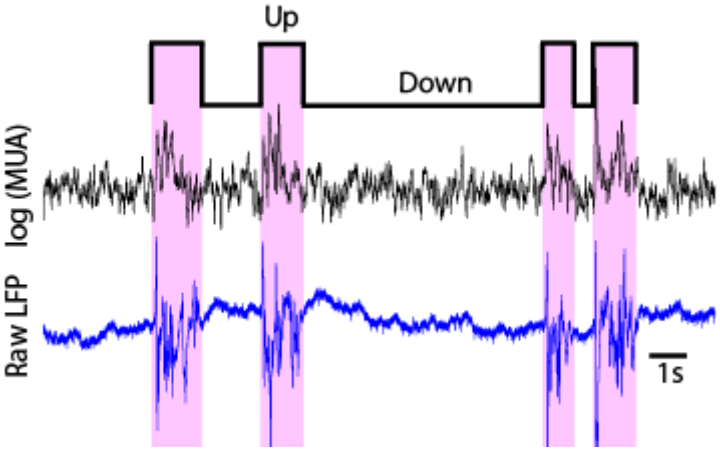

Figure 13. Up and Down state detection
Black line on top shows the Up and Down state selection and the pink rectangle indicates the Up state singled out in the raw extracellular signal (LFP) (blue trace) and the multi-unit activity expressed in logarithmic scale (log MUA) (middle black trace). The Up state is detected from the log MUA, after establishing a threshold, a minimum and maximum duration of the Up states all based in the average level of activity obtained from the log MUA.

(MUA). MUA was logarithmically scaled resulting in the relative measure of the FR (Reig et al., 2010).

Up and Down state duration

To estimate the duration of the Up and Down states, first a minimum threshold for both the amplitude and length of Up and Down states was established to single out both periods. Under these premises, an Up state was defined as the period where the log (MUA) was over the amplitude threshold and fitted within the minimum duration criteria. Segments which did not reach the conditions were considered as Down states. These algorithms have been validated in several published studies (Ruiz-Mejias et al., 2016; D'Andola et al., 2018).

Coefficient of variation of the slow oscillation

In order to have an estimation of changes in the regularity of the cortical activity after the stimulation, we computed the frequency of the slow oscillatory as the inverse of the duration of an Up to Down cycle. Based on this measure, the coefficient of variation of the slow oscillation was obtained by defining it as the ratio between the standard deviation and the mean of the slow oscillatory frequencies from Up-to-Down transitions found for all the analyzed signal.

Statistics

To compare the changes produced in the selected broad time-scale (30 min) after the PF stimulation on the Up and Down state duration, in the firing rate from Up states and in the variation of the slow oscillation, we applied the nonparametric Wilcoxon signed-rank test for dependent samples ($p \leq 0.05$). All the significant p-values are described in the results and all mean values are represented graphically in the results.

The data analysis to study the modulation of cortical activity by thalamic electrical deep brain stimulation was performed by Arnau Manasanch Berengué from our laboratory.

3.3.3. Anatomical reconstruction

After the experiment was concluded, we made an electrolytic lesion to mark the tissue to visualize placement of the electrodes in the PF nucleus. Thereafter the transcardiac perfusion and the brain removal, the brain was fixed in paraformaldehyde (4%). First, a magnetic resonance of the positions of interest was made. If the electrode placement was unclear, the brain was sliced for Cresyl violet staining. Then 80 μm thick slices were cut with a microtome

(HM 450, Thermo Scientific) and placed on gelatin-coated glass slides. After drying overnight, slices were dehydrated with ascending alcohol series followed by an incubation on xylol and a decreasing alcohol series. Then the slices were immersed in the stain for a few seconds and dehydrated again. Finally, slices were mounted in DePeX medium. Images were visualized and captured with a microscope.

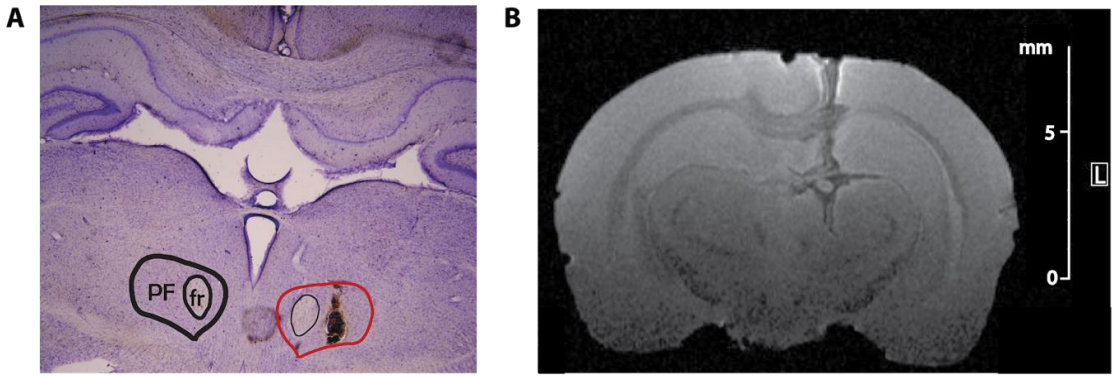

Figure 14. Anatomical reconstruction of the trajectory of the stimulation electrodes in the PF nucleus
(A) Central part of a slice with Cresyl violet staining. Marked in black the localization of the right PF nucleus and the fasciculus retroflexus, structure that guided the identification of the PF nucleus. Marked in red is the stimulated PF nucleus from the left hemisphere with the electrolytic lesion caused after the stimulation. **(B)** Magnetic resonance image from the brain slice with the trajectory of the bipolar stimulation electrode to the PF nucleus.

Chapter 4

Results

4.1. Brain states and transitions in the physiological sleep-wake cycle

4.1.1. Cortical synchronization can discriminate between the distinct stages of the sleep-wake cycle

The results reported in this chapter of the Thesis show cortical networks emergent properties within the distinct sleep-wake stages. Synchronization in particular, seems to have an important role in the dynamics of cognition and behavior across the sleep-wake cycle (Cantero and Atienza, 2005). Considering these premises, we tested the ability of the phenomenon of synchronization between cortical areas and the presence of specific frequency ratios to distinguish among stages and the possible functional implications.

Following the main descriptions in literature that are based primarily in the spectral profile of the different stages as a critical property to its classification (1.2.2), we first estimated the PSD of our manually classified LFP signals.
The spectral values among cortical areas were very similar (Fig. 15A); however, between stages and frequency bands they seemed to vary. A three-way-ANOVA corroborated a significant interaction only between stage and frequency band (Fig. 15B, p=9.7·10-20). We performed a Tukey post-hoc analysis to further examine those interactions and we observed significant changes within the delta, theta and high gamma band. Power in delta was higher in SWS compared with awake (p=0.001) and REM (p=0.000002), while in theta was higher just in

SWS compared to awake (p=0.002). In high gamma there is a broader difference in power between some stages, being significantly higher in awake with respect to SWS (p=0.16x10^{-5}) and REM (p=0.39x10^{-5}), but not finding significant differences within sleep stages. Both the prevalence of delta and theta in SWS and of gamma during wakefulness is in agreement with that described by several previous studies (Sinha et al., 1972; Feinberg and March, 1988; Merica et al., 1991; 1992; Maloney et al., 1997; Gross and Gotman, 1999; Steriade and McCarley, 2005; McCormick et al., 2015), validating our manual classification of the three stages of the cycle.

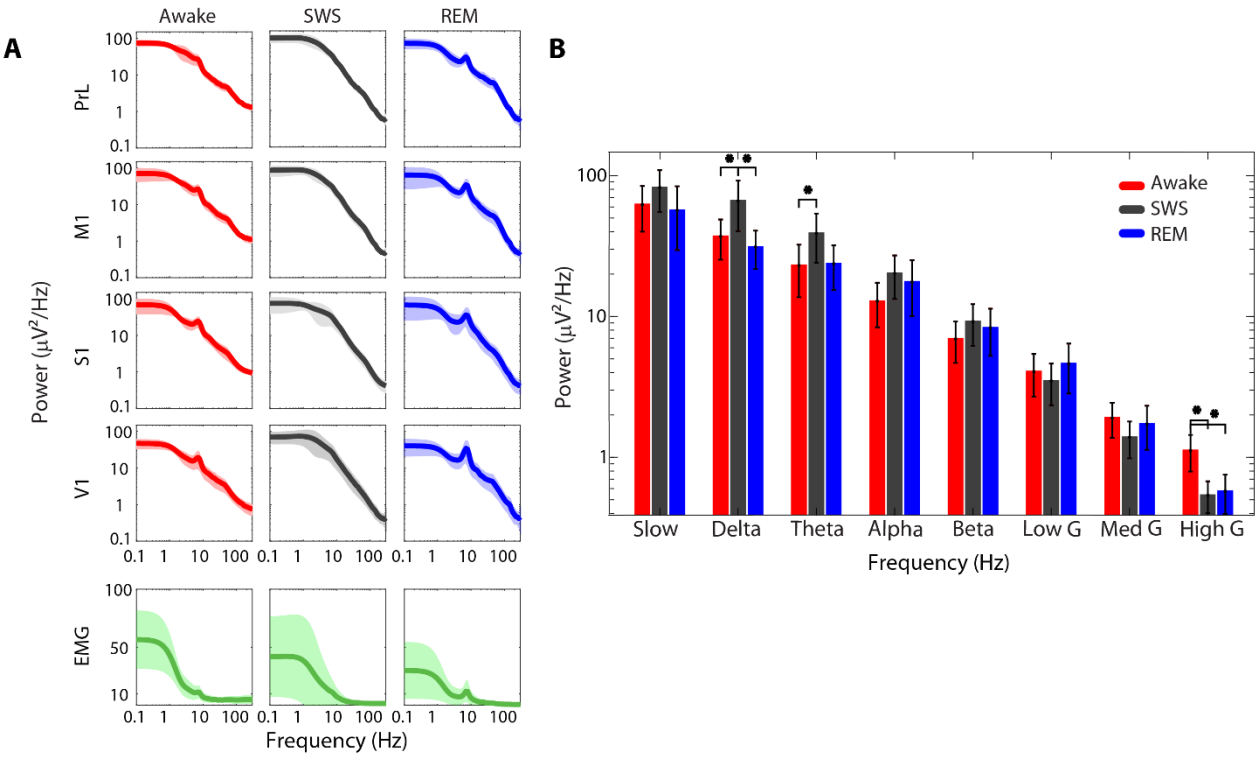

Figure 15. Spectral content in the distinct stages of the sleep-wake cycle
(A) Mean of the population data showing the power spectral density in each cortical area and EMG signal per stage. For cortical areas, the *y*-axis of power is presented in logarithmic scale. **(B)** Mean of the population data comparing the power spectral density from all cortical areas in each stage of the sleep-wake cycle grouped by frequency bands. The *y*-axis axis of power is presented in logarithmic scale. Error bars depict the SE *(p≤0.05).

The examination of the interaction among cortical regions revealed differences in the PLV values across stages, frequencies and area pairs, in contrast with the local power. We observed an overall decrease in the population level of synchrony as the distance among areas increased, finding the lowest values for the furthest areas. However, the distance also seemed to affect the PLV specifically depending on the frequency. A representative example is illustrated in the Fig. 16, for the closest (PrL-M1) and the furthest (PrL-V1) pair of recorded areas in specific frequencies of the theta (6.38 Hz) and high gamma (163.3 Hz) bands. We could observe the remarkable changes of PLV among stages over time and the difference in

magnitude in the PLV values for PrL-V1 between theta and gamma bands. PLV values during wakefulness were constantly higher than during SWS in both theta and gamma frequencies. Although surprisingly, the PLV values for REM sleep in theta were equal and even higher than the exhibited during wakefulness. In the populational data we observed that both theta and alpha bands had these highest PLV values for the stages with a high frequency pattern of activity: Awake and REM, while for the high gamma band this high coupling was observed exclusively in the awake stage.

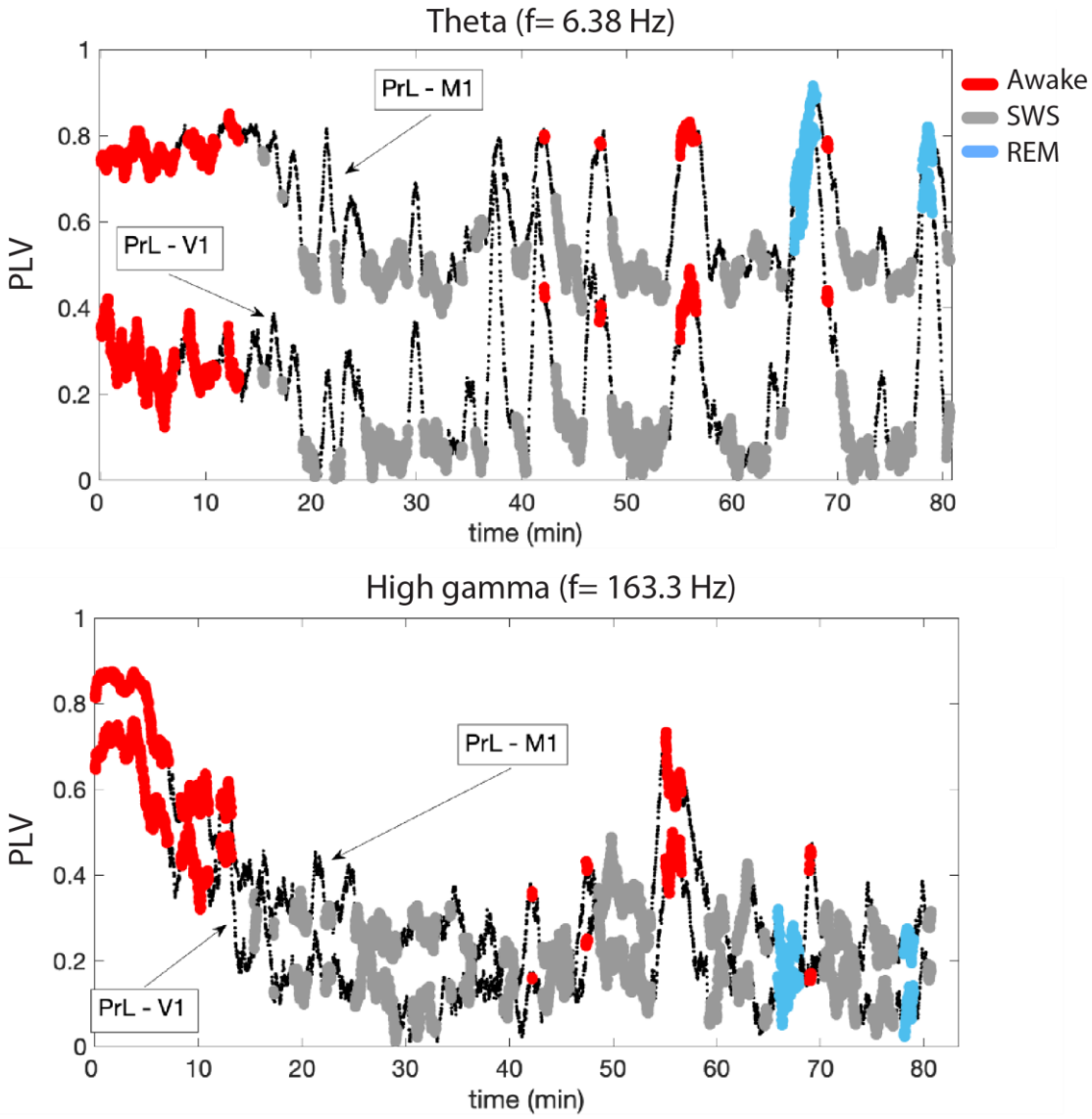

Figure 16. PLV time traces for two pairs of cortical areas (PrL-M1 and PrL-V1) in specific frequencies of the theta (6.38 Hz) and gamma (163.3 Hz) bands

Representative example of a natural transition from wakefulness to sleep in one subject. Each pair of areas is marked by the arrows. Black dots correspond to unclassified periods.

This effect was not observed in the rest of the analyzed frequency bands. Nevertheless, at nearby frequencies like delta or medium gamma (Fig. 17), the gradual onset of this increase in synchronization emerging from anterior regions could be distinguished. These results suggest that the level of cortical synchrony in specific frequency ranges could constitute a hallmark that contributes to the differentiation between stages.

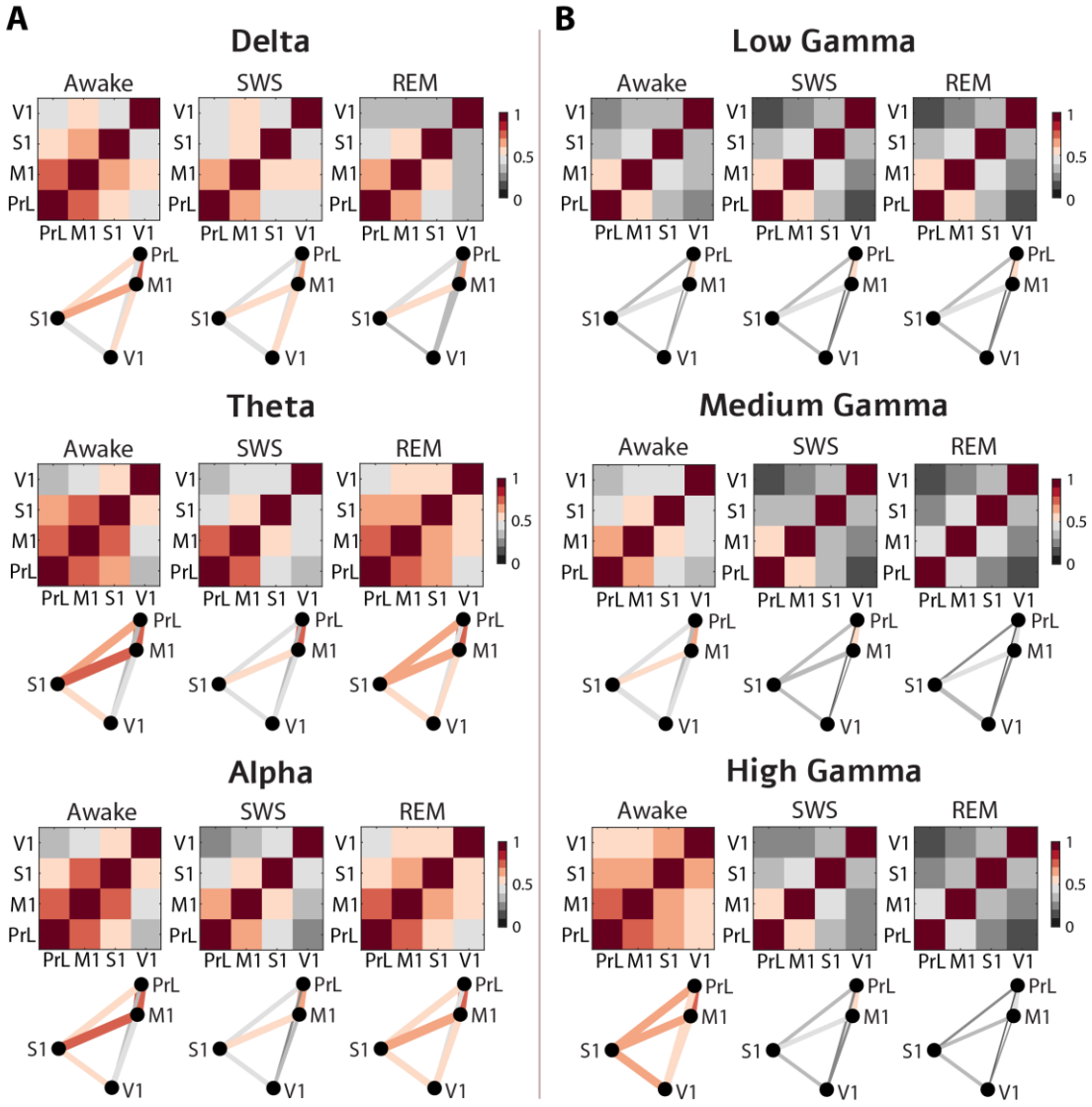

Figure 17. Synchrony among cortical areas in the distinct stages of the sleep-wake cycle
(Top) Matrices of the average PLVs. (Bottom) Spatial representation of the localization of the electrodes (black dots) and the level of synchronization between the areas (line thickness and color code). **(A)** Values for the delta, theta and alpha bands. **(B)** Values for the low, medium and high gamma bands.

Considering the salient values found in the PLV for several features, we tested if the PLV could be robust enough to classify the three different stages of the cycle. Then, we used the MLR to compute the accuracy, defined as the ratio between the correctly classified stages by just using the PLV index and the total number of manually classified stages. When the classifier was unable to distinguish between the three states, it randomly assigned PLV values

to each state. Therefore, the accuracy was equal to ⅓. If the accuracy was above ⅓ but below ⅔ it meant that the classifier was able to discern one of the states from the other two. An accuracy above ⅔, indicated that enough PLV values were unique to each state.

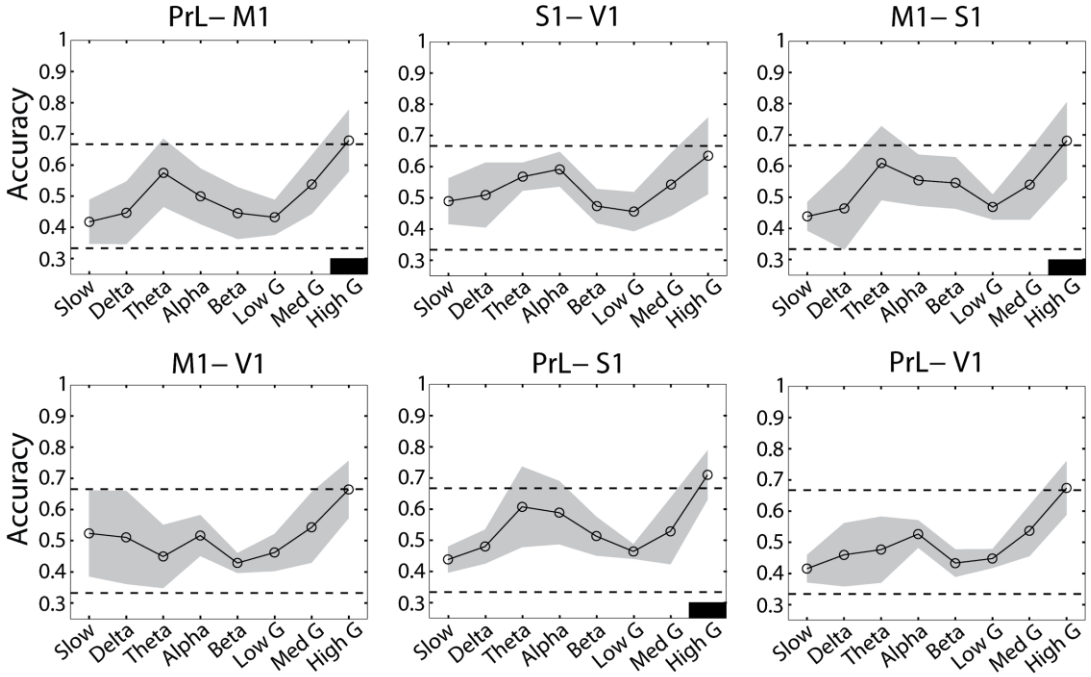

Figure 18. Accuracy exhibited by the PLV in the differentiation between the three stages of the sleep-wake cycle in each frequency band and pair of cortical areas

Population data, showing on a scale the potential for distinction between stages. A value above ⅓, indicates the distinguishability of one stage from the rest, while above ⅔ among the three stages. Both thresholds are marked by dotted lines, and the black solid lines mark the frequency range where the distinction among the three states is statistically significant ($p \leq 0.05$).

These results indicated that, in general, the index of cortical phase synchronization in high gamma has the potential to distinguish between the three stages of the sleep-wake cycle (Fig. 18). Nevertheless, the highest level of accuracy in the differentiation was exhibited by the synchronization among any pair of cortical areas that did not contain V1, where the distinction between the three stages was statistically significant in high gamma ($p < 0.05$).
In order to distinguish which specific stages contributed more to high accuracy values, we also computed the ratio of each correctly classified stage and the total number of manually classified stages (Fig. 19).

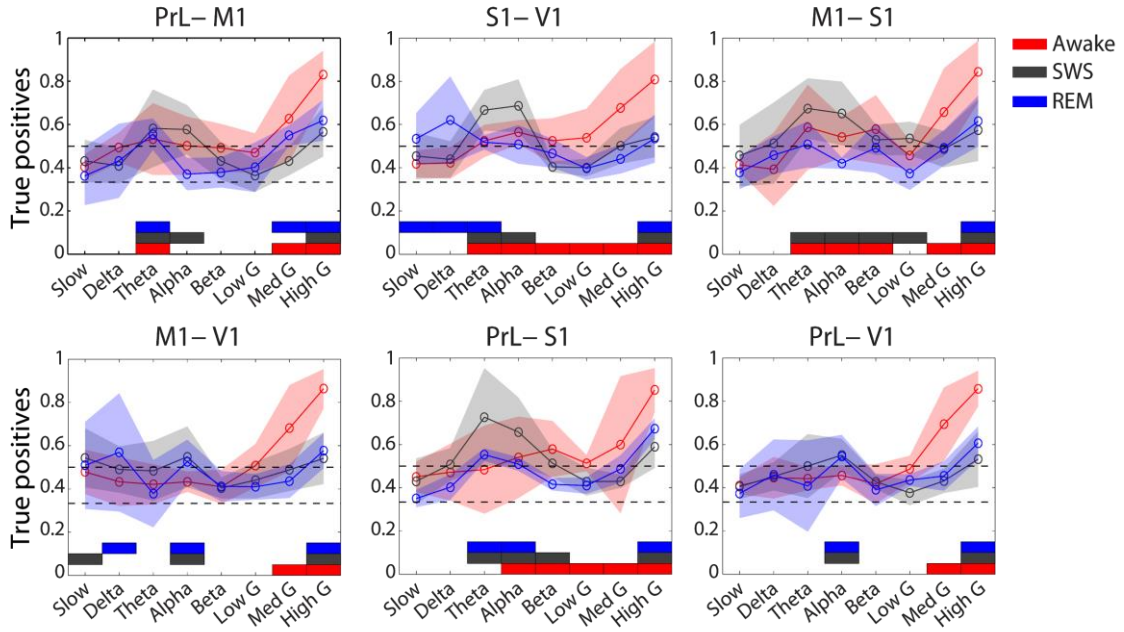

Figure 19. Ratio of true positives classifications among the three stages using the PLV
Population data, showing on a scale the potential for classify each stage correctly. A value above 1/2 (top black dotted line) shows a capacity for distinction above chance. The solid patches mark the frequency range and the stage (color coded) where the correct classification with the PLV is statistically significant ($p \leq 0.05$).

The estimation of the classification ratio of true positives confirmed the ability to distinguish between the three stages by high gamma, finding the highest accuracy in the awake stage of the cycle. On the other hand, it showed that, in general, theta and alpha frequency had remarkable accuracy values classifying the stage of SWS by the cortical PLV.

Together, these results suggest that cortical synchronization measured by means of the PLV in high gamma has the potential to distinguish between behavioral stages of the sleep-wake cycle (wakefulness versus sleep), while synchronization in the theta and alpha bands could distinguish between their brain patterns of activity (SWS versus awake and REM stages).

4.1.2. Development of an algorithm for the automatic online classification of the sleep-wake stages

In parallel to testing the capacity of the index of cortical network synchronization to distinguish among stages, we also explored features from the electrophysiological signal that allows the online identification of the stage from the sleep-wake cycle. In this way, the studied features were the LFP power spectral density ratios among distinct ranges of frequency bands in combination with data on muscular tension and active displacement of the animal provided by the EMG.

Using once more the classifier based in a multi-class logistic regression, we found that the LFP power ratios of beta (20-30 Hz)-low/medium gamma (30-80 Hz) and theta (5-10 Hz)-delta (1-5 Hz) in time windows of 60 s could correctly classify and predict each of the stages. Then, we tested if adding the information of the fluctuations of the EMG recordings from its standard deviation (σEMG) could enhance the precision in the classification.

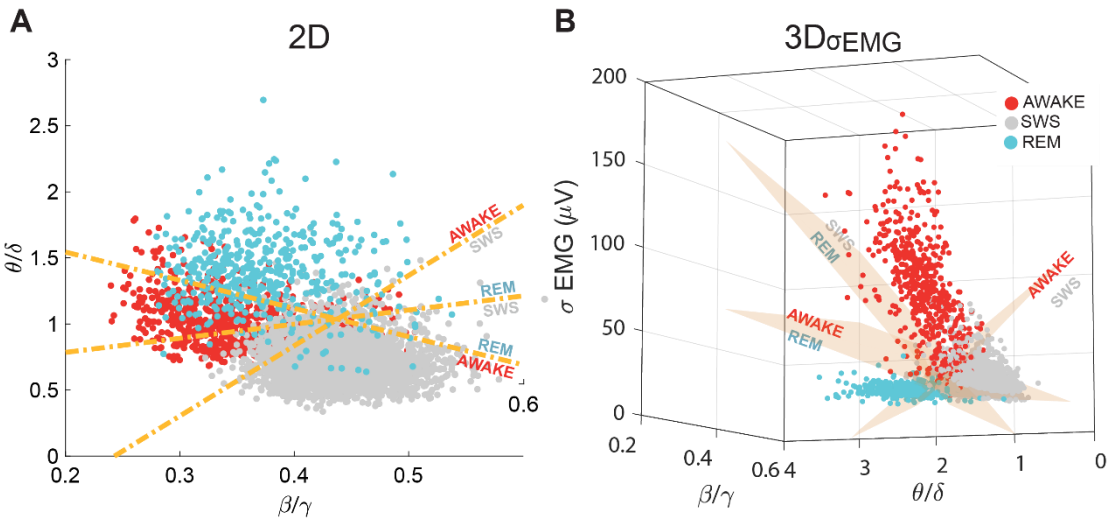

Figure 20. Classification of the multi-class logistic regression-based classifier with different number of variables

(A) Outcome of the classifier for two independent variables, namely the ratio between the PSD in the theta and delta bands and the ratio between the PSD in the beta and gamma bands. The orange lines are the optimized boundaries for the three classes. **(B)** Outcome of the classifier for three independent variables, when considering the standard deviation of the EMG. The orange planes are the optimized boundaries for the three classes. Each coloured dot is the average value of the independent variables in a 60 s window.

We further tested the performance of the classifier with different choices of features. In addition to the EMG fluctuations (σEMG) we also analyzed the mean displacement of the animal (<R>) during each stage, extracted from the video tracking (Fig. 20).

We observed that the addition of the EMG fluctuations increased the accuracy of the predictions of the 2D model, while the addition of the mean displacement of the animal had no effect. As illustrated in Fig. 21 (bottom, right), because the distribution of <R> during sleep was similar in the SWS and REM stages, the two distributions overlap and did not add information to the classifier to distinguish between the two stages. Thus, the highest performance is obtained for a 3D model that combines the spectral content of the LFP and the fluctuations of the EMG.

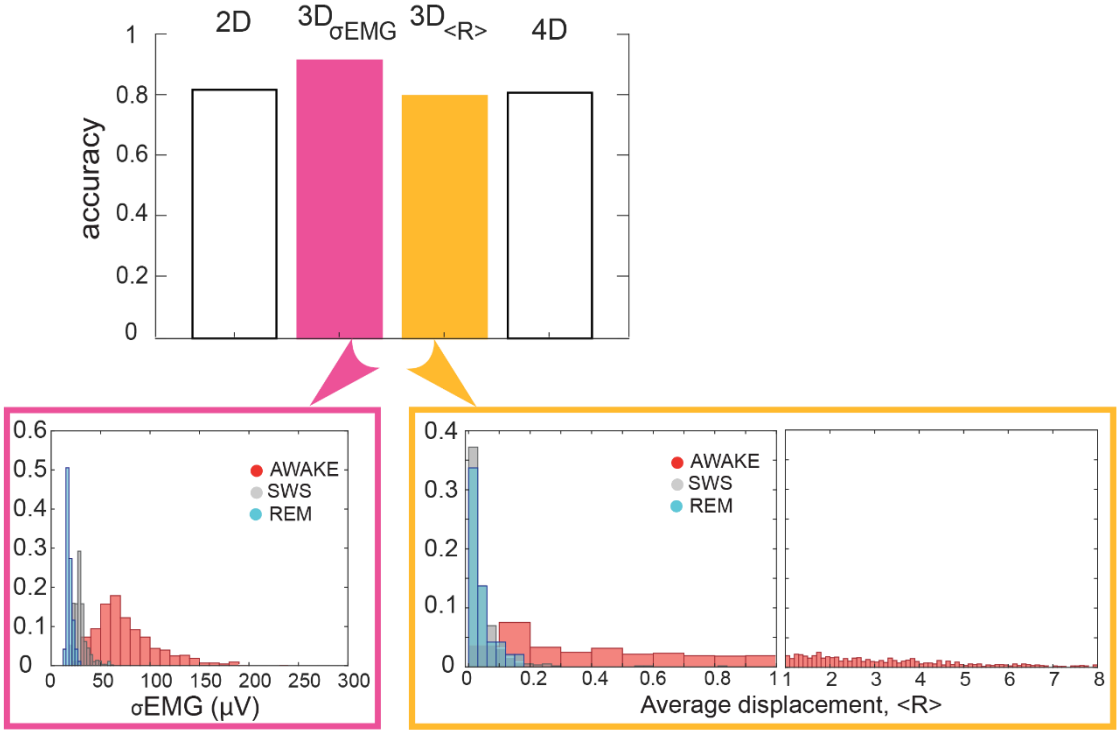

Figure 21. Performance of the multi-class logistic regression-based classifier with different sets of variables
(Top) The bar plot shows the accuracy (percentage of successful predictions) when considering four different sets of independent variables: 2D is as in Fig. 12A and 3DσEMG (pink) as in Fig. 12B. In the 3D<R> (yellow) the standard deviation of the EMG is replaced by the mean displacement of the rat. In 4D all variables were considered. (Bottom) The distribution of σEMG (left, pink) and <R> (right, yellow).

Based on these findings, we developed an algorithm for the online detection of all the stages. As described before, our online algorithm used three independent variables: the standard deviation of the EMG, the ratio between the LFP power in the theta/delta bands and in the beta/gamma (30-80 Hz) bands. Each of these quantities were computed in windows of 60 s.

Derived from these experiments in physiological states our objectives expanded to also explore how auditory sensory processing is modulated by the particular properties of each stage of the sleep-wake cycle leading to changes in the cortical network dynamics. This algorithm allowed us to avoid the online visual scoring to classify the stages during long-lasting experiments with chronic animals that were time-consuming and subject to errors (Hamrahi et al., 2001). Moreover, when in addition to the stages classification the experiment required the delivery of an auditory stimulus in a specific state, performing everything manually may be inaccurate.

4.1.3. *Pilot study:* Auditory evoked cortical responses in the distinct stages of the sleep-wake cycle

As cited before (1.2.4), there is a variety of results about the level of auditory processing during the sleep stages, reflected in distinct modulations of cortical responses, or even a lack of response (Portas et al., 2000; Atienza and Cantero, 2001; Issa and Wang, 2008; Nir et al., 2013). We designed an experimental protocol in order to investigate the cortical dynamics at the distinct stages of the sleep-wake cycle in the presence of auditory stimuli of a different nature. To test this protocol, we recorded 6 cortical areas (3.1.2) comprising primary, secondary and sensory integration areas, auditory related and non-related. We recorded this variety of cortical regions to have a broader perspective of the possible effect mediated by the physiological brain state at a network level. In this section we present some preliminary results.

Within the testing session with this single subject, we recorded the natural sleep-wake cycle of the rat for 3 hours along with the delivery of the auditory stimulation. A total of (3596) trials were presented for all conditions: (1224) 4 kHz (620 at 45 dB; 241 awake, 360 SWS, 19 REM and 604 at 60 dB; 252 awake, 333 SWS, 19 REM), 1237 at 8kHz (605 45 dB; 280 awake, 315 SWS, 10 REM and 632 at 60 dB; 271 awake, 340 SWS, 21 REM) and 1135 in white noise (565 at 45 dB; 211 awake, 333 SWS, 21 REM and 570 at 60 dB; 202 awake, 339 SWS, 29 REM), performing with the algorithm an equitable distribution of the conditions of the sounds for its delivery between stages.

We chose to show the results pertaining to the 45 dB intensity condition, while at 60 dB of intensity the traces in the LFP and the EMG were identical. Therefore, both intensities seemed to affect the cortical response in a very similar way. Performing an average of the raw LFP signals we observed that the two pure tones presented seemed to elicit a neural response in contrast to the presentation of white noise (Figs. 22, 23). More specifically, the auditory stimulation at 4 kHz evoked in general a clear response very similar across all the recorded cortical areas and restricted to the SWS period (Fig. 22A). However, a constant early response of A1 could be differentiated, consistent with the many observations of an activation of primary auditory areas during sleep that supported the preservation of the first steps of the auditory processing in this stage (Peña, 1999; Portas et al., 2000; Cote, 2002; Issa and Wang, 2008; Strauss et al., 2015). On the other hand, the presentation of the 8 kHz tone evoked a broad cortical response that was very similar among all stages (Fig. 22B). This tone had the particularity of also eliciting a clear behavioral response reflected in the EMG, in the form of a twitch, that was visible in the video recording. Surprisingly, even with this striking motor response there were no signs that this type of auditory stimulus evoked a change of stage,

since brain activity in the LFP stabilized and continued with the same pre-stimulation pattern and no postural change was observed.

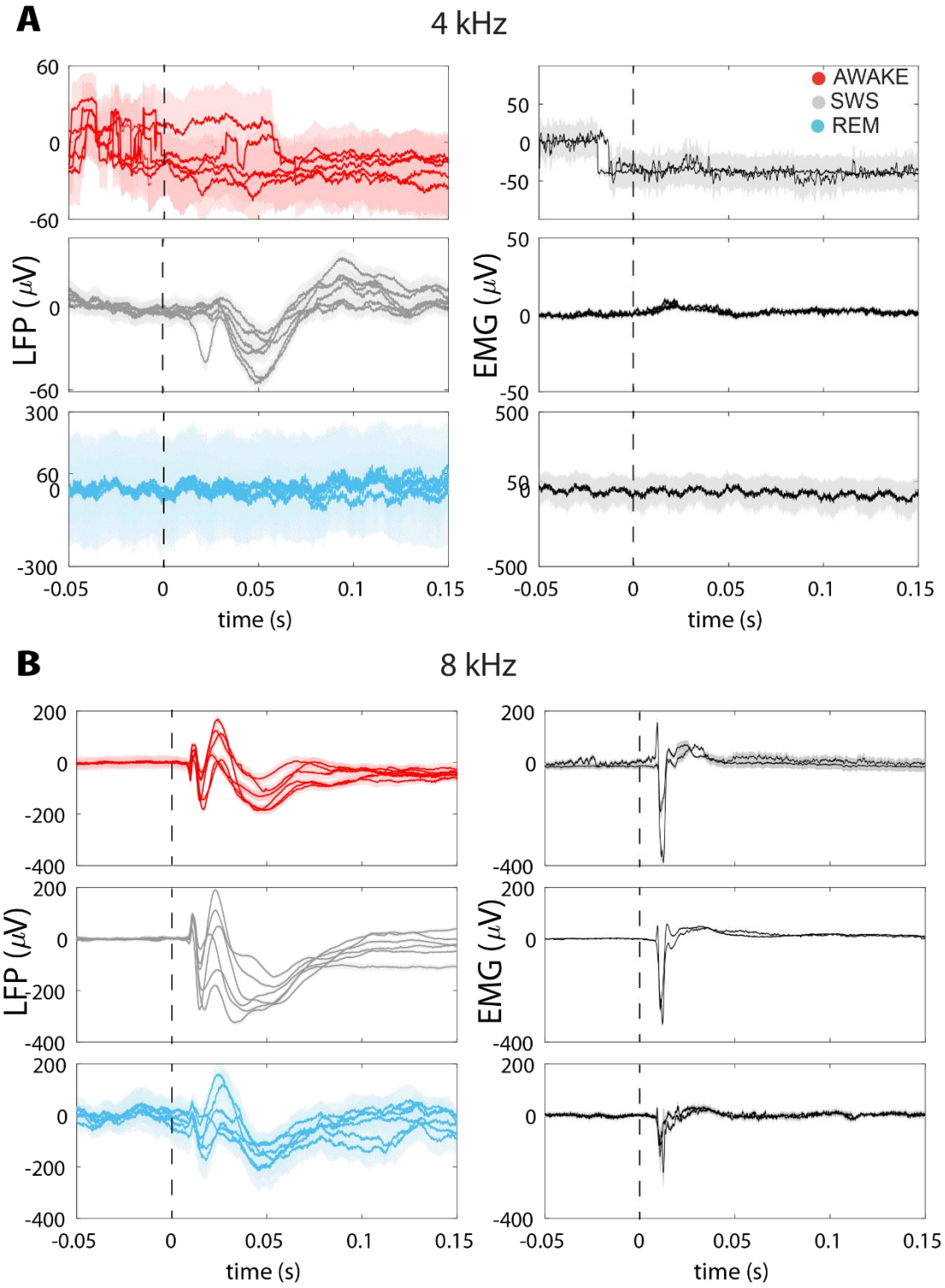

Figure 22. Evoked cortical responses to auditory stimulation with pure tones in the three stages of the sleep-wake cycle

Each trace corresponds to a recorded cortical area showing the average of the responses exhibited in all the trials in the LFP (left) and EMG (right) raw signals, separated by stages. The dotted black line indicates the moment of the auditory stimulation. **(A)** Auditory stimulation at 4 kHz. **(B)** Auditory stimulation at 8 kHz.

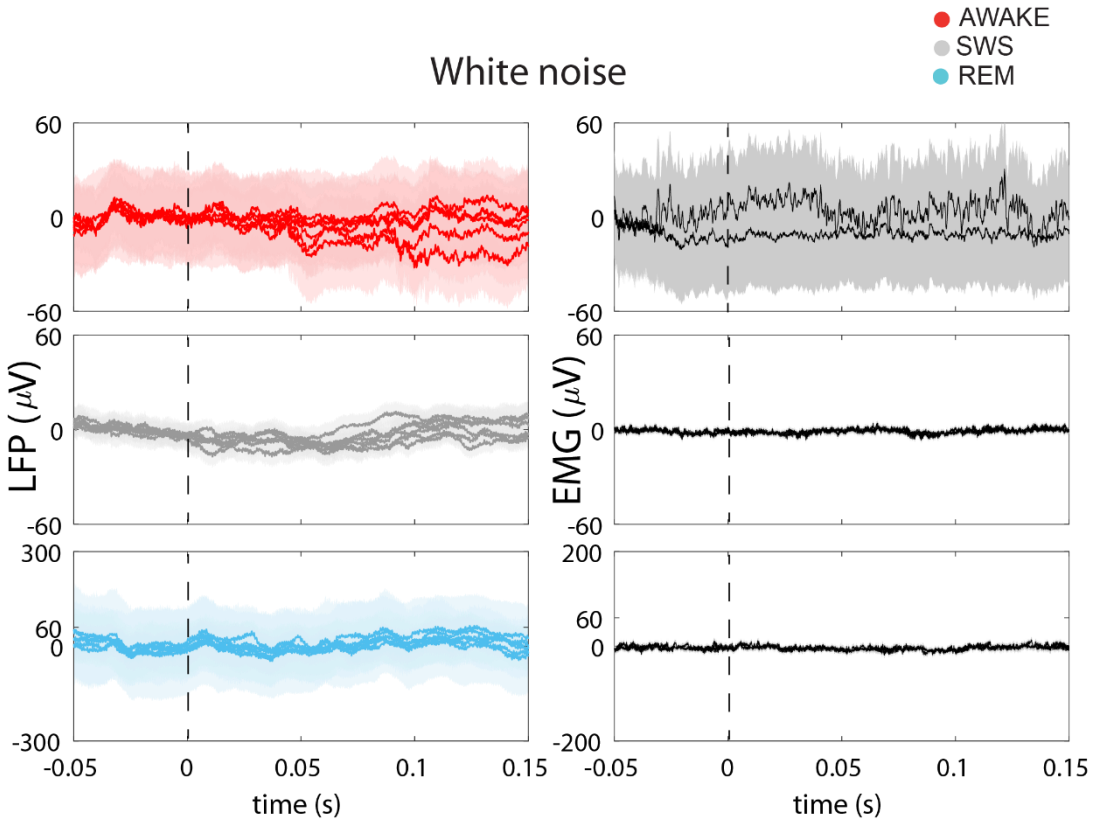

Figure 23. Evoked cortical responses with auditory stimulation with white noise in the three stages of the sleep-wake cycle

Each trace corresponds to a recorded cortical area showing the average of the responses exhibited in all the trials in the LFP (left) and EMG (right) raw signals, separated by stages. The shaded areas represent the standard error of the mean. The dotted black line indicates the moment of the auditory stimulation.

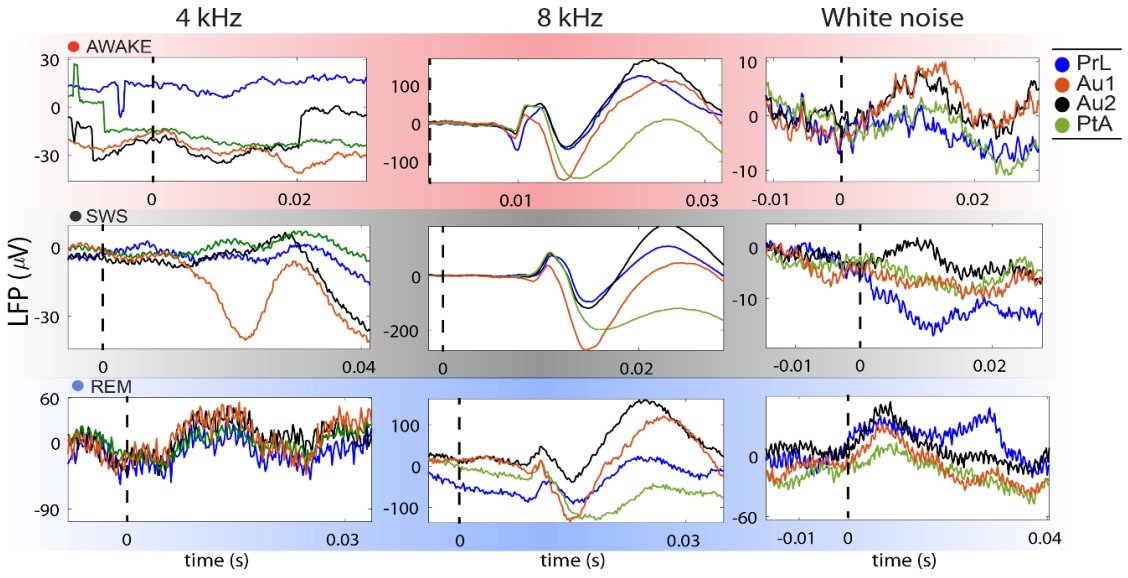

Figure 24. Detailed view of the evoked cortical responses with the auditory stimulation in the three stages of the sleep-wake cycle
Enlarged view of the LFP average signal of the most relevant cortical areas around the moment of the auditory stimulation. Each row of plots corresponds to a stage of the cycle (color coded). Each trace shows the average LFP signal from a recorded cortical area (color coded). PrL= Prelimbic cortex, A1= Primary auditory cortex, A2= Secondary auditory cortex, PtA= Parietal association cortex.

An enlarged view of the most relevant areas for cortical auditory processing showed that A1 was the region with the lowest latency response during SWS, clearly discernible at 4kHz stimulation. The same occurs at 8 kHz and not only restricted to SWS, during wakefulness PrL seemed to respond simultaneously with A1, even with an increased amplitude. It should be mentioned that the responses to 8 kHz stimulation were rather large, and it must be explored in future experiments if they were influenced by the movement elicited in the animal.

A general conclusion that could be derived from these preliminary results is that, as expected, both the frequency of the auditory stimulus and the stage of the sleep-wake cycle play a role in the modulation of the cortical response. Further experiments are being currently performed in order to explore in detail the relationship between cortical dynamics, stimulus properties, and cortical responsiveness.

4.2. Brain states and transitions in anesthetized states

4.2.1. Spectral-based characterization of the cortical dynamics during anesthesia

We know that the anesthetized unconscious state is dominated by slow oscillations which also prevail in the slow wave sleep. It is also known that the awake state has been classically described as an asynchronous state, although we know that it contains synchronization in high frequencies as described above. However, how is the transition between these dynamics? Is it a linear or a nonlinear progression? How is the relation between the local activity and the global patterns, the multiscale aspects? Is it a unidirectional transition, or is it one with hysteresis? Is it a continuous transition or are there "jumps" between states? Does the system need to go through all stages to reach the awake state? When we study physiological cycles sleep-awake, as in the first part of this Thesis, the system autonomously switches between states. However, the gradual change in anesthesia levels allows us to experimentally investigate these different dynamic states, the transitions between them and therefore to propose the cellular and network mechanisms involved in each level.

The starting point for the cortical dynamic's characterization was the identification of the basic elements contained within an entire experimental session. Considering the signal from all the recorded areas from a global point of view, a recurrence in the pattern of temporal appearance of the two types of activity patterns (slow wave and awake-like) were observed among experiments. During the induction there was a fast change of activity patterns (Fig. 8), that then got stabilized into a period that we called "steady-stage" (blue cloud in Fig. 7). This period generally consisted in slow oscillations that did not alternate with other activity patterns. After a variable period of time (between 30-75 min) the steady-stage was abandoned, and the system started transitioning with a continuous back and forth jumping of the activity between slow oscillations and awake-like periods that followed the same spatial path of the induction with distinct temporal dynamic (Fig. 25). this period was referred to as "fade-out". This recurrent trajectory suggested that this temporal-based division could have functional mechanisms coinciding with the anesthetic induction.

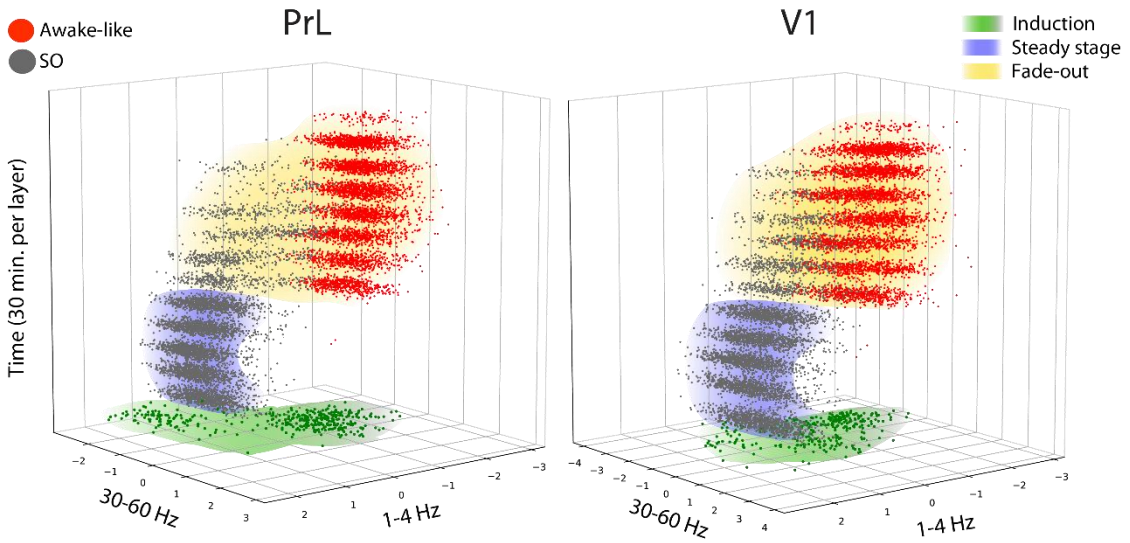

Figure 25. Spatiotemporal representation of the cortical dynamics from two spectral predictors during an experiment with a light dose

The dynamics from most distant cortical regions are illustrated (PrL and V1) with the two frequency bands that best classify among activity patterns in this experiment (delta and gamma bands). The power values exhibited in the *x* and *y*-axis are normalized by z-scoring. Green dots belonging to the induction period contain both awake-like and slow oscillatory activity patterns. They are not differentiated in this figure since their distinction was manual. Differences in the spatial distribution of both activity patterns during the induction and fade-out are noticeable, while all the stages remain very resembling in the temporal distribution. It can be also observed that during the induction the same spatial path generated in both the steady-stage and the fade-out is reproduced in a short lapse.

Moreover, the elemental division was based in the two observable activity patterns: awake-like and slow oscillation. The induction comprised these two patterns of activity in all its variants in a relative short period of time. Having the manual classification of the awake-like and slow oscillatory activity patterns from the induction, a logistic regression model was able to classify the rest of the experiment into these two main patterns of activity. The logistic regression model allowed also the comparison of the dynamics established between activity patterns and further sub-comparisons sorted by frequency bands and cortical areas.

Influence of related variables in the spectral-based characterization of the anesthetized state

In order to have a first general characterization of the cortical dynamics during the anesthetized state, we analyzed the relevance of multiple related variables (activity pattern, frequency band and cortical area) by applying a linear regression model for each experimental

session. We found that the linear model in each experiment described the data very accurately (Table 1) and the three predictor coefficients were statistically significant with a $p<0.001$.

estimate + CI	β_0	β_1	β_2	β_3	β_4	β_5	R^2
Subj.1-Light	0.201 [0.199-0.203]	-0.0056 [-0.006--0.006]	0.288 [0.286-0.290]	0.285 [0.283-0.288]	0.182 [0.180-0.184]	-0.169 [-0.171--0.168]	0.767
Subj. 1-Light	0.196 [0.195-0.198]	-0.0057 [-0.006--0.006]	0.269 [0.266-0.271]	0.246 [0.244-0.249]	0.136 [0.134-0.138]	-0.163 [-0.164--0.161]	0.765
Subj. 1-Light	0.262 [0.260-0.264]	-0.0058 [-0.006--0.006]	0.174 [0.172-0.177]	0.163 [0.161-0.165]	0.197 [0.195-0.199]	-0.159 [-0.161--0.157]	0.775
Subj. 2-Deep	0.131 [0.129-0.133]	-0.0056 [-0.006--0.006]	0.294 [0.292-0.296]	0.199 [0.196-0.201]	0.194 [0.192-0.197]	-0.036 [-0.038--0.034]	0.722
Subj. 3-Deep	0.2624 [0.260-0.265]	-0.0056 [-0.006--0.006]	0.0382 [0.036-0.041]	---	---	-0.047 [-0.044--0.049]	0.710

Table 1. Predictor coefficient and the coefficient of determination values from all experimental sessions.

This implied that all the evaluated predictors had the capacity to explain the changes that take place in the spectral content of both activity patterns throughout the experiments. Furthermore, these results indicated that the PSD comparisons of cortical areas, activity patterns and frequencies were statistically significant.

These results supported the validity of our supervised classification based in the PSD and opens the possibility of an additional approach based in several components of the cortical network for the classification of the potential different stages of an anesthetized state.

Spectral profile of the anesthetized state

In a general view of the PSD values sorted by areas, doses, activity pattern and functional stages, the most salient differences in power were observed between distinct doses, activity patterns and functional stages. The overall changes in power seemed more pronounced when the anesthetic dose was light (Fig. 26).

Examining the differences between the two types of activity patterns we found that in general, when the cortical areas were in the slow oscillatory regimen of activity, the power levels in the frequency bands ranging from slow to beta were higher compared to when they were in the awake-like activity pattern. In the gamma frequencies the trend was reversed, the power being higher when the cortical activity was in the awake-like regime. The dominance in the power of low frequencies during slow oscillation and of gamma during the awake-like activity was consistent with the spectral dynamics described for the induction period with GABAergic anesthetics (John et al., 2001; McCarthy et al., 2008; Breshears et al., 2010; Purdon et al., 2013; Lee et al., 2017; Prerau et al., 2017) and during stages of the sleep-wake cycle (Sinha et al., 1972; Feinberg and March, 1988; Merica et al., 1991; 1992; Maloney et al., 1997; Gross and Gotman, 1999; Steriade and McCarley, 2005; McGinley et al., 2015).

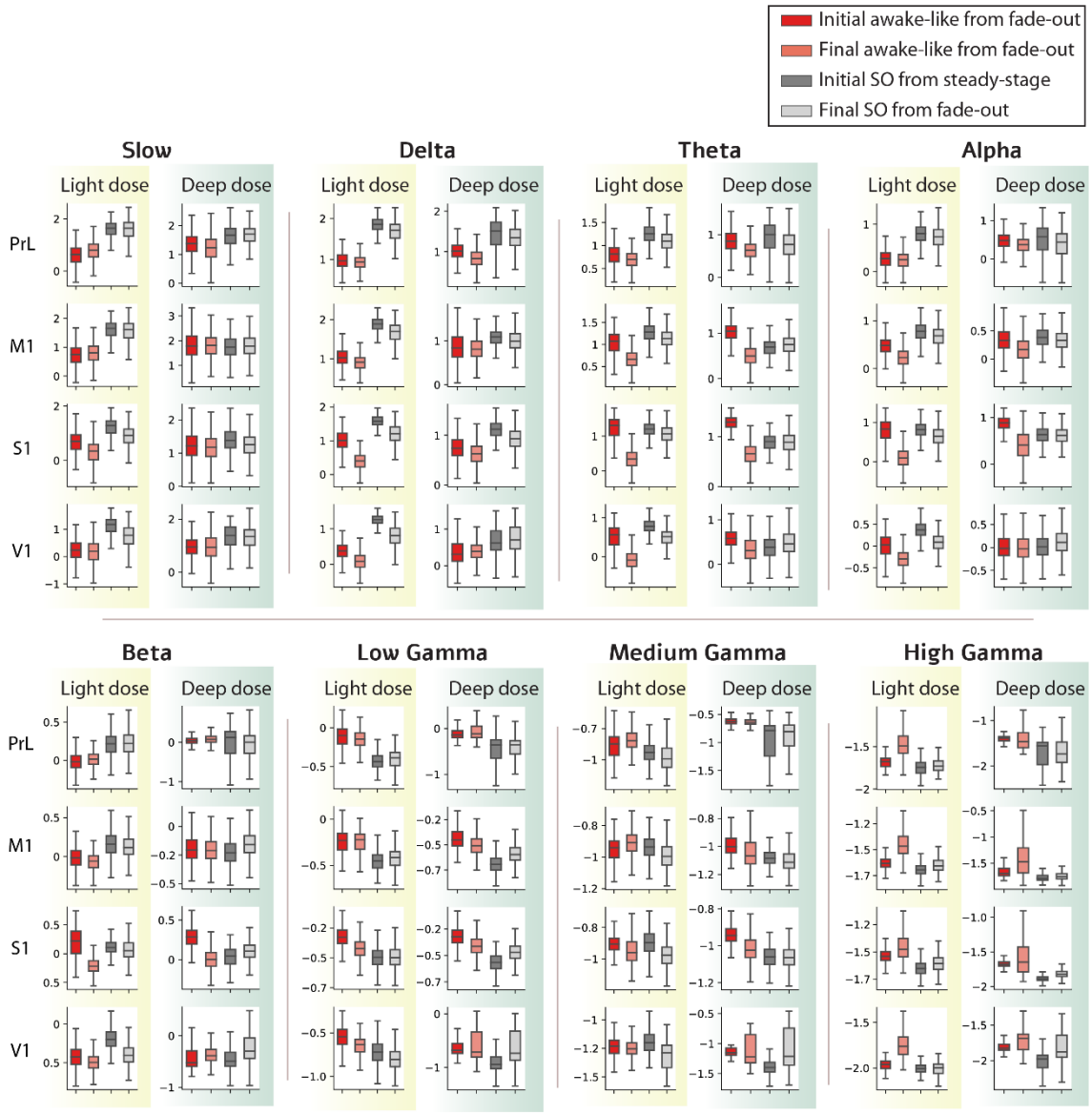

Figure 26. Spectral content in each experimental condition
Mean of the population data showing the power spectral density in each cortical area, for the 2 different doses (light dose N: 1 subject with 3 exp. sessions, deep dose N: 2 subjects with 1 exp. session each), in each activity pattern and from different moments of the functional stages. PSD from the first and last fragments of signal with awake-like pattern in the fade-out and initial fragments with SO= slow oscillatory pattern from the steady-stage and last from fade-out. The power is normalized by z-scoring.

We also observed differences in the PSD from the awake-like pattern at different moments of the experiment. In the delta, theta, alpha and beta frequency bands from the lighter dose and just in the theta and alpha frequency bands for the deeper dose the power drops noticeably in fragments of awake-like activity detected at the end of the fade-out in comparison to those from the beginning of the transition. Following the same general trend, in those final awake-like activity fragments the dominance of power was inverted, being higher in high gamma than in the onset of the fade-out.

Interestingly, the slow oscillatory activity pattern showed a PSD fairly constant at different moments of the experiment regardless of the dose, supported by the comparison of fragments from the onset of the slow oscillation in the steady-stage against fragments of slow oscillation from the fade-out.

These results suggest that the slow oscillation during an anesthetized state could be maintained by a robust mechanism, which allows its characteristics to be invariant at any context. Conversely, the changes found in the awake-like pattern of activity on different functional stages opened the question of whether they could be distinct patterns and consequently, their differences and classification should be further investigated.

4.2.2. Cortical synchronization dynamics during anesthesia

For this analysis, the comparison of the results among doses could not be performed due to the disparity in the number of analyzed subjects for each category. However, there appeared some differences that could be worth mentioning.
From an overall view it was observed that the level of synchronization between all the areas decreased progressively as the value of the frequency range increased (Fig. 27).

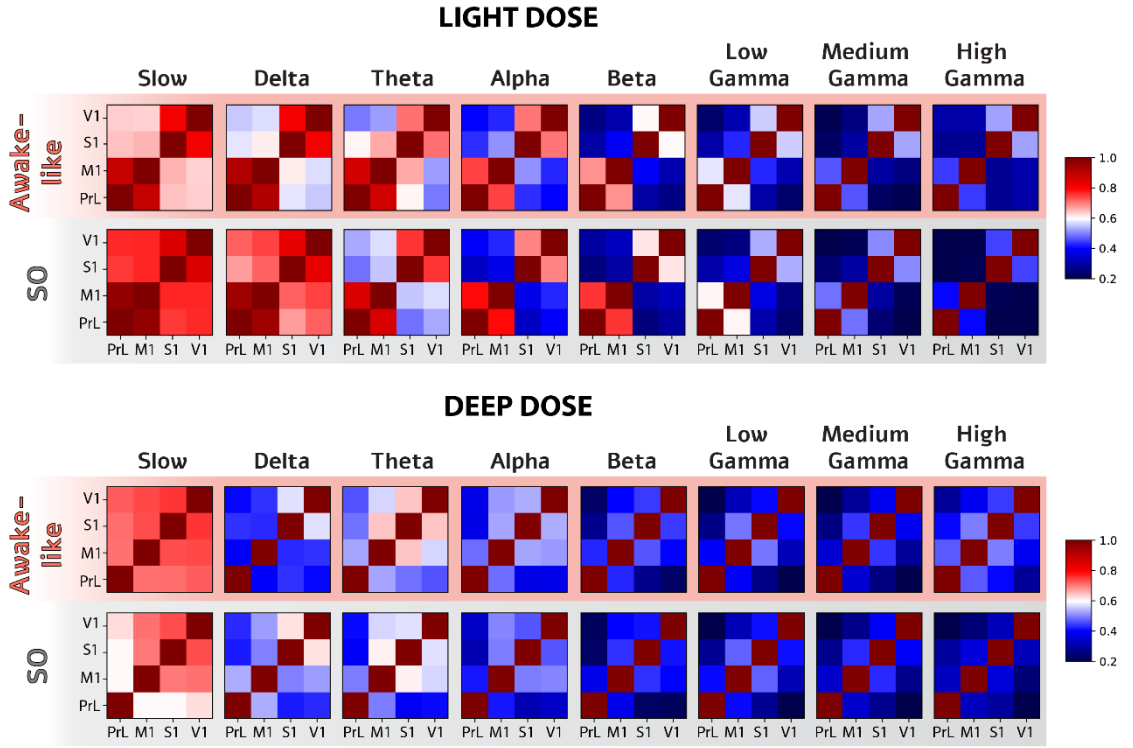

Figure 27. Synchrony among cortical areas in several experimental conditions

Matrices showing the average of PLV values for the 2 different doses (light dose N: 1 subject with 3 exp. sessions, deep dose N: 1 subject in 1 exp. session), in each activity pattern and from different moments of the defined functional stages.

The overall lowest levels of synchronization were observed with the deep dosage, which could be due to the extensive disruption of connectivity characteristic of general anesthesia (Alkire et al., 2008; Pawela et al., 2009; Mashour, 2013; Bettinardi et al., 2015; Paasonen et al., 2017; Krzeminski et al., 2017).

From the experiments with a lighter dose, it was found a synchronization pairing among the anterior (PrL-M1) and posterior pair of areas (S1-V1) that were preserved at all frequency bands. This phenomenon was consistent with the recurrent description of alterations in the frontoparietal axis connectivity in the anesthetic-induced transition to unconsciousness, when the anesthetic is going through different depth levels (White and Alkire, 2003; Lee et al., 2009; 2011; 2013; Boly et al., 2012; Hudetz, 2012; Ranft et al., 2016; Sanders et al., 2018a; Li et al., 2019b). This clustering was also in line with the observed enhancement of local connectivity produced by anesthetic agents (Lee et al., 2017).
On the contrary, with a deeper dose, this clustering was not observed, although the higher level of synchronization was again grouped among posterior regions.

Synchronization values sorted by activity patterns were substantially different among doses. Considering all the recorded regions, the higher levels of synchronization were found for the light dose during the slow oscillatory activity in the slow and delta band, while in the deep dose the higher synchronization level was observed basically in the slow frequency range during the awake-like activity. There were no matching dynamics of synchronization predominance between types of activity, probably due to the lack of samples from the deep dosage for this specific analysis.

Surprisingly, a peak of synchronization during the awake-like pattern within the theta band was found, comprising nearby areas in the light dose among and restricted to posterior areas in the deep dose. A similar pattern of results was obtained in our previous experiments during physiological states (1.4.1), where it was shown that the cortical PLV from theta and alpha bands had the potential to discriminate among an active or a slow oscillatory pattern of activity. Together, these results suggest that cortical synchronization in the theta band could be distinguishing specific features from an active activity pattern, regardless of the conscious state.

4.2.3. Presence of distinct types of Up states during wakefulness and anesthesia

Recording a section of the auditory cortex with calcium imaging allowed the observation of both single neurons and population activity. As result, we were able to observe that, even when awake states are clearly more asynchronous than those anesthetized, we can still detect in the recordings transient periods of synchronous activity during wakefulness. These events seemed similar to the clear Up states recorded from the same subjects in anesthesia, but instead of silent Down states, these awake Up-states were embedded among periods of more active and asynchronous spiking.

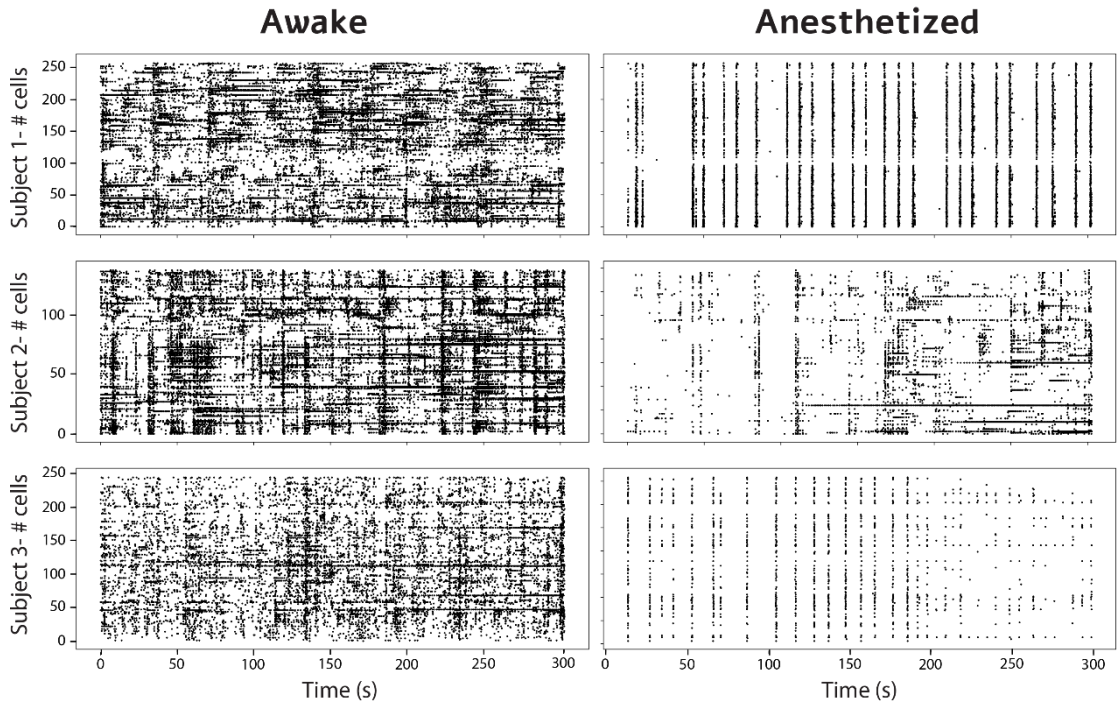

Figure 28. Raw neural activity from awake and anesthetized states within the same subjects
Each dot corresponds to a spike onset.

The ability to detect these synchronous events during wakefulness was due to the high spatial resolution of the calcium imaging technique. The visualization of the firing from single neurons allowed the detection of very local activity patterns of neural interaction, in contrast to LFP in which is not possible to determine the contribution of each neuron to the recorded activity, missing these small-scale phenomena.

To further study the dynamics of these two states from the basis of this synchronous and oscillatory activity, we first detected the synchronous events as Up-states by means of a

detection algorithm (3.2.4) and then estimated several parameters from the slow oscillation: Up and Down-state FR, duration and Up-state size.

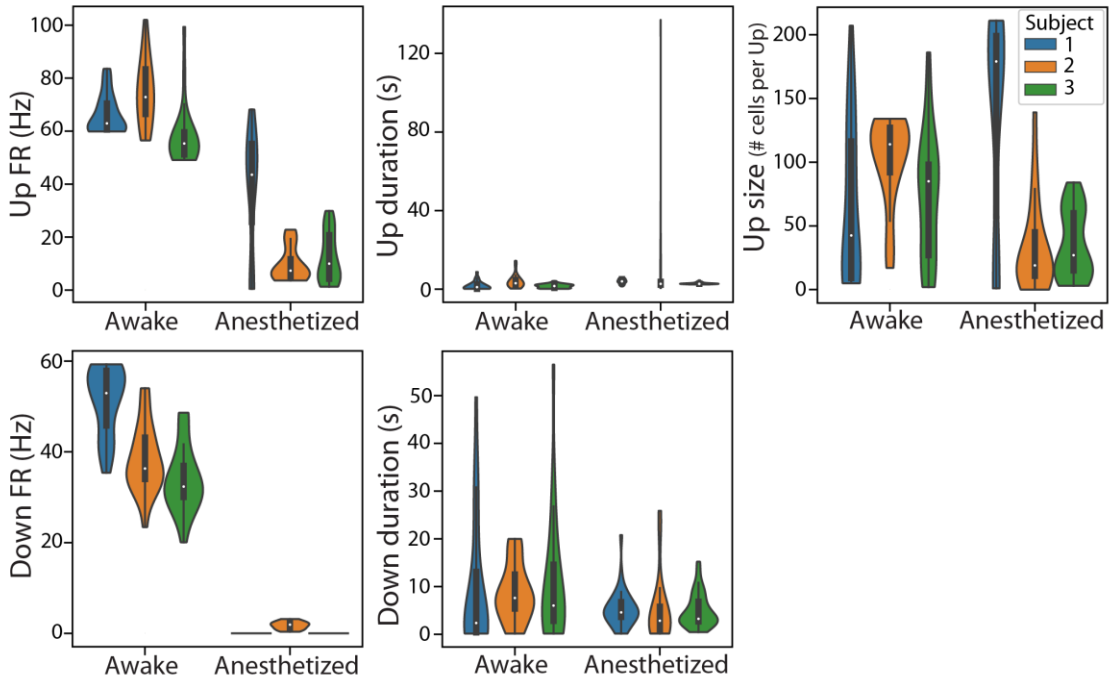

Figure 29. Distribution of the parameters from the slow oscillation for each animal in awake and anesthetized states
No outlier removal has been performed.

The parameters from the slow oscillation indicated that the Up and Down states from wakefulness and anesthesia seemed to differ notably in the FR and the Up states duration (Fig. 29). The Up states duration from wakefulness presented more variability and were shorter than those occurring during anesthesia. However, surprisingly, in two subjects the size of the awake Up state indicated in general a slightly higher involvement of a larger number of neurons. Therefore, although the same type of synchronous event could be visually and conceptually distinguished, the quantification of its components could reveal that they differ functionally. However, for further explore this hypothesis a larger sample is needed. It should also be taken into account that the firing detected with calcium imaging has lower temporal resolution than electrophysiological firing, and therefore no assumptions should be made about firing synchrony.

Considering these results, we visualized for each subject a scatter plot with their parameters distribution by pairs. An interesting relation among the Up FR and size was noted consistently in the three subjects independently from the brain state.

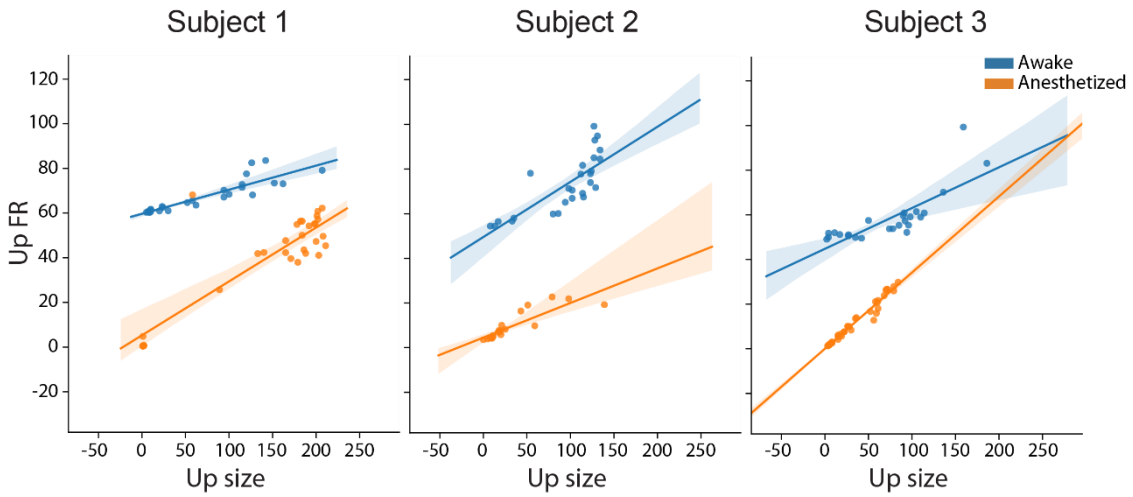

Figure 30. Correlation between the FR and size of the Up states in awake and anesthesia
Illustration on each subject data of the regression line and the 95% confidence intervals of the linear model. No outlier detection and removal has been applied.

Then we estimated the regression line of a linear model for these two parameters (Fig. 30), finding that the linear model explained the data to a good extent, as shown more quantitatively in the table below.

Subject	State	99% CI of slope	R^2
1	Awake	[0.07,0.13]	0.76
1	Anesthetized	[0.18,0.30]	0.78
2	Awake	[0.13,0.36]	0.61
2	Anesthetized	[0.09,0.22]	0.75
3	Awake	[0.10,0.26]	0.64
3	Anesthetized	[0.31,0.37]	0.97

This high and constant relation between the FR and the size of the Up state could be indicative of a robust dynamic of activity, where the augmentation in firing of a neuron during an Up state provokes the recruitment of other sets of neurons in specific and stable proportions, augmenting the size of the Up state as a result.

4.2.4. Differences in neuronal functional connectivity during wakefulness and anesthesia

In order to investigate the functional connectivity, we estimated the partial correlation between each time series of DF/F0 using a Gaussian graphical model.

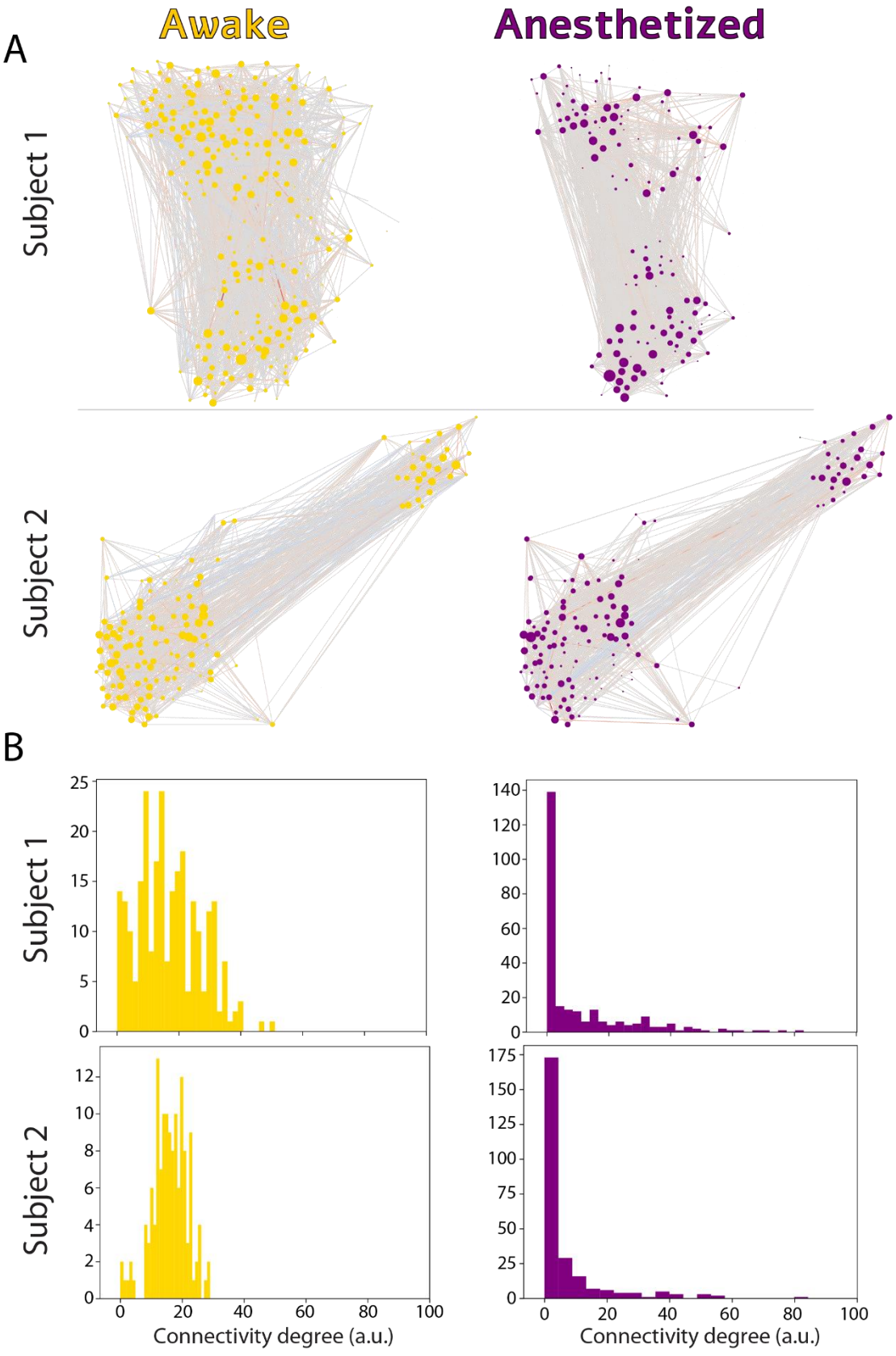

Figure 31. Neuronal connectivity pattern within the same subjects during wakefulness and anesthesia

(A) Networks are illustrated with connectivity graphs. Each node represents a neuron in its real position from the recording and the size of the node indicates its connectivity degree **(B)**Histogram showing the differences on the connection weights for the group of active neurons.

During wakefulness in general, an extensive number of neurons are engaged in the asynchronous activity and consequently multiple connections are established. However, this number decreases substantially during anesthesia, where connections are sparser and weaker. Estimating the functional connectivity, we observed this phenomenon in our data (Fig. 31), but with the exception of a few neurons that during the anesthetized state exhibited a higher correlation of activity than any neuron during wakefulness (Fig. 31B). This could be coherent with the intrinsic dynamic of the slow oscillatory activity, where the synchronous firing produced during the Up state enhances the possibility of coupled activity among the small amount of active neurons.

4.3. Thalamic stimulation during an anesthetized state

We evaluated the effect produced by the PF stimulation under anesthesia in the activity of a PF-connected (PrL) and non-connected (V1) cortical areas by quantifying the changes in the spatiotemporal and frequency values.

4.3.1. Regularization of the oscillatory activity of the prelimbic cortex after the stimulation of the parafascicular nucleus

The spectrograms from 30 min before and after the stimulation showed that, although the PrL activity both prior and post-PF stimulation varies among subjects, in all cases there are discernible changes after the stimulation compared to its own previous activity (Fig. 32). Furthermore, those changes did not seem to be restricted to the moment immediately after the stimulation, but in general, they showed relatively long-lasting effects, with a minimum duration of 30 min.

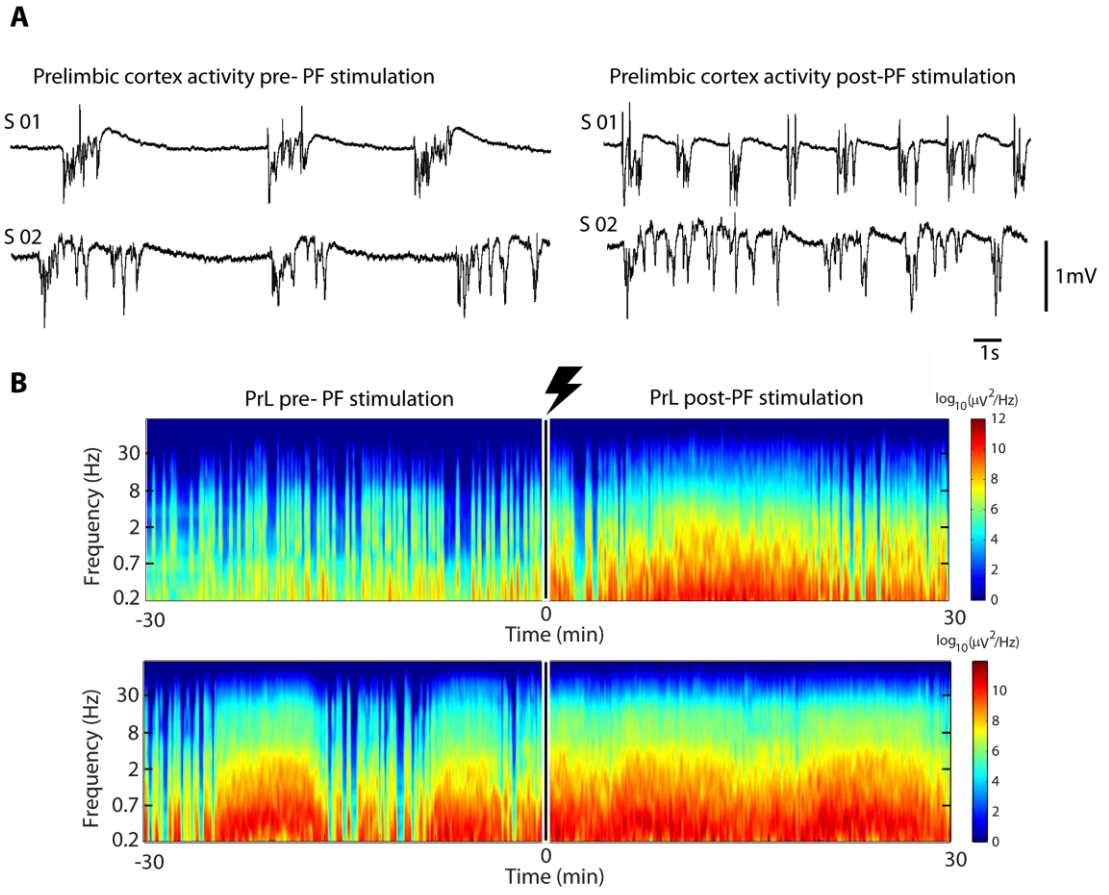

Figure 32. Prelimbic activity before and after parafascicular nucleus stimulation
(A) Extracts of the LFP raw signal from the PrL cortex before (left) and after (right) the PF nucleus stimulation in two different subjects where the changes in activity are observable. **(B)** Spectrogram from the LFP recordings

in the PrL the whole analyzed time: 30 min before and after the PF nucleus stimulation (marked with a black and white horizontal line and a black ray) in two different subjects.

To quantify the average changes across the population, different parameters of the slow oscillation were analyzed: the average of the slow oscillation frequency, the slow oscillation coefficient of variation (CV), the FR over time, the FR cycle, the Up and Down durations, and their respective FR.

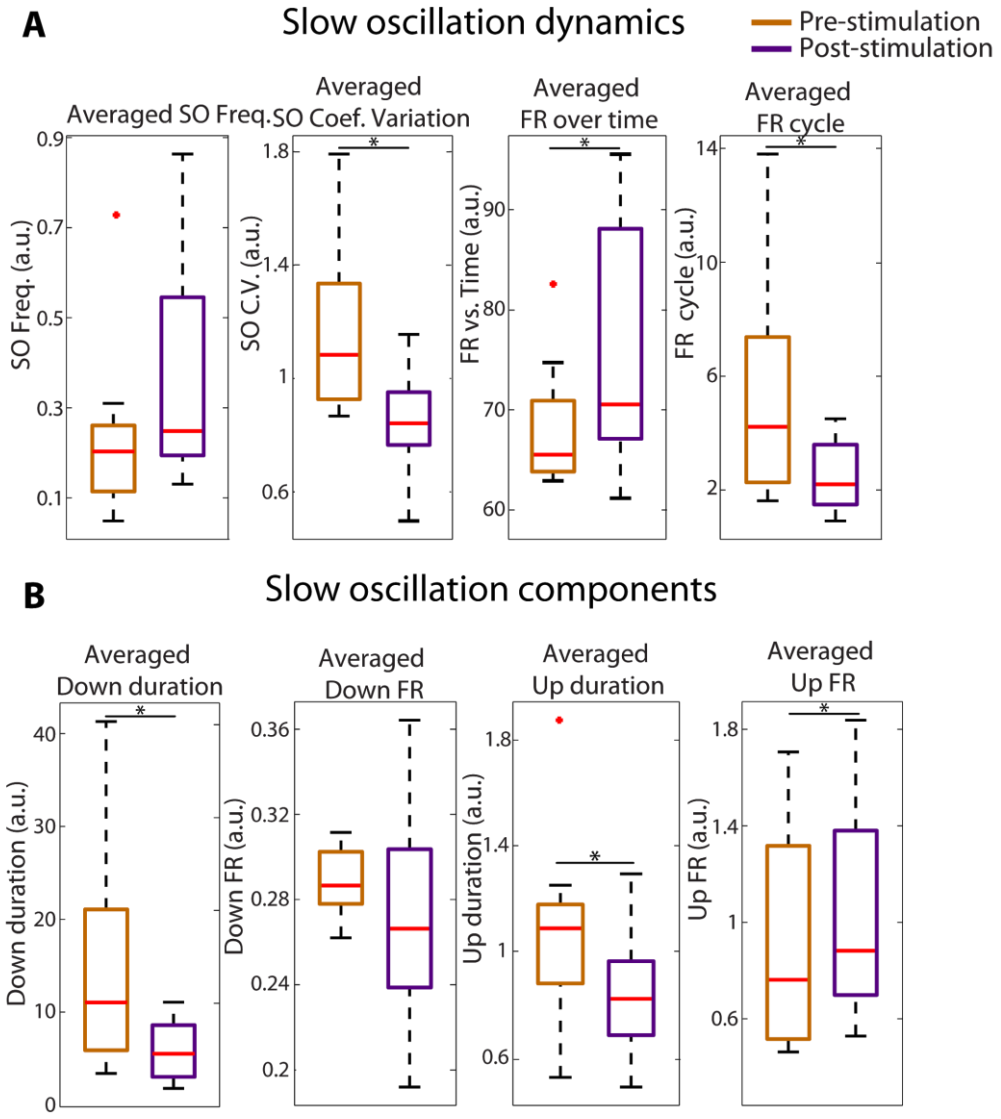

Figure 33. Modulation of slow oscillation in the PrL cortex by the PF stimulation
Population data showing the changes in the different SO= slow oscillation parameters 30 min before and after the PF stimulation **(A)** Parameters that explain the dynamic of the whole signal. **(B)** Measurements of the Up and Down states.

Our observed changes following stimulation were compatible with an increase in the excitability of the cortical network. The FR across the analyzed time increased significantly (p=0.039063), and the slow oscillation frequency tended to increase, although not

significantly (p=0.25). At the level of the slow oscillation components, a shortening of the duration of the Up (p=0.023438) and the Down states (p=0.039063) was consistent with an increase in arousal. Besides, the CV decreased significantly (p=0,039063) what seemed to explain the regularization of the activity shown in the spectrograms (Fig. 32B).

Consistent with previous results, the analysis of the different parameters of the slow oscillation seemed to suggest that the PF stimulation regularized the activity and had an activating effect in the PrL cortex, coherent with the innervation received from the PF and the involvement of this nucleus in the ARAS system, the activation network.

4.3.2. Alterations in the gamma band after stimulation of the PF nucleus

We also explored how the PF stimulation affected the spectral content and the synchrony between the two cortical recorded areas.

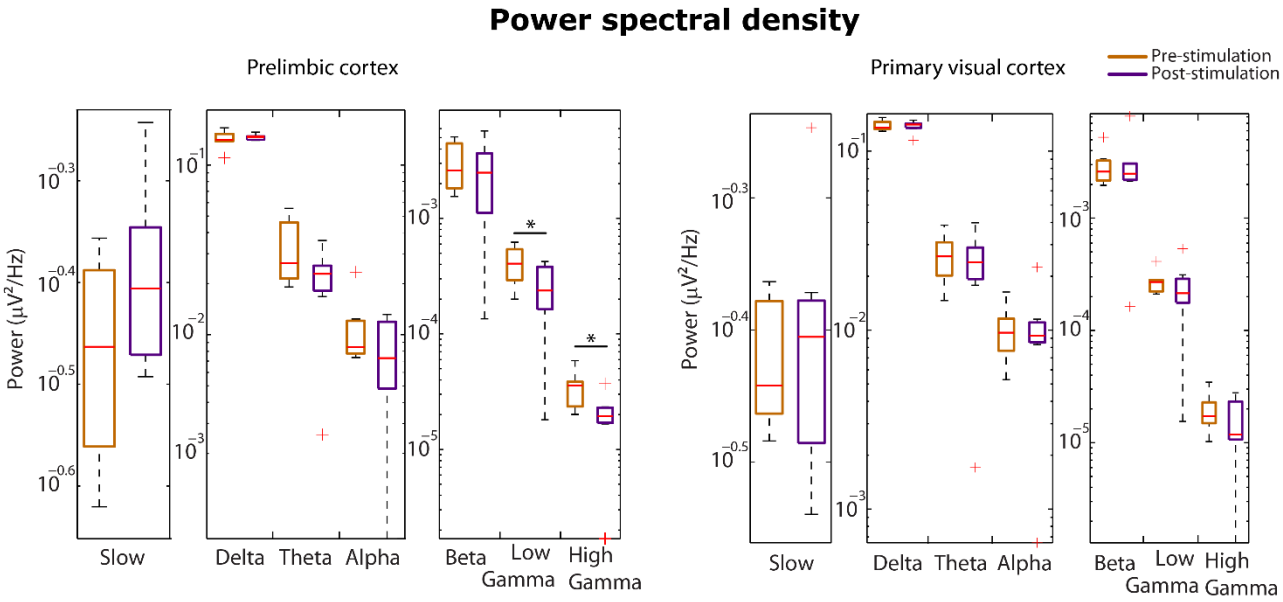

Figure 34. Spectral content in PrL and V1 before and after the PF stimulation
Mean raw power spectral density changes after the PF stimulation.

These results indicated a decrease in the gamma band (30-100 Hz) after the PF stimulation produced in both recorded areas. This decreasing trend is consistent with the general idea that the effects observed after thalamic stimulation are produced widespread in the cortex (Morison and Dempsey, 1942; Jasper, 1949; Hanbury et al., 1954). However, this descent in the gamma band was only significant in PrL cortex (p=0.0156) which could be suggesting

a possible specific effect probably due to the existent innervation from the PF nucleus to the PrL cortex in opposition to V1.

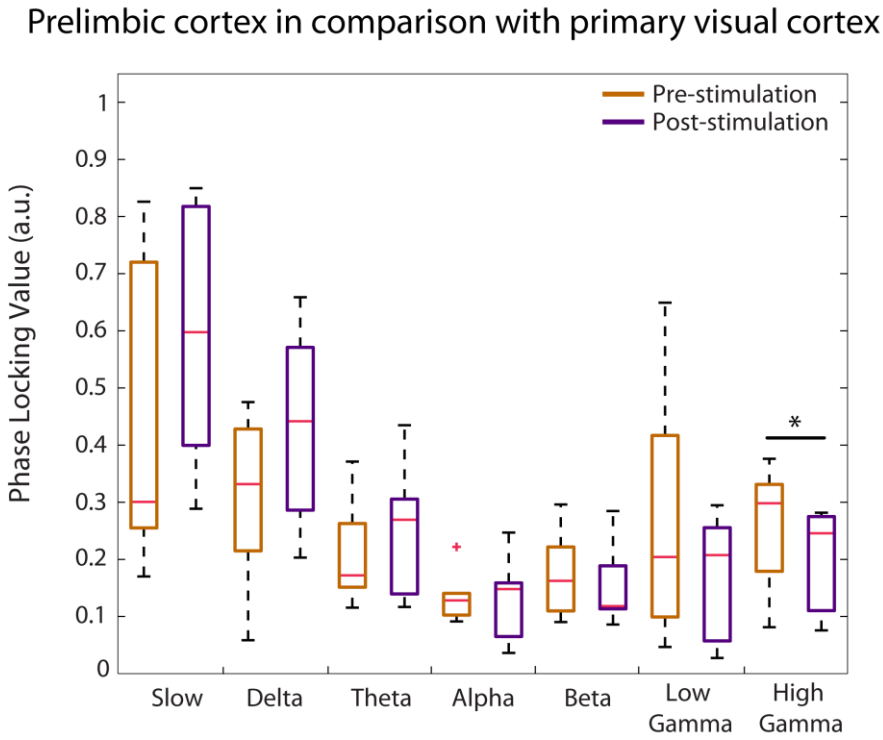

Figure 35. Phase synchronization between PrL and V1 before and after the PF nucleus stimulation
0 is the minimum and 1 the maximum value indicating respectively the coupling or uncoupling of the phases of the signals from the two regions recorded regions.

In addition to the gamma decrease in the spectral content, we also observed a decrease in phase synchronization at the gamma band between PrL cortex and V1 (p=0.015625) (Fig. 35). Given the global nature of the slow oscillation in the cortex and the anatomical connectivity of the recorded structures, it seems comprehensible to assume that a perturbational thalamic stimulus would affect the PrL cortex, as a connected area, and consequently interrupt the previous cortico-cortical synchronization among non-connected areas, in this case V1.

Our results suggested that the PF stimulation induces long-lasting effects in the PrL cortex, reflected in changes that remained 30 min after the stimulation in the spectral content and in different parameters of the slow oscillation. The two main effects observed were a regularization of the oscillatory activity, evidenced in the changes in the variance coefficient of the slow oscillation, and an increase in cortical arousal indicated by an increase in the relative firing rate. Moreover, in terms of spectral content, a variation in the gamma band

power in PrL cortex and a decrease in the gamma band synchronization was observed between two distant cortical areas which differ in their innervation by the PF nucleus.

Chapter 5

Discussion

The work performed in this Thesis has comprised the study of physiological states of sleep and wakefulness and pharmacologically induced brain states (with anesthesia) from different perspectives and scales. The data obtained from the LFP and two-photon calcium imaging recordings of their spontaneous and evoked brain activity patterns was used to classify those states into differentiated stages and further analyze their intrinsic cortical dynamics. Finally, the impact of thalamic -specifically, the parafascicular nucleus- activation on the cortical state was investigated, as an stratategy that may be relevant also in the clinic.

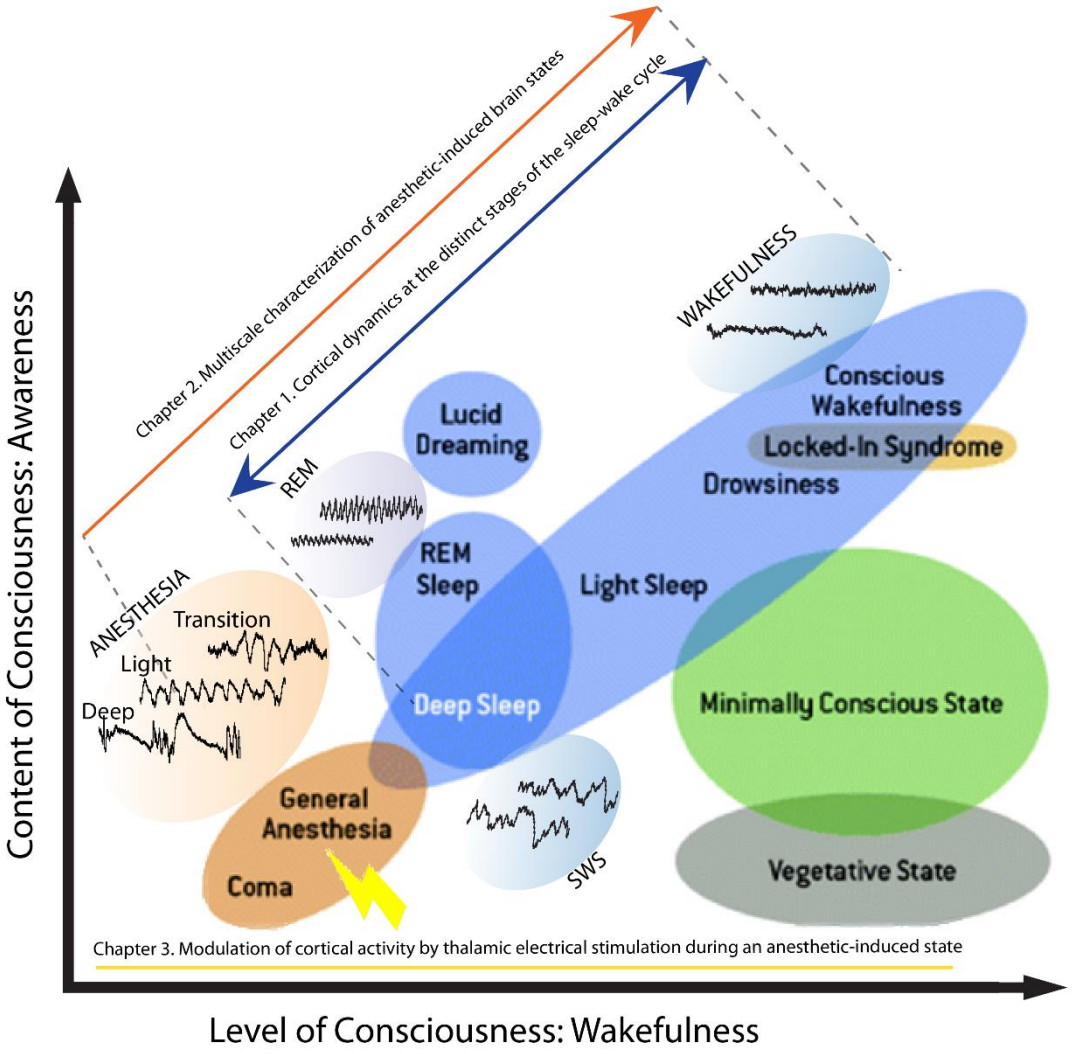

Adapted from Laureys (2007)

Figure 36. Distribution of the different brain states in correlation with the main components of consciousness: level of wakefulness (or arousal) and awareness (Laureys et al., 2007)
Illustration of the characteristic activity patterns of the studied anesthetic-induced and non-pathological physiological brain states. Yellow ray depicts the electrical stimulation delivered.

The potential role of power ratios and cortical synchronization at specific frequency bands to classify stages in both physiological and pharmacologically induced conditions and to describe some of their functional aspects was highlighted with this work. An accurate identification and classification of states and their stages is crucial to unveil stage-specific phenomena and underlying mechanisms. The relevance of discovering robust indexes able to categorize stages is not only restricted to the neuroscientific study of the underlying mechanisms of the brain states, but it also has a clinical application. Evidence of the necessity

of a unitary and reliable method of brain states classification in the clinical field is the existence of multiple scorings scales and methods based on numerous features such as behavioral indicatives of the level of consciousness, in patients with disorders of consciousness, or diverse traits and rhythms observed in the electrophysiological activity during physiological states.

5.1. Brain states and transitions in the physiological sleep-wake cycle

Synchrony within a neural system has been proposed as a potential mechanism for the integration of information, essential for the emergence of mental processes and behavior (Hebb, 1949; Nicolelis et al., 1995; Singer, 1995; Engel et al., 2001; Varela et al., 2001; O'Connor et al., 2002). In particular, the enhancement of synchrony between distributed cortical regions has been considered a specific mechanism of brain processing directly dependent of the brain state (Fries, 2005). Furthermore, Gervasoni et al. (2004) affirmed that wakefulness and sleep specifically exhibit different values of phase synchrony of the LFP oscillations. However, previous studies have focused on either a frequency band, large cortical territories or a small subset of cortical pairs when exploring relevant features that define each physiological brain state, which can lead to partial and biased conclusions.

Following these premises, we explored synchrony from the perspective of the cortical network, considering multiple distributed cortical areas and frequency bands simultaneously. In this context we investigated the efficiency of the PLV as a potential index to differentiate distinct stages of a physiological sleep-wake cycle. Specifically, we showed that cortical synchrony in high gamma could accurately differentiate between a state of wakefulness and sleep while in the theta and alpha range, could classify differentiate between an active or a slow wave pattern of brain activity.

Cortical oscillations in the gamma frequency band seem to be closely involved in perception, cognitive binding and consciousness (Gray and Singer, 1989; Llinás, 1991; Singer and Gray, 1995; Rodriguez et al., 1999; Hwang et al., 2019). This is consistent with the fact that the level of cortical phase synchronization in this frequency band could distinguish between physiological states that differ in the degree of consciousness.
Previous studies reported divergent dynamics of cortical synchrony in the gamma bandwidth across the different stages of the sleep-wake cycle; however, all coincided in the description of a stage-dependent prominent role for this band. Some authors affirmed that gamma

cortical synchrony was high during those stages with an activated pattern of activity (awake and REM) and correlated with the presence of cognition (in REM in the form of dream content) (Llinás and Ribary, 1993; Bragin et al., 1995; Maloney et al., 1997; Achermann and Borbely, 1998a). Our results were in agreement with the decreases found in gamma coherence both in SWS and REM stages of sleep that was interpreted as a sign of the decrease in the capacity for integrate and process information among cortical regions that is produced in sleep (Gross and Gotman, 1999; Perez-Garci et al., 2001; Cantero et al., 2004; Voss et al., 2009; Castro et al., 2013, 2014; Cavelli et al., 2015; Pal et al., 2016). Furthermore, within individual brain states there are differences in the stimulus processing, described both for different phases of slow waves (Up/Down states) (Reig et al., 2015) or, within the awake state, depending on the engagement in the task (Abolafia et al., 2011). A further involvement of gamma phase in these modulations should be taken into account.

On the other hand, our data additionally showed that cortical synchrony in the theta and alpha frequency range were able to distinguish stages of the sleep-wake cycle according to the brain activity pattern. The values of synchrony in theta and alpha rhythms accurately separated between the stage of SWS from the awake and REM stages. Awake and REM have an active and desynchronized pattern of activity and share some common neural substrates that promote arousal, such as a cholinergic transmission (Llinás and Pare, 1991; Jouvet, 1999; Steriade, 2000; Pace-Schott and Hobson, 2002). Therefore, the fact that the properties of cortical synchrony at this frequency range were indistinguishable among these two stages, could have a functional basis given its common physiology. Pal et al. (2016) showed a correlation of cortical connectivity in the theta band with the cholinergic tone regardless of behavioral arousal; therefore, in both awake and REM, the synchronization in theta was similar, since the transmission of acetylcholine in both states is high. Pal et al. (2016) emphasized that the value of synchronization in theta does not consider behavior, while we suggest that synchronization in the theta band distinguishes between distinct patterns of brain activity.

In conclusion, we observed that cortical synchrony in high gamma can differentiate the stages of the sleep-wake cycle based on its behavioral level of arousal (wakefulness and sleep), whilst in theta and high gamma based on the pattern of brain activity (active in wakefulness and REM against slow in SWS).

In agreement with Lustenberger et al. (2018) which showed that neural responses were modulated by the physiological state, from our preliminary data we observed that the auditory evoked responses in primary and secondary auditory areas and in the multimodal parietal associative cortex depended on the physiological state and in the frequency content

of the sound. In contrast to white noise, pure tones elicited cortical responses. In particular, 8 kHz tones elicited responses in all physiological state, whereas 4 kHz only produced noticeable responses in SWS. This does not imply the absence of a response to 4 kHz tones during wakefulness, but rather that the modulation produced is of lower amplitude. This is in line with studies reporting that the cortical response to an auditory stimulus is larger during a state of synchronous activity (dominated by slow oscillations) than during a state of desynchronized activity (Castro-Alamancos, 2004a; Marguet et al., 2011). It is also coherent with the fact that the same stimulus induces larger synaptic responses in Down states, than in Up states (Reig and Sanchez-Vives, 2007: Reig et al 2015), Up states that indeed share many features with wakefulness (Compte et al 2008; Destexhe et al 2007). Furthermore, there is a different relationship between intensity of stimulation and amplitude of responses between Down and Up states (Reig et al., 2015). If we add up the frequency specificity be location, we find that the responsiveness to sensory stimulation, in this case auditory, is multifactorial.

Moreover, the 8 kHz tones elicited large-scale responses in all states accompanied by a constant muscular response. During sleep specifically, this stimulation provoked an adequate arousal level to elicit a behavioral reaction but not for inducing a switch in the state from REM to SWS or causing awakening.

In order to further explore how the brain state and the frequency modulates the cortical response a larger experimental sample is needed, which is currently ongoing work.

5.2. Brain states and transitions in anesthetized states

Even when there are many changes in cortical dynamics during anesthesia, we still lack a mechanistic understanding of the evolution of network properties of the different levels that anesthesia goes through. Among the most recurrent traits in the literature that explores those dynamics are: the variations in power in different frequency bands and its topographical predominance (Hudson et al., 1983; Long et al., 1989; John et al., 2001; Gugino et al., 2001; McCarthy et al., 2008; Breshears et al., 2010; Cimenser et al., 2011; Lewis et al., 2012; Ní Mhuircheartaigh et al., 2013; Purdon et al., 2013; Lee et al., 2013; Vijayan et al., 2013; Warnaby et al., 2017; Lee et al., 2017; Prerau et al., 2017), alterations in synchrony among areas, thus disruptions of functional connectivity (Engel and Singer, 2001; Alkire et al., 2008; Ferrarelli et al., 2010; Mashour, 2013; Guldenmund et al., 2013; Purdon et al., 2013; Bettinardi et al., 2015; Bonhomme et al., 2016; Chander et al., 2014; Lee et al., 2017;

Mashour and Hudetz, 2017; Krzeminski et al., 2017; Pal et al., 2019) and the suppression of activity in specific areas (Fiset et al., 1999; Alkire, 1998; Paasonen et al., 2018).

The search for the establishment of functionally defined stages during anesthesia has the added difficulty of the wide variety of neurochemical, neuroanatomical and neurophysiological functioning derived from the use of distinct anesthetics and dosage. Tort-Colet et al. (2019) described the existence of two activity patterns that alternated during the decrease in the level of anesthesia with ketamine and medetomidine. Considering these findings, we used the same mixture of anesthesia at two different doses and based in the spectral dynamics of the two main detected activity patterns during the anesthetic induction we build a model able to classify the entire period of anesthesia. However, a critical difference in the current study is that, being a chronic recording, we did reach a wider range of anesthesia levels, including from deep anesthesia to fully awake.

With this work, we have proposed a methodology that could be systematically used to classify anesthetic patterns of activity. From this classification we also suggested a stages division based on the observation of the pattern of temporal appearance of the two types of activity. Changes in the PSD of the awake-like pattern at distinct moments of the anesthetic state supported the viability of this functional classification, which could be a starting point to further investigate this division criteria at a larger scale.

During this anesthetized-induced state of unconsciousness we found the emergence of activity patterns that are also characteristic of well-defined physiological stages, as wakefulness or SWS. The analysis of the spectral content of both patterns revealed that also their dynamics were convergent. Per contra, wakefulness implies consciousness and SWS absence of consciousness, leaving a shared pattern of activity and spectral profile among physiological and pharmacological states, regardless of the conscious state. This could be suggesting that this spectral dynamic is strongly related with the patterns of activity and not to the same level with the behavior.

Synchronization during anesthesia with a light dosage was restricted to nearby areas following an anteroposterior division, while with a deeper dosage no clustering was observed. This clustering in activity coupling from the lighter dose is consistent with the disruption of the frontoparietal connectivity (White and Alkire, 2003; Lee et al., 2009; 2011; 2013; Boly et al., 2012; Hudetz, 2012; Ranft et al., 2016; Sanders et al., 2018a; Li et al., 2019b) and the enhancement of local connectivity observed with GABAergic agents (Lee et al., 2017). However, previous studies did not found a consistent pattern of the spatiotemporal dynamics and alterations in connectivity with the administration of ketamine (Liao et al., 2012;

Scheidegger et al., 2012; Niesters et al., 2012; Sarasso et al., 2015; Bonhomme et al., 2016). Our results could be suggesting that the dose of the ketamine and medetomidine mixture could be important to the trend of the cortical connectivity dynamics.

The synchronization values within the theta band during the awake-like pattern of activity suggested a relation with the results found in the sleep-wake cycle. Synchronization in the theta and alpha bands seemed to accurately distinguish between the SWS sleep stage against wakefulness and REM sleep stages. In the anesthetized state was observed the emergence of high values in theta contrasting with the progressive decrease experienced by the rest of frequency bands at each tested dosage. These results showed a convergence in the relevance of the synchrony in the theta band related with desynchronized and active patterns of activity in both physiological and anesthetized states. Considering this, cortical synchronization at this frequency band could be indicating a correlation restricted to features from the activity pattern regardless of the state of consciousness.

Within this work we also approached the study of the cortical neural population dynamics in an anesthetized state from a single-neuron scale. We applied definitions and measurements that are also used in the analysis of LFP data. More specifically, the single-neuron scale allowed the observation of synchronous events similar to the Up states produced in anesthesia (Steriade et al., 1993). It has been already described that features such as the spatiotemporal and membrane potential dynamics from the activity during wakefulness and the Up states in anesthesia and SWS are also similar (Destexhe et al., 1999; 2007). Although, the quantification performed of their parameters of the slow oscillation suggested that despite the dynamics at a single-neuronal scale seemed analogous, the Up states from wakefulness and anesthesia differed in parameters from the slow oscillation such as the FR and the Up states duration and functional connectivity. However, in order to further explore both these similarities and differences is important to increase the sample and to determine the extent to which a freely-moving animal presents this type of Up-state like synchronization which we observe in the head-fixed animal.

This study has provided data from different scales of the cortical dynamics that are established as the level of anesthesia varies among their distinct stages: from wakefulness, within the induction, maintenance and fade-out all the way to awakening.

Given the large heterogeneity of results described in the scientific literature about this line of research, it seems necessary to characterize as many features as possible using a common methodology during the anesthetic period with distinct types of anesthetics and doses. With these multi-scale data, we can address the search for a consistency in the brain patterns of

activity over time that allows a functional distinction of stages and eventually clarify how those correspond to distinct neural mechanisms and their levels of consciousness.

5.3. Thalamic stimulation during an anesthetized state

Electrical stimulation of nuclei belonging or connected to the ARAS resulted in an increase in behavioral arousal (Moruzzi and Magoun, 1949; Cohadon et al., 1985; Tsubokawa et al., 1990; Schiff et al., 2007; Alkire et al., 2007; Yamamoto et al., 2010; Brown et al., 2012; Kundishora et al., 2017). However, the reported consequences on cortical activity have not been homogeneous, reporting both a cortical desynchronization with a high frequency stimulation and a reduction of the arousal with a low frequency stimulation (Moruzzi and Magoun, 1949).

In our experiments we applied the parameters proven to be of functional relevance when were delivered in the PF nucleus as well as in other intralaminar thalamic nuclei (Moruzzi and Magoun, 1949; Cohadon and Richer, 1993; Tsubokawa et al., 1990; Vale-Martínez et al., 1999; Guillazo-Blanch et al., 1999; Sos-Hinojosa et al., 2003; Lin et al., 2007; Andero et al., 2007; Yamamoto et al., 2010; Cervera-Ferri et al., 2016). We delivered a stimulation consisted in 120 s of square pulse trains of 500 ms each at 50 Hz of frequency and 60 μA of intensity. According to the literature, this stimulation is considered as a low frequency which in rats has not only shown to be able to reverse memory deficits (Sos-Hinojosa et al., 2003) but even to enhance memory consolidation (Guillazo-Blanch et al., 1999).

With this stimulation we observed a change in the oscillatory activity of the prefrontal cortex compatible with an increase in the excitability, which according to our studies of cortical activity in different levels of anesthesia, is compatible with a lower level of anesthesia and therefore, with a step closer in the state of arousal. Interestingly, in the studies in our group in lighter levels of anesthesia it was found, as here, a higher slow oscillatory frequency, higher regularity, decreased duration of Up and Down states, all changes compatible with increased excitability and a state closer to arousal (D'Andola et al., 2018; Tort-Colet et al, 2019; Dasilva et al, 2020).

We did not consider that this stimulation evoked a shift in the brain state, as seen in the aforementioned studies, since the cortical activity never ceased the bistability of the slow oscillation. Therefore, we suggest that the thalamic stimulation produced an increase in cortical arousal, reflected in the enhancement of the regularity in the slow oscillatory activity (Tort-Colet et al, 2019; Dasilva et al, 2020).

It also should be noted that isoflurane, like other anesthetics severely depressed essential components of the ARAS, critical for consciousness (Rudolph and Antkowiak, 2004). In this context of deep anesthesia, even this validated stimulation may not be an enough input to activate these nuclei at a level required to provoke a complete shift of brain state. Interestingly, the changes observed in the gamma synchronization are opposite, suggesting that changes in slow oscillations and gamma components can be dissociated depending on the underlying mechanism.

As mentioned above, the coupling of gamma oscillations is suggested to have an important role in cognitive binding and conscious perception (Gray and Singer, 1989; Srinivasan et al., 1999; Meador et al., 2002; Doesburg et al., 2005; Nakatani et al., 2005; Palva et al., 2005; Hwang et al., 2019). However, we found a disruption in gamma cortico-cortical synchrony from distant regions. This is consistent with the results found with multiple other anesthetics, where they reported a decrease in gamma coherence particularly pronounced across distant cortical regions (John et al., 2001; Alkire et al., 2008; Lewis et al., 2012). It has been suggested that this impairment in gamma also affects the transmission and integration of information, crucial elements of an activated state with conscious perception (Gray and Singer, 1989; Llinás, 1991; Singer and Gray, 1995; Tassi and Muzet, 2001; Hwang et al., 2019).

Chapter 6

Conclusions

1. The PLV of cortical synchronization in the high gamma band distinguishes with high accuracy between behavioral stages of the sleep-wake cycle (wakefulness versus sleep), while synchronization within the theta and alpha bands could distinguish between their brain patterns of activity (SWS versus awake and REM stages).

2. The LFP power ratios of beta (20-30 Hz)-low/medium gamma (30-80 Hz) and theta (5-10 Hz)-delta (1-5 Hz) together with the information from the EMG fluctuations precisely predict and allow the online classification of awake, SWS and REM sleep stages of the sleep-wake cycle.

3. Preliminary results show that not only the frequency of an auditory stimulus but also the stage of the sleep-wake cycle plays a role in the modulation of an auditory evoked cortical response. The online classification of stages will allow a detailed investigation of stimulus processing in different states.

4. The existence of two distinct patterns of activity (awake-like and slow oscillation) during different levels of anesthesia, is evidenced by their differences in their PSD that allows the performance of a supervised classification in unclassified signals.

5. In each of the two defined types of activity (awake-like and slow oscillation) during different levels of anesthesia, similar dynamics can be observed to those that appear in distinct stages of physiological states (wakefulness and slow wave sleep), which consist in an enhancement of the power in low frequencies and a decrease of gamma during the slow oscillatory pattern and an increase of the gamma band and decrease of low frequency ranges during an awake-like pattern of activity.

6. The anesthetic mixture of ketamine and medetomidine disrupts spatial cortical synchrony, also called functional connectivity, in all frequency bands more broadly at a deeper dose compared to a lighter dose. This suggests that in deep anesthesia the dynamics are more local, even when the temporal synchronization in slow waves is larger.

7. A synchronization peak in the theta band during the awake-like activity pattern of an anesthetized state, further supports the hypothesis that cortical synchronization in this frequency band could distinguish specific features from a desynchronized and active activity pattern, regardless of the conscious state.

8. The recording by means of calcium imaging of neural populations with a single-neuron resolution reveals the spatiotemporal activity in ≈300 local neurons in synchronous vs asynchronous states. In spite of the asynchrony that characterizes the awake state, this technique allows the detection and measurement of synchronous oscillatory events during wakefulness (Up states).

9. The Up states or synchronized events recording in the awake differ from anesthetized Up states presenting a more variable duration, higher FR and the involvement of a larger number of neurons, suggesting different underlying network basis.

10. The linear relation among the FR and the spatial size of the Up state indicates a stable and balanced neural recruitment dynamic within each Up state occurrence.

11. Cortical connectivity at a single-neuronal scale during an anesthetized state engages a lesser number of neurons than during an awake state.

12. PF electrical stimulation of the thalamic parafascicular nucleus induces long-lasting changes in the slow oscillatory activity pattern of its innervated PrL cortex. Those changes are compatible with an enhancement in excitability and an activating effect during deep anesthesia, therefore inducing the cortical dynamics corresponding to a more awake state.

13. Electrical stimulation of the parafascicular nucleus disrupted the synchrony at the gamma band among the PrL and V1 cortical regions.

Bibliography

Abel T, Havekes R, Saletin JM and Walker MP. (2013) Sleep, plasticity and memory from molecules to whole-brain networks. *Curr Biol*, 23:R774–R788.

Abolafia JM, Martinez-Garcia M, Deco G and Sanchez-Vives MV. (2011) Slow modulation of ongoing discharge in the auditory cortex during an interval-discrimination task. *Front Integr Neurosci*, 1-6. doi:10.3389/fnint.2011.00060

Abolafia JM, Martinez-Garcia M, Deco G and Sanchez-Vives MV. (2013). Variability and information content in auditory cortex spike trains during an interval-discrimination task. *Journal of neurophysiology*, 110(9), 2163-2174.

Achermann P and Borbely AA. (1998a) Coherence analysis of the human sleep electroencephalogram. *Neuroscience*, 85:1195–1208.

Agnew HW and Webb WB. (1972). Measurement of sleep onset by EEG criteria. *Am J EEG Technol*, 12:127–34.

Akeju O and Brown EN. (2017) Neural oscillations demonstrate that general anesthesia and sedative states are neurophysiologically distinct from sleep. *Current opinion in neurobiology*, 44:178–185.

Akeju O, Westover, BM, Pavone KJ, Sampson AL, Hartnack KE, Brown EN and Purdon PL. (2014) Effects of Sevoflurane and Propofol on Frontal Electroencephalogram Power and Coherence. *Anesthesiology*, 121(5): 990–998.

Alkire MT, Haier RJ and Fallon JH. (2000). Toward a unified theory of narcosis: brain imaging evidence for a thalamocortical switch as the neurophysiologic basis of anesthetic-induced unconsciousness. *Conscious Cogn*, 9: 370–386.

Alkire MT, Hudetz AG and Tononi G. (2008) Consciousness and anesthesia. Science 322 (5903):876–880.

Alkire MT, McReynolds JR, Hahn EL, Trivedi AN. (2007) Thalamic microinjection of nicotine reverses sevoflurane-induced loss of righting reflex in the rat. *Anesthesiology*, 107(2):264–72.

Alkire MT. (1998) Quantitative EEG correlations with brain glucose metabolic rate during anesthesia in volunteers. *Anesthesiology*, 89:323–333.

Alonso LM, Proekt A, Schwartz TH, Pryor KO, Cecchi GA and Magnasco MO. (2014). Dynamical criticality during induction of anesthesia in human ECoG recordings. *Front. Neural Circ*, 8: 20. http://dx.doi.org/10.3389/fncir.2014.00020.

Amico E, Gomez F, Di Perri C, Vanhaudenhuyse A, Lesenfants D, Boveroux P, Bonhomme V, Brichant JF, Marinazzo D and Laureys S. (2014) Posterior cingulate cortex-related co-activation patterns: A resting state FMRI study in propofol-induced loss of consciousness. *PLoS One,* 9:e100012

Andero R, Torras-Garcia M, Quiroz-Padilla MF, Costa-Miserachs D and Coll-Andreu M. (2007) Electrical stimulation of the pedunculopontine tegmental nucleus in freely moving awake rats: Time- and site-specific effects on two-way active avoidance conditioning. *Neurobiology of Learning and Memory*, 87(4), 510–521.

Angel A. The G. L. Brown lecture. Adventures in anaesthesia. (1991). *Exp. Physiol,* 76: 1–38.

Antognini JF and Carstens E. (2002). In vivo characterization of clinical anaesthesia and its components. *Br. J. Anaesth,* 89:156–166.

Aouad MT and Nasr VG. 2005. Emergence agitation in children: an update. *Curr. Opin. Anaesthesiol,* 18: 614–619.

Arcelli P, Frassoni C, Regondi MC, De Biasi S, Spreafico R. (1997) GABAergic neurons in mammalian thalamus: a marker of thalamic complexity? *Brain Res Bull,* 42(1):27-37.

Atienza M, Cantero JL, Escera C. (2001) Auditory information processing during human sleep as revealed by event-related brain potentials. *Clin Neurophysiol,* 112(11):2031-2045. doi:10.1016/s1388-2457(01)00650-2

Axmacher N et al. (2010) Cross-frequency coupling supports multi-item working memory in the human hippocampus. *Proc Natl Acad Sci USA,* 107:3228–3233.

Aydore S, Pantazis D and Leahy RM. (2012) A Note on the Phase Locking Value and its Properties. doi:10.1016/j.neuroimage.2013.02.008

Bai D, Pennefather PS, MacDonald JF and Orser BA (1999) The general anesthetic propofol slows deactivation and desensitization of GABA(A) receptors. *J Neurosci,* 19 (24):10635–10646.

Barash PG. (2009). Clinical anesthesia. 6th ed. Philadelphia: Wolters Kluwer/Lippincott Williams and Wilkins.

Barttfeld P, Uhrig L, Sitt JD, Sigman M, Jarraya B and Dehaene S. (2015). Signature of consciousness in the dynamics of resting-state brain activity. *Proc. Natl. Acad. Sci. U.S.A,* 112 (3): 887–892.

Bastuji H, Garcia-Larrea L. (1999). Evoked potentials as a tool for the investigation of human sleep. *Sleep Med Rev*, 3:23–45.

Becker K, Eder M, Ranft A, Meyer L and Zieglgänsberger W. (2012). Low Dose Isoflurane Exerts Opposing Effects on Neuronal Network Excitability in Neocortex and Hippocampus. *PLoS ONE,* 7(6): 39346. https://doi.org/10.1371/journal.pone.0039346

Bedwell SA, Billett EE, Crofts JJ and Tinsley CJ. (2014) The topology of connections between rat prefrontal, motor and sensory cortices. *Frontiers in Systems Neuroscience,* 177(8).

Bedwell SA, Billett EE, Crofts JJ and Tinsley CJ. (2017). Differences in anatomical connections across distinct areas in the rodent prefrontal cortex. *European Journal of Neuroscience,* 45(6), 859–873.

Belelli D, Peden DR, Rosahl TW, Wafford KA and Lambert JJ. (2005). Extrasynaptic GABAA receptors of thalamocortical neurons: a molecular target for hypnotics. *J. Neurosci,* 25: 11513–11520.

Benington JH and Heller HC. (1995) Restoration of brain energy metabolism as the function of sleep. *Prog Neurobiol*, 45:347–360.

Bettinardi RG, Tort-Colet N, Ruiz-Mejias M, Sanchez-Vives MV and Deco G. (2015) Gradual emergence of spontaneous correlated brain activity during fading of general anesthesia in rats: Evidences from fMRI and local field potentials. *NeuroImage,* 114, 185–198.

Billard V, Gambus PL, Chamoun N, Stanski DR, Shafer SL. (1997) A comparison of spectral edge, delta power, and bispectral index as EEG measures of alfentanil, propofol, and midazolam drug effect. *Clin Pharmacol Ther,* 61:45–58.

Blain-Moraes S, Lee U, Ku S, Noh G and Mashour GA. (2014). Electroencephalographic effects of ketamine on power, cross-frequency coupling, and connectivity in the alpha bandwidth. *Front. Syst. Neurosci*, 8, 114.

Blumenfeld H et al. (2004) Ictal neocortical slowing in temporal lobe epilepsy. Neurology, 63(6):1015–1021.

Blumenfeld H. (2012) Impaired consciousness in epilepsy. *Lancet Neurol,* 11:814–826. [PubMed: 22898735]

Bogen JE. (1995) On the neurophysiology of consciousness: I. An overview. *Consciousness and Cognition,* 4:52–62. [PubMed: 7497102].

Boly M, Moran R, Murphy M, et al. (2012) Connectivity changes underlying spectral EEG changes during propofol-induced loss of consciousness. *J Neurosci*, 32: 7082–90.

Boly M, Tshibanda L, et al. (2009) Functional connectivity in the default network during resting state is preserved in a vegetative but not in a brain dead patient. *Human brain mapping,* 30(8):2393– 400. [PubMed: 19350563].

Bonhomme V et al. (2001). Propofol anesthesia and cerebral blood flow changes elicited by vibrotactile stimulation: a positron emission tomography study. *J. Neurophysiol,* 85:1299–1308.

Bonhomme V, Vanhaudenhuyse A, Demertzi A, Bruno MA, Jaquet O, Bahri MA, et al. (2016) Resting-state network-specific breakdown of functional connectivity during Ketamine alteration of consciousness in volunteers. *Anesthesiology,* 125: 873–888.

Boveroux P, Vanhaudenhuyse A, Bruno MA, Noirhomme Q, Lauwick S, Luxen A et al. (2010). Breakdown of within- and between-network resting state functional magnetic resonance imaging connectivity during propofol-induced loss of consciousness. *Anesthesiology,* 113: 1038–1053. doi: 10.1097/ALN.0b013e3181f697f5.

Bradfield LA, Bertran-Gonzalez J, Chieng B, and Balleine BW. (2013) The thalamostriatal pathway and cholinergic control of goal-directed action: interlacing new with existing learning in the striatum. *Neuron,* 79, 153-166.

Bragin A, Jando G, Nadasdy Z, Hetke J, Wise K and Buzsáki G. (1995). Gamma (40–100 Hz) oscillation in the hippocampus of the behaving rat. *J. Neurosci.* 15:47-60.

Breshears JD, Roland JL, Sharma M, Gaona CM, Freudenburg ZV, Tempelhoff R, … Leuthardt EC. (2010) Stable and dynamic cortical electrophysiology of induction and emergence with propofol anesthesia. *PNAS,* 107(49): 21170–21175.

Broughton R. (1982). Human consciousness and sleep/waking rhythms: a review of some neuropsychological considerations. *J Clin Neuropsychol*, 4(3):193-218.

Brown EN and Purdon PL. (2013). The aging brain and anesthesia. *Curr. Opin. Anaesthesiol*, 26: 414–419.

Brown EN, Lydic R and Schiff ND. (2010). General anesthesia, sleep, and coma. *N. Engl. J. Med*, 363:2638–2650.

Brown EN, Purdon PL and Van Dort CJ (2011) General anesthesia and altered states of arousal: A systems neuroscience analysis. *Annu Rev Neurosci*, 34: 601–628.

Brown RE, Basheer R, McKenna JT, Strecker RE and McCarley RW. (2012) Control of sleep and wakefulness. *Physiological Reviews*, 92(3):1087–1187.

Bruhn J, Röpcke H and Hoeft A. (2000) Approximate entropy as an electroencephalographic measure of anesthetic drug effect during desflurane anesthesia. *Anesthesiology,* 92(3):715-726. doi:10.1097/00000542-200003000-00016

Bullock TH, McClune MC and Enright JT. (2003). Are the electroencephalograms mainly rhythmic? Assessment of periodicity in wide-band time series. *Neuroscience*, 121:233–52.

Buzsáki G and Chrobak JJ. (1995). Temporal structure in spatially organized neuronal ensembles: a role for interneuronal networks. *Curr. Opin. Neurobiol.* 5:504-510.

Buzsáki G. (1989). Two-stage model of memory trace formation: a role for "noisy" brain states. *Neuroscience*, 31:551–570.

Buzsáki G. (1996) The hippocampo-neocortical dialogue. *Cereb. Cortex*, 6: 81-92.

Buzsáki G. (2002) Theta oscillations in the hippocampus. *Neuron,* 33:325–340.

Buzsáki G. (2006). Rhythms of the Brain. *Oxford Univ. Press*, Oxford.

Campagna JA, Miller KW and Forman SA. (2003) Mechanisms of actions of inhaled anesthetics. *N. Engl. J. Med,* 348, 2110–2124.

Canolty RT et al. (2006) High gamma power is phase-locked to theta oscillations in human neocortex. *Science,* 313:1626–1628.

Cantero JL, Atienza M, Madsen JR and Stickgold R. (2004). Gamma EEG dynamics in neo- cortex and hippocampus during human wakefulness and sleep. *Neuroimage*, 22:1271–80.

Cantero JL, Atienza M. (2005) The role of neural synchronization in the emergence of cognition across the wake-sleep cycle. *Rev Neurosci*, 16(1):69-83. doi:10.1515/revneuro.2005.16.1.69

Cariani P. (2000). Anesthesia, neural information processing, and conscious awareness. *Conscious Cogn,* 9(3):387–95.

Casali AG, Gosseries O, Rosanova M, Boly M, Sarasso S, Casali KR, Casarotto S, Bruno M-A, Laureys S, Tononi G and Massimini M. (2013) A Theoretically Based Index of Consciousness Independent of Sensory Processing and Behavior. *Sci Transl Med,* 5:198ra105-198ra105.

Castano-Prat P, Perez-Zabalza M, Perez-Mendez L, Escorihuela RM, Sanchez-Vives MV. (2017) Slow and Fast Neocortical Oscillations in the Senescence-Accelerated Mouse Model SAMP8. *Front Aging Neurosci,* 9:141. doi:10.3389/fnagi.2017.00141.

Castro S, Cavelli M, Vollono P, Chase MH, Falconi A and Torterolo P. (2014) Inter-hemispheric coherence of neocortical gamma oscillations during sleep and wakefulness. *Neurosci Lett*, 578:197–202.

Castro S, Falconi A, Chase MH and Torterolo P. (2013) Coherent neocortical 40-Hz oscillations are not present during REM sleep. *Eur J Neurosci*, 37: 1330–9.

Castro-Alamancos MA. (2004a) Absence of rapid sensory adaptation in neocortex during information processing states. *Neuron,* 41:455–464. [PubMed: 14766183]

Cauda F, Micon BM, Sacco K, et al. (2009) Disrupted intrinsic functional connectivity in the vegetative state. *J Neurol Neurosurg Psychiatry,* 80:429–431. [PubMed: 19289479].

Cavelli M, Castro S, Schwarzkopf N, Chase MH, Falconi A and Torterolo P. (2015). Coherent neocortical gamma oscillations decrease during REM sleep in the rat. *Behavioural Brain Research*, 281:318–325.

Ceballo S, Bourg J, Kempf A, Piwkowska Z, Daret A, Pinson P… Bathellier B. (2019). Cortical recruitment determines learning dynamics and strategy. *Nature Communications*, 10(1479). https://doi.org/10.1038/s41467-019-09450-0

Cervera-Ferri A, Teruel-Marti V, Barcelo-Molina M, Martinez-Ricos J, Luque-Garcia A, Martinez-Bellver S and Adell A. (2016) Characterization of oscillatory changes in hippocampus and amygdala after deep brain stimulation of the infralimbic prefrontal cortex. *Physiol Rep,* 4(14).

Chander D, García PS, MacColl JN, Illing S and Sleigh JW. (2014) Electroencephalographic variation during end maintenance and emergence from surgical anesthesia. *PLoS One*, 9, e106291.

Chase MH, Morales FR. (1990). The atonia and myoclonia of active (REM) sleep. *Annu Rev Psychol*, 41:557–584.

Chen J, Li W, Hu X and Wang D. 2010. Emergence agitation after cataract surgery in children: a comparison of midazolam, propofol and ketamine. *Paediatr. Anaesth,* 20 (9): 873–879.

Chen T-W, Wardill TJ, Sun Y, Pulver SR, Renninger SL, Baohan A… Kim DS. (2013). Ultra-sensitive fluorescent proteins for imaging neuronal activity. *Nature,* 499(7458): 295–300.

Chennu S, O'Connor S, Adapa R, Menon DK and Bekinschtein TA. (2016). Brain connectivity dissociates responsiveness from drug exposure during propofol-induced transitions of consciousness. *PLoS Comput. Biol,* 12, e1004669.

Ching S, Cimenser A, Purdon PL, Brown EN, Kopell NJ. (2010) Thalamocortical model for a propofol-induced alpha-rhythm associated with loss of consciousness. *Proc Natl Acad Sci USA*, 107: 22665–22670.

Chudy D, Deletis V, Rogic M, Paradzik V and Grahovac G. (2012) Deep brain stimulation for the early treatment of the minimal consciousness state and vegetative state. Stereotactic and Functional *Neurosurgery,* 90: 1–10.

Cimenser A, Purdon PL, Pierce ET, Walsh JL, Salazar-Gomez AF, et al. (2011) Tracking brain states under general anesthesia by using global coherence analysis. *Proc Natl Acad Sci USA*, 108: 8832–8837.

Clemens Z, Fabo D and Halasz P. (2006) Twenty-four hours retention of visuospatial memory correlates with the number of parietal sleep spindles. *Neurosci. Lett.* 403:52–56.

Cohadon F and Richer E. (1993) Deep cerebral stimulation in patients with post-traumatic vegetative state. 25 cases. *Neurochirurgie,* 39:281–292, (Fr).

Cohadon F, Richer E, Rougier A, et al. (1985) Deep brain stimulation in cases of prolonged post-traumatic unconsciousness. In: Y. Lazorthes, A. R. M. Upton, eds. *Neurostimulation: an Overview.* pp. 247–250. Mt. Kisco, New York: Futura Publishing Company.

Cohen MR and Maunsell JH. (2010). A neuronal population measure of attention predicts behavioral performance on individual trials. *The Journal of neuroscience: the official journal of the Society for Neuroscience*, 30:15241–15253. [PubMed: 21068329].

Cohen MR and Maunsell JH. (2011). When attention wanders: how uncontrolled fluctuations in attention affect performance. *The Journal of neuroscience: the official journal of the Society for Neuroscience*, 31:15802–15806.

Compte A, Reig R, Descalzo VF, Harvey MA, Puccini GD, et al. (2008) Spontaneous High-Frequency (10–80 Hz) Oscillations during UP states in the cerebral cortex in vitro. J Neurosci, 28: 13828–13844.

Cote KA, Epps TM and Campbell KB. (2000). The role of the spindle in human information processing of high-intensity stimuli during sleep. *Journal of Sleep Research,* 9(1): 19–26.

Cote KA. (2002). Probing awareness during sleep with the auditory odd-ball paradigm. *Int J Psychophysiol.* 46:227–241.

Crick F, Mitchison G. (1983) The function of dream sleep. *Nature*, 304:111–114.

Crochet S and Petersen CC. (2006). Correlating whisker behavior with membrane potential in barrel cortex of awake mice. *Nat. Neurosci*, 9:608–610.

Crone NE et al. (2001) Electrocorticographic gamma activity during word production in spoken and sign language. *Neurology,* 57:2045–2053.

Cull-Candy S, Brickley S and Farrant M. (2001). NMDA receptor subunits: diversity, development and disease. *Curr. Opin. Neurobiol,* 11: 327–335.

Czisch M, Wetter TC, Kaufmann C, Pollmächer T, Holsboer F and Auer DP. (2002) Altered processing of acoustic stimuli during sleep: reduced auditory activation and visual deactivation detected by a combined fMRI/EEG study. *Neuroimage,*16(1):251-258. doi:10.1006/nimg.2002.1071.

Damoiseaux JS, Rombouts SA, Barkhof F, et al. (2006). Consistent resting-state networks across healthy subjects. *Proc Natl Acad Sci* U S A; 103:13848–13853.

D'Andola M, Rebollo B, Casali AG, et al. (2018) Bistability, Causality, and Complexity in Cortical Networks: An In Vitro Perturbational Study. *Cereb Cortex,* 28(7):2233-2242. doi:10.1093/cercor/bhx122

Dang-Vu TT, Bonjean M, Schabus M, Boly M, Darsaud A, et al. (2011) Interplay between spontaneous and induced brain activity during human non-rapid eye movement sleep. *Proc Natl Acad Sci U S A,* 108: 15438–15443.

Dang-Vu TT, Schabus M, Desseilles M, Albouy G, Boly M, Darsaud A, … Maquet P. (2008). Spontaneous neural activity during human slow wave sleep. *Proceedings of the National Academy of Sciences of the United States of America*, 105(39):15160–15165.

Dang-Vu TT. (2012) Neuronal Oscillations in Sleep: Insights from Functional Neuroimaging. *Neuromol Med,* 14: 154–167.

Dasilva M, Navarro-Guzman A, Ortiz-Romero P, et al. (2020) Altered Neocortical Dynamics in a Mouse Model of Williams-Beuren Syndrome. *Mol Neurobiol,* 57(2):765-777. doi:10.1007/s12035-019-01732-4

Datta, S. (2000). Avoidance task training potentiates phasic pontine- wave density in the rat: A mechanism for sleep-dependent plasticity. *Journal of Neuroscience*, 20(22), 8607–8613.

De Gennaro L, Ferrara M and Bertini M. (2001). The boundary between wakefulness and sleep: quantitative electroencephalo- graphic changes during the sleep onset period. *Neuroscience*, 107:1–11.

Delacour J. (1969). Role of a medial thalamic structure in various types of instrumental defensive conditioning. *Physiol. Behav,* 4: 969–974.

Dement WC and Kleitman N. (1957). The relation of eye movements during sleep to dream activity: an objective method for the study of dreaming. *J Exp Psychol*, 53:339–46.

Deneux T, Faugeras O. (2010) EEG-fMRI fusion of paradigm-free activity using Kalman filtering. *Neural Comput*, 22(4):906-948. doi:10.1162/neco.2009.05-08-793

Deneux T, Kaszas A, Szalay G, et al. (2016) Accurate spike estimation from noisy calcium signals for ultrafast three-dimensional imaging of large neuronal populations in vivo. *Nat Commun,* 7:12190. doi:10.1038/ncomms12190

Destexhe A, Contreras D, Steriade M. (1999) Spatiotemporal analysis of local field potentials and unit discharges in cat cerebral cortex during natural wake and sleep states. *J Neurosci*, 19: 4595–4608.

Destexhe A, Hughes SW, Rudolph M and Crunelli V. (2007) Are corticothalamic UP states fragments of wakefulness? The dynamics of single neurons during "activated" states and SWS. *Trends Neurosci.* 30(7):334-342. doi:10.1016/j.tins.2007.04.006.

Di Perri C, Stender J, Laureys S and Gosseries O. (2014). Functional neuroanatomy of disorders of consciousness. *Epilepsy Behav*, 30: 28–32.

Dickson CT, Biella G and de Curtis M. (2003). Slow periodic events and their transition to gamma oscillations in the entorhinal cortex of the isolated Guinea pig brain. *J Neurophysiol*, 90: 39–46.

Dinges DF, Orne MT and Orne EC. (1985). Assessing performance upon awakening from naps during quasi-continuous operations. *Behav Res Methods Instrum Comput*, 17:37–45.

Doesburg S, Kitajo K and Ward L. (2005) Increased gamma-band synchrony precedes switching of conscious perceptual objects in binocular rivalry. *NeuroReport,* 16:1139–1142.

Driesen NR, McCarthy G, Bhagwagar Z, Bloch M, Calhoun V, D'Souza DC, Gueorguieva R, He G, Ramachandran R, Suckow RF, Anticevic A, Morgan PT and Krystal JH. (2013) Relationship of resting brain hyperconnectivity and schizophrenia-like symptoms produced by the NMDA receptor antagonist ketamine in humans. *Mol Psychiatry,* 18:1199–204.

Edeline JM, Dutrieux G, Manunta Y and Hennevin E. (2001) Diversity of receptive field changes in auditory cortex during natural sleep. *Eur J Neurosci,* 14(11):1865-1880. doi:10.1046/j.0953-816x.2001.01821.x

Edlow BL, Takahashi E, Wu O, Benner T, Dai G, Bu L, … Folkerth RD. (2012) Neuroanatomic Connectivity of the Human Ascending Arousal System Critical to Consciousness and Its Disorders. *J Neuropathol Exp Neurol,* 71(6): 531–546.

Elton M, Winter O, Heslenfeld D, Loewy D, Campbell K and Kok A. (1997). Event-related potentials to tones in the absence and presence of sleep spindles. *Journal of Sleep Research,* 6(2): 78–83.

Engel AK and Singer W. (2001). Temporal binding and the neural correlates of sensory awareness. *Trends Cogn. Sci*, 5: 16–25.

Esser SK, Hill SL, Tononi G (2009) Breakdown of effective connectivity during slow wave sleep: investigating the mechanism underlying a cortical gate using large-scale modeling. *JNeurophysiol*, 102(4):2096-2111. doi:10.1152/jn.00059.2009

Fagerholm ED, Scott G, Shew WL, et al. (2016) Cortical entropy, mutual information and scale-free dynamics in waking mice. *Cerebral Cortex*, 26: 3945–52.

Feinberg I and March JD. (1988). Cyclic delta peaks during sleep result of a pulsatile endocrine process? *Arch Gen Psychiatry*, 45:1141–2.

Ferrara M, Curcio G, Fratello F, Moroni F, Marzano C, Pellicciari MC, et al. (2006). The electroencephalographic substratum of the awakening. *Behav Brain Res*, 167:237–44.

Ferrarelli F, Massimini M, Sarasso S, Casali A, Riedner BA, Angelini G… Pearce RA. (2010) Breakdown in cortical effective connectivity during midazolam-induced loss of consciousness. *Proceedings of the National Academy of Sciences of the United States of America,* 107(6): 2681–2686.

Ferrer-Allado T, Brechner VL, Dymond A, Cozen H and Crandall P. (1973) Ketamine-induced electroconvulsive phenomena in the human limbic and thalamic regions. *Anesthesiology*, 38:333–44.

Feshchenko VA, Veselis RA and Reinsel RA. (2004) Propofol-induced alpha rhythm. *Neuropsychobiology*, 50:257-266.

Fingelkurts AA, Bagnato S, Boccagni C and Galardi G. (2012). Toward operational architectonics of consciousness: basic evidence from patients with severe cerebral injuries. *Cogn. Process,* 13: 111–131.

Fiset P et al. (1999) Brain mechanisms of propofol-induced loss of consciousness in humans: a positron emission tomographic study. *J. Neurosci*, 19: 5506–5513.

Fishbein W. (1971). Disruptive effects of rapid eye movement sleep deprivation on long-term memory. *Physiol Behav*, 6:279–282.

Flores FJ, Hartnack KE, Fath AB, et al. (2017) Thalamocortical synchronization during induction and emergence from propofol-induced unconsciousness. *Proc Natl Acad Sci U S A,* 114(32):E6660-E6668. doi:10.1073/pnas.1700148114

Franks N and Lieb W. (1994). Molecular and cellular mechanisms of general anaesthesia. *Nature,* 367: 607–614. https://doi.org/10.1038/367607a0

Franks NP and Lieb WR. (1988). Volatile general anaesthetics activate a novel neuronal K+ current. *Nature,* 333:662–664.

Franks NP. (2008) General anaesthesia: from molecular targets to neuronal pathways of sleep and arousal. *Nat Rev Neurosci,* 9(5): 370–386.

French JD, Vezeano M and Magoun HW. (1953). A neural basis of the anesthetic state. A.*M.A. Arch. Neurol. Psychiat*, 69:519–529.

Fries P. (2005). A mechanism for cognitive dynamics: neuronal communication through neuronal coherence. *Trends Cogn. Sci*, 9: 474–480.

Gao YR, Ma Y, Zhang Q, Winder AT, Liang Z, Antinori L, Drew PJ and Zhang N. (2017). Time to wake up: studying neurovascular coupling and brain-wide circuit function in the un-anesthetized animal. *Neuroimage,* ;153:382-398. doi:10.1016/j.neuroimage.2016.11.069

Garfield JM, Garfield FB, Stone JB, Hopkins D and Johns LA. (1972). A comparison of psychologic responses to ketamine and thiopental-nitrous oxide-halothane anesthesia. *Anesthesiology*, 36:329–338.

Gentet LJ, Avermann M, Matyas F, Staiger JF and Petersen CC. (2010). Membrane potential dynamics of GABAergic neurons in the barrel cortex of behaving mice. *Neuron*, 65: 422–435.

Gervasoni D, Lin SC, Ribeiro S, Soares ES, Pantoja J and Nicolelis MAL. (2004) Global Forebrain Dynamics Predict Rat Behavioral States and Their Transitions. *The Journal of Neuroscience*, 24(49): 11147–11137.

Gibbs F, Gibbs E, Lennox W. (1937) Effect on the electroencephalogram of certain drugs which influence nervous activity. *Arch Intern Med*, 60:154–166.

Goldman-Rakic PS and Porrino LJ. (1985). The primate mediodorsal (MD) nucleus and its projection to the frontal lobe. *J. Comp. Neurol,* 242: 535–560.

Gottesmann, C. (1973). Le stade intermédiaire du sommeil chez le rat. Rev. Electroencéphalogr. *Neurophysiol. Clin*, 3:65–68. doi: 10.1016/S0370-4475(73) 80026-7

Grandjean J, Schroeter A, Batata I and Rudin M. (2014). Optimization of anesthesia protocol for resting-state fMRI in mice based on differential effects of anesthetics on functional connectivity patterns. *Neuroimage,* 102 (Pt 2): 838–847.

Gray CM and Singer W. (1989). Stimulus-specific neuronal oscillations in orientation columns of cat visual cortex. *Proc Natl Acad Sci USA*, 86(5):1698–1702.

Grenier F, Timofeev I and Steriade M (2001) Focal synchronization of ripples (80– 200 Hz) in neocortex and their neuronal correlates. *J Neurophysiol*, 86: 1884–1898.

Groenewegen HJ and Berendse HW. (1994) The specificity of the 'nonspecific' midline and intralaminar thalamic nuclei. *Trends in Neurosciences,* 17(2): 52–57.

Gross DW and Gotman J. (1999) Correlation of high-frequency oscillations with the sleep-wake cycle and cognitive activity in humans. *Neuroscience*, 94:1005–1018.

Gugino LD et al. (2001) Quantitative EEG changes associated with loss and return of consciousness in healthy adult volunteers anaesthetized with propofol or sevoflurane. *Br. J. Anaesth*, 87: 421–428.

Guillazo-Blanch G, Vale-Martínez AM, Martí-Nicolovius M, Coll-Andreu M and Morgado-Bernal I. (1999) The parafascicular nucleus and two-way active avoidance: effects of electrical stimulation and electrode implantation. *Experimental Brain Research,* 129(4): 605–614.

Guldenmund P, Demertzi A, Boveroux P, Boly M, Vanhaudenhuyse A, Bruno MA, Gosseries O, Noirhomme Q, Brichant JF, Bonhomme V, Laureys S and Soddu A. (2013) Thalamus, brainstem and salience network connectivity changes during propofol-induced sedation and unconsciousness. *Brain Connect, 3:273–85.*

Gummadavelli A, Motelow JE, Smith N, Zhan Q, Nicholas D, Blumenfeld H… Haven N. (2015). Thalamic stimulation to improve level of consciousness after seizures: Evaluation of electrophysiology and behavior. *Epilepsia,* 56(1): 114–124.

Hall RD and Borbely AA. (1970). Acoustically evoked potentials in the rat during sleep and waking. *Exp Brain Res*,11(1):93-110. doi:10.1007/BF00234203.

Hamilton C, Ma Y and Zhang N. (2017) Global reduction of information exchange during anesthetic-induced unconsciousness. *Brain Struct. Funct*, 222 (7): 3205–3216.

Hamrahi H, Stephenson R, Mahamed S, Liao KS, Horner RL. (2001) Selected Contribution: Regulation of sleep-wake states in response to intermittent hypoxic stimuli applied only in sleep. *J Appl Physiol*, 90(6):2490-2501. doi:10.1152/jappl.2001.90.6.2490

Hanbury J, Ajmone-Marsan C and Dilworth M. (1954) Pathways of non-specific thalamocortical projection system. *Electroencephalogr Clin Neurophysiol,* 6:103–118.

Hashmi JA, Loggia ML, Khan S, et al. (2017) Dexmedetomidine Disrupts the Local and Global Efficiencies of Large-scale Brain Networks. *Anesthesiology,* 126(3):419-430. doi:10.1097/ALN.0000000000001509

Hebb DO. (1949). The organization of behavior: a neuropsychological theory. New York: Wiley.

Hennevin E, Hars B, Maho C and Bloch V. (1995). Processing of learned information in paradoxical sleep: relevance for memory. *Behav Brain Res*, 69:125–135.

Hennevin E, Huetz C and Edeline JM. (2007) Neural representations during sleep: from sensory processing to memory traces. *Neurobiol Learn Mem*, 87: 416–440.

Hentschke H, Raz A, Krause BM, Murphy CA and Banks MI. (2017). Disruption of cortical network activity by the general anaesthetic isoflurane. *Br J Anaesth,* 119(4):685-696. doi:10.1093/bja/aex199

Herculano-Houzel S, Munk MH, Neuenschwander S and Singer W. (1999) Precisely synchronized oscillatory firing patterns require electroencephalographic activation. *J Neurosci,* 19:3992–4010.

Höflich A, Hahn A, Küblböck M, Kranz GS, Vanicek T, Windischberger C, Saria A, Kasper S, Winkler D and Lanzenberger R. (2015) Ketamine-induced modulation of the thalamo-cortical network in healthy volunteers as a model for schizophrenia. *Int J Neuropsychopharmacol,* 18.

Hori T, Hayashi M and Morikawa T. (1994). Topographical EEG changes and the hypnagogic experience. In Ogilvie RD and Harsh JR (Eds.), *Sleep onset: Normal and abnormal processes* (pp. 237-253). Washington, DC, US: American Psychological Association.

Hori T, Tanaka H and Hayashi M. (1998). Topographic mapping of EEG spectral power and coherence in the hypnagogic period. In: Koga Y, Nagata K and Hirata K, editors. *Brain topography today.* Amsterdam.

Horner RL and Peever JH. (2017) Brain Circuitry Controlling Sleep and Wakefulness. *Sleep Neurology*, 4 (Vol. 23), p 955–972.

Hudetz AG and Mashour GA. (2016) Disconnecting Consciousness: Is There a Common Anesthetic End Point? *Anesth Analg,* 123(5):1228-1240. doi:10.1213/ANE.0000000000001353

Hudetz AG, Liu X and Pillay S. (2015). Dynamic repertoire of intrinsic brain states is reduced in propofol-induced unconsciousness. *Brain Connect,* 5 (1): 10–22.

Hudetz AG, Vizuete JA, Pillay S and Mashour GA. (2016). Repertoire of Mesoscopic cortical activity is not reduced during anesthesia. *Neuroscience,* 17:402–417. http://dx.doi.org/10.1016/j.neuroscience.2016.10.023.

Hudetz AG. (2012) General anesthesia and human brain connectivity. *Brain Connect*, 2:291–302.

Hudson AE, Calderon DP, Pfaff DW and Proekt A. (2014) Recovery of consciousness is mediated by a network of discrete metastable activity states. *Proc Natl Acad Sci U S A,* 111:9283–9288.

Hudson RJ, Stanski DR, Saidman LJ, Meathe E. (1983) A model for studying depth of anesthesia and acute tolerance to thiopental. *Anesthesiology,* 59: 301– 308.

Hunt MJ, Raynaud B and Garcia R. (2006). Ketamine dose-dependently induces high-frequency oscillations in the nucleus accumbens in freely moving rats. *Biol. Psychiatry,* 60: 1206–1214.

Hwang E, Brown RE, Kocsis B, Kim T, Mckenna JT, Mcnally JM… Choi JH. (2019). Optogenetic stimulation of basal forebrain parvalbumin neurons modulates the cortical topography of auditory steady-state responses. *Brain Structure and Function*, 1-3.

Iber C, Ancoli-Israel S, Chesson A and Quan SF. The AASM Manual for the Scoring of Sleep and Associated Events: Rules, Terminology and Technical Specifications (American Academy of Sleep Medicine, Westchester, IL, 2007).

Imas OA, Ropella KM, Ward BD, Wood JD and Hudetz AG. (2005) Volatile anesthetics disrupt frontal-posterior recurrent information transfer at gamma frequencies in rat. NeurosciLett, 387: 145–50.

Inostroza M and Born J. (2013) Sleep for preserving and transforming episodic memory. *Annu Rev Neurosci*, 36:79–102.

Ishizawa Y et al. (2016). Dynamics of propofol-induced loss of consciousness across primate neocortex. *J. Neurosci,* 36, 7718.

Issa EB and Wang X. (2008). Sensory responses during sleep in primate primary and secondary auditory cortex. *J Neurosci,* 28: 14467–14480.

Jagannathan SR, Ezquerro-Nassar A, Jachs B, Pustovaya OV, Bareham CA & Bekinschtein TA. (2018). Tracking wakefulness as it fades: Micro-measures of alertness. *NeuroImage*, 176:138–151.

Jasper HH, Naquet R and King LE. (1955) Thalamocortical recruiting responses in sensory receiving areas in the cat. *Electroencephalogr. Clin. Neurophysiol.,* 7: 99–114.

Jasper HH. (1949) Diffuse projection systems: the integrative action of the thalamic reticular system. *Electroencephalogr Clin Neurophysiol,* 1:405–419.

Jia F et al. (2005). An extrasynaptic GABAA receptor mediates tonic inhibition in thalamic VB neurons. J. *Neurophysiol,* 94: 4491–4501.

Johansen-Berg H, Behrens TEJ, Sillery E, Ciccarelli O, Thompson AJ, Smith SM and Matthews PM. (2005a). Functional–anatomical validation and individual variation of diffusion tractography-based segmentation of the human thalamus. *Cereb. Cortex,* 15: 31–39. http://dx.doi.org/10.1093/cercor/bhh105

John ER et al. (2001) Invariant reversible QEEG effects of anesthetics. *Conscious Cogn*,10: 165–183.

John ER, Prichep LS. (2005). The anesthetic cascade: a theory of how anesthesia suppresses consciousness. *Anesthesiology,* 102, 447–471.

John ER. (2002) The neurophysics of consciousness. *Brain Res Brain Res Rev*, 39:1–28.

Jonckers E, Delgado y Palacios R, Shah D, Guglielmetti C, Verhoye M and Van der Linden A. (2014). Different anesthesia regimes modulate the functional connectivity outcome in mice. *Magn. Reson. Med*, 72 (4): 1103–1112.

Jones EG. (1981) Functional subdivision and synaptic organization of the mammalian thalamus. *Int Rev Physiol,* 25:173-245.

Jones EG. (1985) The intralaminar nuclei. In: The thalamus. (ed) *Plenum Press*, New York, pp 606–645.

Jones EG. (1991). The anatomy of sensory relay functions in the thalamus. *Prog. Brain Res,* 87: 29–52.

Jones EG. (1998) A new view of specific and nonspecific thalamocortical connections. *Adv Neurol,* 77:49–71. discussion 72-43. [PubMed: 9709817]

Jones EG. (2007). Thalamus 2 Vol. Set. *Cambridge*.

Jordan D, Ilg R, Riedl V, Schorer A, Grimberg S, Neufang S et al. (2013). Simultaneous electroencephalographic and functional magnetic resonance imaging indicate impaired cortical top–down processing in association with anesthetic-induced unconsciousness. *Anesthesiology,* 119: 1031–1042. doi: 10.1097/ALN.0b013e3182a7ca92.

Jouvet M. (1999) The paradox of sleep: the story of dreaming. Cambridge, MA: MIT.

Kaisti KK et al. (2003) Effects of sevoflurane, propofol, and adjunct nitrous oxide on regional cerebral blood flow, oxygen consumption, and blood volume in humans. *Anesthesiology,* 99:603–613.

Kalthoff D, Po C, Wiedermann D and Hoehn M. (2013). Reliability and spatial specificity of rat brain sensorimotor functional connectivity networks are superior under sedation compared with general anesthesia. *NMR in Biomedicine,* 26: 638–650. https://doi.org/10.1002/nbm.2908.

Kavanau JL. (1994). Sleep and dynamic stabilization of neural circuitry: A review and synthesis. *Behav Brain Res*, 63:111–126.

Kearse LA, Jr., Manberg P, Chamoun N, deBros F, Zaslavsky A. (1994) Bispectral analysis of the electroencephalogram correlates with patient movement to skin incision during propofol/nitrous oxide anesthesia. *Anesthesiology*, 81:1365–1370.

Kiersey DK, Bickford RG, Faulconer A, Jr. (1951) Electroencephalographic patterns produced by thiopental sodium during surgical operations; description and classification. *Br J Anaesth*, 23:141–152.

Kim M et al. (2016) Functional and topological conditions for explosive synchronization develop in human brain networks with the onset of anesthetic-induced unconsciousness. *Front. Comput. Neurosci*, 10, 1.

Kinomura S, Larsson J, Gulya's B, Roland PE. (1996) Activation by attention of the human reticular formation and thalamic intralaminar nuclei. *Science,* 271: 512–5.

Kiviniemi VJ, Haanpää H, Kantola JH, Jauhiainen J, Vainionpää V, Alahuhta S, and others. (2005). Midazolam sedation increases fluctuation and synchrony of the resting brain BOLD signal. *Magn Reson Imaging*, 23(4):531–7.

Kochs E, Stockmanns G, Thornton C, Nahm W and Kalkman CJ. (2001). Wavelet analysis of middle latency auditory evoked responses: calculation of an index for detection of awareness during propofol administration. *Anesthesiology,* 95: 1141–1150.

Kocsis B. 2012. Differential role of NR2A and NR2B subunits in N-methyl-D- aspartate receptor antagonist-induced aberrant cortical gamma oscillations. *Biol. Psychiatry,* 71: 987–995.

Kreuzer M, Hentschke H, Antkowiak B, Schwarz C, Kochs EF and Schneider G. (2010) Cross-approximate entropy of cortical local field potentials quantifies effects of anesthesia: a pilot study in rats. *BMC Neurosci,* (11)122.

Krueger JM and Obál F Jr. (1993) A neuronal group theory of sleep function. *J Sleep Res*, 2:63–69.

Krueger JM, Frank M, Wisor J and Roy S. (2016) 'Sleep Function: Toward Elucidating an Enigma', *Sleep Med Rev*, 28: 46–56. doi: 10.1016/j.smrv.2015.08.005.

Krueger JM, Huang Y, Rector DM and Buysse DJ. (2013) Sleep: A synchrony of cell activity-driven small network states. *Eur J Neurosci*, 38: 2199–2209. [PubMed: 23651209].

Krzeminski D, Nski K, Marchewka A and Bola M. (2017) Breakdown of long-range temporal correlations in brain oscillations during general anesthesia. *NeuroImage,* 159: 146–158.

Ku SW, Lee U, Noh GJ, Jun IG and Mashour GA. (2011) Preferential inhibition of frontal-to-parietal feedback connectivity is a neurophysiologic correlate of general anesthesia in surgical patients. *PLoS One,* 6:e25155.

Kumar VJ, Van Oort E, Scheffler K, Beckmann CF and Grodd W. (2017). Functional anatomy of the human thalamus at rest *Neuroimage,* 12.071 https://doi.org/10.1016/j.neuroimage

Kundishora AJ, Gummadavelli A, Ma C, Liu M, Mccafferty C, Schiff ND… Blumenfeld H. (2017) Restoring Conscious Arousal During Focal Limbic Seizures with Deep Brain Stimulation. *Cerebral Cortex*, 27: 1964–1975.

Kuramoto E et al. (2017). Individual mediodorsal thalamic neurons project to multiple areas of the rat prefrontal cortex: A single neuron-tracing study using virus vectors. *J. Comp. Neurol,* 525: 166–185.

Lachaux JP, Rodriguez E, Martinerie J and Varela FJ. (1999) Measuring phase synchrony in brain signals. *Hum. Brain Mapp*, 8: 194–208.

Laitio RM et al. (2007). Effects of xenon anesthesia on cerebral blood flow in humans: a positron emission tomography study. *Anesthesiology,* 106: 1128–1133.

Långsjö JW et al. (2003). Effects of subanesthetic doses of ketamine on regional cerebral blood flow, oxygen consumption, and blood volume in humans. *Anesthesiology,* 99: 614–623.

Långsjö JW, Maksimow A, Salmi E, Kaisti K, Aalto S, Oikonen V, Hinkka S, Aantaa R, Sipilä H, Viljanen T, Parkkola R and Scheinin H. (2005) S-ketamine anesthesia increases cerebral blood flow in excess of the metabolic needs in humans. *Anesthesiology,* 103:258–268. [PubMed: 16052107].

Laureys S and Tononi G (2009) The Neurology of Consciousness. *Elsevier*, Amsterdam, 21.

Laureys S, Boly M. (2007) What is it like to be vegetative or minimally conscious?. *Curr Opin Neurol,* 20(6):609-613. doi:10.1097/WCO.0b013e3282f1d6dd

Laureys S, Faymonville ME, Goldman S, Degueldre C, Phillips C, Lambermont B, Aerts J, Lamy M, Luxen A, Franck G and Maquet P. (2000a) Impaired cerebral connectivity in vegetative state. In: *Physiological Imaging of the Brain with PET*, A. Gjedde, S.B. Hansen, G.M. Knudsen and O.B. Paulson, eds, San Diego, Academic Press, pp. 329– 334.

Laureys S, Faymonville ME, Luxen A, Lamy M, Franck G and Maquet P. (2000b) Restoration of thalamocortical connectivity after recovery from persistent vegetative state. *Lancet,* 355(9217):1790–1791.

Laureys S, Goldman S, Phillips C, Van Bogaert P, Aerts J, Luxen A, Franck G and Maquet P. (1999) Impaired effective cortical connectivity in vegetative state: preliminary investigation using PET. *Neuroimage,* 9(4):377–382.

Laureys S, Peigneux P, Phillips C, Fuchs S, Degueldre C, Aerts J, Del Fiore G, Petiau C, Luxen A, van der Linden M, Cleeremans A, Smith C and Maquet P. (2001). Experience-dependent changes in cerebral functional connectivity during human rapid eye movement sleep. *Neuroscience*, 105:521–525.

Le Van Quyen M, Staba R, Bragin A, Dickson C, Valderrama M, et al. (2010). Large-scale microelectrode recordings of high frequency gamma oscillations in human cortex during sleep. *J Neurosci*, 30: 7770–7782.

Lee H, Mashour GA, Noh GJ, Kim S and Lee U. (2013) Reconfiguration of network hub structure after propofol-induced unconsciousness. *Anesthesiology,* 119: 1347–1359.

Lee M, Sanders RD, Yeom S, Won D, Seo K, Kim HJ… Lee S. (2017). Network Properties in Transitions of Consciousness during Propofol-induced Sedation. *Nature Scientific Reports,* 7(16791), 1–13.

Lee U, Kim S, Noh G-J, Choi B-M, Hwang E and Mashour GA. (2009) The directionality and functional organization of frontoparietal connectivity during consciousness and anesthesia in humans. *Conscious Cogn,* 18:1069–1078.

Lee U, Ku S, Noh G, Baek S, Choi B and Mashour GA. (2013) Disruption of frontal-parietal communication by ketamine, propofol, and sevoflurane. *Anesthesiology,* 118: 1264–75.

Lee U, Mueller M, Noh G-J, Choi B and Mashour GA. (2011) Dissociable network properties of anesthetic state transitions. *Anesthesiology,* 114: 872–881.

Lenz C, Rebel A, van Ackern K, Kuschinsky W, Waschke KF. (1998) Local cerebral blood flow, local cerebral glucose utilization, and flow– metabolism coupling during sevoflurane versus isoflurane anesthesia in rats. *Anesthesiology,* 89(6): 1480–1488.

Lepousé C, Lautner CA, Liu L, Gomis P and Leon A. (2006). Emergence delirium in adults in the post-anaesthesia care unit. *Br. J. Anaesth,* 96: 747–753.

Leung LS, Luo T, Ma J and Herrick I. (2014) Brain areas that influence general anesthesia. *Prog Neurobiol,* 122:24-44. doi:10.1016/j.pneurobio.2014.08.001

Leung LWS. (1985). Spectral analysis of hippocampal EEG in the freely moving rat: effects of centrally active drugs and relations to evoked potentials. *Electroencephalogr. Clin. Neurophysiol*, 60: 65–77.

Lewis LD, Piantoni G, Peterfreund RA, et al. (2018) A transient cortical state with sleep-like sensory responses precedes emergence from general anesthesia in humans. *Elife,* 7:e33250. doi:10.7554/eLife.33250

Lewis LD, Weiner VS, Mukamel EA, Donoghue JA, Eskandar EN, Madsen JR… Purdon PL. (2012). Rapid fragmentation of neuronal networks at the onset of propofol-induced unconsciousness. *PNAS,* 109(49): E3377–E3386.

Li D and Mashour GA (2019a) Cortical dynamics during psychedelic and anesthetized states induced by ketamine. *NeuroImage*, 196:32–40. 784.

Li D, Hambrecht-Wiedbusch VS and Mashour GA. (2017). Accelerated Recovery of Consciousness after General Anesthesia Is Associated with Increased Functional Brain Connectivity in the High-Gamma Bandwidth. *Frontiers in Neuroscience,* 11: 16. https://doi.org/10.3389/fnsys.2017.00016.

Li D, Vlisides PE, Kelz MB, Avidan MS and Mashour GA. (2019b) Dynamic Cortical Connectivity during General Anesthesia in Healthy Volunteers. *Anesthesiology,* 130:870–884.

Li D, Voss LJ, Sleigh JW and Li X. (2013) Effects of volatile anesthetic agents on cerebral cortical synchronization in sheep. *Anesthesiology,* 119:81–8.

Liao Y, Tang J, Fornito A, Liu T, Chen X, Chen H, Xiang X, Wang X and Hao W. (2012) Alterations in regional homogeneity of resting-state brain activity in ketamine addicts. *Neurosci Lett,* 522:36–40.

Lin FK, Xin Y, Gao DM, Xiong Z and Chen JG. (2007) Effects of electrical stimulation of the parafascicular nucleus on the neuronal activities of the subthalamic nucleus and the ventromedial nucleus in rats. *Acta Physiologica Sinica,* 59(1): 79–85.

Lissek T, Obenhaus HA, Ditzel DAW, et al. (2016) General anesthetic conditions induce network synchrony and disrupt sensory processing in the cortex. *Front Cell Neurosci,* 10:64.

Liu X, Zhu XH, Zhang Y and Chen W. 2013a. The change of functional connectivity specificity in rats under various anesthesia levels and its neural origin. *Brain Topogr,* 26 (3): 363–377.

Livingstone MS and Hubel DH. (1981) Effects of sleep and arousal on the processing of visual information in the cat. *Nature*, 291: 554–561.

Llinás R and Ribary U. (2001) Consciousness and the brain. The thalamocortical dialogue in health and disease. *Ann N Y Acad Sci,* 929:166-175.

Llinás R, Ribary U, Contreras D and Pedroarena C. (1998) The neuronal basis for consciousness. *Philos Trans R Soc Lond B Biol Sci*, 353(1377):1841-1849. doi:10.1098/rstb.1998.0336

Llinás R. and Ribary U. (1993). Coherent 40Hz oscillation characterizes dream state in humans. *Proc. Natl. Acad Sci. U.S.A.* 90: 2078-2081.

Llinás RR and Pare D. (1991). Of dreaming and wakefulness. *Neuroscience,* 44:521–535.

Llinás RR, Leznik E and Urbano FJ. (2002) Temporal binding via cortical coincidence detection of specific and nonspecific thalamocortical inputs: a voltage-dependent dye-imaging study in mouse brain slices. *Proc Natl Acad Sci USA,* 99:449–454.

Long CW, Shah NK, Loughlin C, Spydell J and Bedford RF. (1989) A comparison of EEG determinants of near-awakening from isoflurane and fentanyl anesthesia. Spectral edge, median power frequency, and delta ratio. *Anesth Analg,* 69: 169–173.

Long JL, Shen B, Luo T, Stewart L, McMurran TJA and Leung LS. (2009). Pilocarpine model of temporal lobe epilepsy shows enhanced response to general anesthetics. *Exp. Neurol*, 219: 308–318.

Loomis AL, Harvey E and Hobart GA. (1937). Cerebral states during sleep, as studied by human brain potentials. *J Exp Psychol*, 21:127–44.

Lorente de No, R. (1938) Cerebral cortex: architecture, intra-cortical connections, motor projections. In: Fulton, J., editor. *Physiology of the Nervous System.* London: Oxford University Press; p. 291-340.

Lu H, Zuo Y, Gu H, Waltz JA, Zhan W, Scholl CA, Rea W, Yang Y and Stein EA. (2007). Synchronized delta oscillations correlate with the resting-state functional MRI signal. *Proc. Natl. Acad. Sci. U.S.A,* 104 (46):18265–18269.

Lustenberger C, Patel YA, Alagapan S, et al. (2018) High-density EEG characterization of brain responses to auditory rhythmic stimuli during wakefulness and NREM sleep. *Neuroimage,* 169:57-68. doi:10.1016/j.neuroimage.2017.12.007

Ma J and Leung LS. (2007). The supramammillo-septal-hippocampal pathway mediates sensorimotor impairment and hyperlocomotion induced by MK-801 and ketamine in rats. *Psychopharmacology (Berl.)*, 19:961–974.

Ma J, Shen B, Stewart LS, Herrick IA and Leung LS. (2002). The septohippocampal system participates in general anesthesia. *J. Neurosci,* 22 (RC200), 1–6.

Macchi G and Bentivoglio M. (1986) The thalamic intralaminar nuclei and the cerebral cortex. In: *Cerebral Cortex,* edited by Jones E and Peters A. New York: Plenum, vol. 5, p. 355–401.

MacDonald AA, Naci L, MacDonald PA and Owen AM. (2015). Anesthesia and neuroimaging: investigating the neural correlates of unconsciousness. *Trends Cogn. Sci*, 19: 100–107.

Maekawa T, Tommasino C, Shapiro HM, Keifer-Goodman J and Kohlenberger RW. (1986) Local cerebral blood flow and glucose utilization during isoflurane anesthesia in the rat. *Anesthesiology,* 65(2): 144–151.

Magnuson ME, Thompson GJ, Pan WJ and Keilholz SD. (2014) Time-dependent effects of isoflurane and dexmedetomidine on functional connectivity, spectral characteristics, and spatial distribution of spontaneous BOLD fluctuations. *NMR Biomed,* 27 (3): 291–303.

Majeed W, Magnuson M and Keilholz SD. (2009) Spatiotemporal dynamics of low frequency fluctuations in BOLD fMRI of the rat. *J. Magn. Reson. Imag,* 30 (2): 384–393.

Maksimow A, Sarkela M, Langsjo JW, Salmi E, Kaisti KK, Yli-Hankala A, Hinkka- Yli-Salomaki S, Scheinin H and Jaaskelainen SK. (2006). Increase in high frequency EEG activity explains the poor

performance of EEG spectral entropy monitor during S-ketamine anesthesia. *Clin. Neurophysiol,* 117: 1660–1668.

Maloney KJ, Cape EG, Gotman J and Jones BE. (1997). High frequency gamma electroencephalogram activity in association with sleep-wake states and spontaneous behaviors in the rats. *Neuroscience*, 76: 541–555.

Mann A, Gondard E, Tampellini D, Milsted JAT, Marillac D, Hamani C… Lozano AM. (2017) Brain Stimulation Chronic deep brain stimulation in an Alzheimer's disease mouse model enhances memory and reduces pathological hallmarks. *Brain Stimulation,* 1–10.

Marguet SL, Harris KD. (2011) State-dependent representation of amplitude-modulated noise stimuli in rat auditory cortex. *J Neurosci,* 31(17):6414-6420. doi:10.1523/JNEUROSCI.5773-10.2011

Marini G, Pianca L. (1996) Thalamocortical projection from the parafascicular nucleus to layer V pyramidal cells in frontal and cingulate areas of the rat. *Neuroscience Letters,* 203: 81–84.

Marshall L, Helgadottir H, Molle M and Born J. (2006). Boosting slow oscillations during sleep potentiates memory. *Nature,* 444(7119):610–613.

Marzano C, Ferrara M, Moroni F and De Gennaro L. (2011). Electroencephalographic sleep inertia of the awakening brain. *Neuroscience*, 176:308–17.

Mashour GA and Hudetz AG. (2017) Bottom-Up and Top-Down Mechanisms of General Anesthetics Modulate Different Dimensions of Consciousness. *Front Neural Circuits,* 11:44.

Mashour GA. (2004) Consciousness unbound: Toward a paradigm of general anesthesia. *Anesthesiology,* 100(2):428–433.

Mashour GA. (2006) Integrating the science of consciousness and anesthesia. *Anesth Analg,* 103:975–82.

Mashour GA. (2013) Cognitive unbinding: a neuroscientific paradigm of general anesthesia and related states of unconsciousness. *Neurosci Biobehav Rev,* 37: 2751–9.

Massimini M, Ferrarelli F, Huber R, Esser SK, Singh H, and Tononi G. (2005) Breakdown of cortical effective connectivity during sleep. *Science*, 309: 2228–2232.

Massimini M, Ferrarelli F, Sarasso S and Tononi G. (2012) Cortical mechanisms of loss of consciousness: insight from TMS/EEG studies. *Arch Ital Biol,* 150: 44–55.

Massimini M, Huber R, Ferrarelli F, Hill S and Tononi G. (2004) The sleep slow oscillation as a traveling wave. *J. Neurosci,* 24: 6862–6870.

Massimini M, Rosanova M and Mariotti M. (2003). EEG slow (approximately 1 Hz) waves are associated with nonstationarity of thalamo-cortical sensory processing in the sleeping human. *Journal of Neurophysiology,* 89(3):1205–1213.

Mattia M, Del Giudice P. (2002) Population dynamics of interacting spiking neurons. *Phys Rev E,* 66:051917.

McCarthy MM, Brown EN and Kopell N. (2008) Potential network mechanisms mediating electroencephalographic beta rhythm changes during propofol-induced paradoxical excitation. *J. Neurosci,* 28: 13488–13504.

McCormick DA and Bal T. (1997) SLEEP AND AROUSAL: Thalamocortical Mechanisms. *Annu. Rev. Neurosci* (Vol. 20).

McCormick DA, McGinley MJ and Salkoff DB. (2015) Brain state dependent activity in the cortex and thalamus. *Current Opinion in Neurobiology*, 31: 133-140.

Mcginley MJ, Vinck M, Reimer J, Batista-Brito R, Zagha E, Cadwell CR… Mccormick DA. (2015). Waking State: Rapid Variations Modulate Neural and Behavioral Responses. *Neuron*, 87(6): 1143–1161.

Meador K, Ray P, Echauz J, Loring D and Vachtsevanos G. (2002) Gamma coherence and conscious perception. *Neurology,* 59:847–854.

Mena-Segovia J, Sims HM, Magill PJ, Bolam JP. (2008). Cholinergic brainstem neurons modulate cortical gamma activity during slow oscillations. *J Physiol*, 586: 2947–2960.

Merica H and Fortune RD. (2004) State transitions between wake and sleep, and within the ultradian cycle, with focus on the link to neuronal activity. *Sleep Medicine Reviews*, 8: 473–485.

Merica H and Gaillard JM. (1992). The EEG of the sleep onset period in insomnia: a discriminant analysis. *Physiol Behav*, 52: 199–204.

Merica H, Fortune RD and Gaillard JM. (1991). Hemispheric temporal organization during the onset of sleep in normal subjects. In: Terzano MG, Halasz PL and Declerck AC, editors. *Phasic events and dynamic organization of sleep*. New York: Raven Press.

Merker B. (2013). Cortical gamma oscillations: the functional key is activation, not cognition. *Neurosci. Biobehav. Rev, 37*: 401–417. doi: 10.1016/j.neubiorev.2013.01.013

Merker BH. (2016). Cortical Gamma Oscillations: details of their genesis preclude a role in cognition. *Front. Comput. Neurosci,* 10:78. doi: 10.3389/fncom.2016.00078

Minamimoto T, and Kimura M. (2002) Participation of the thalamic CM–Pf complex in attentional orienting. *J. Neurophysiol,* 87: 3090–3101.

Minamimoto T, Hori Y and Kimura M. (2009) Roles of the thalamic CM-PF complex-basal ganglia circuit in externally driven rebias of action. *Brain Res. Bull,* 78: 75–79.

Moghaddam B, Adams B, Verma A and Daly D. (1997). Activation of glutamatergic neurotransmission by ketamine: a novel step in the pathway from NMDA receptor blockade to dopaminergic and cognitive disruptions associated with the prefrontal cortex. *J. Neurosci,* 17: 2921–2927.

Montgomery SM, Sirota, A., & Buzsáki, G. (2008). Theta and Gamma Coordination of Hippocampal Networks during Waking and Rapid Eye Movement Sleep. *The Journal of Neuroscience*, 28(26): 6731–6741.

Morel A, Magnin M and Jeanmonod D. (1997). Multiarchitectonic and stereotactic atlas of the human thalamus. *J. Comp. Neurol,* 387: 588–630. http://dx.doi.org/10.1002

Morison RS and Dempsey EW. (1942) A study of thalamo-cortical relations. *Am J Physiol,* 135: 281– 292.

Mormann F, Lehnertz K, David P, and Elger C. (2000) Mean phase coherence as a measure for phase synchronization and its application to the EEG of epilepsy patients. *Phys D Nonlinear Phenom,* 144(3):358-369. doi:10.1016/S0167-2789(00)00087-7

Moruzzi G and Magoun HW. (1949) Brainstem reticular formation and activation of the EEG. *Electroencephalogr Clin Neurophysiol,* 1: 455-473.

Mukamel EA, Pirondini E, Babadi B, et al. (2015) A transition in brain state during propofol-induced unconsciousness *J Neurosci*, 3;35(22):8684-5. doi:10.1523/JNEUROSCI.5813-12.2014

Mumford D. (1991) On the computational architecture of the neocortex. I. The role of the thalamo-cortical loop. *Biol Cybern,* 65(2):135-145. doi:10.1007/BF00202389

Munk MH, Roelfsema PR, Konig P, Engel AK, Singer W. (1996) Role of reticular activation in the modulation of intracortical synchronization. *Science,* 272:271–274. [PubMed: 8602512].

Muthukumaraswamy SD, Shaw AD, Jackson LE, Hall J, Moran R and Saxena N. (2015) Evidence that Subanesthetic Doses of Ketamine Cause Sustained Disruptions of NMDA and AMPA-Mediated Frontoparietal Connectivity in Humans. *J Neurosci,* 35: 11694–11706.

Muzet A. (1990). Reactivité de l'homme endormi. In: Benoît O, Foret J, editors. *Le sommeil humain: bases experimentales, physiologiques et physiopathologiques.* Paris: Masson,. P. 77-83.

Naghavi HR and Nyberg L. (2005). Common fronto-parietal activity in attention, memory, and consciousness: shared demands on integration? *Conscious Cogn,* 14(2):390–425.

Naitoh P, Kelly T and Babkoff H. (1993). Sleep inertia: best time not to wake up. *Chronobiol Int*, 10:109–18.

Nakatani C, Ito J, Nikolaev A, Gong P and van Leeuwen C (2005) Phase synchronization analysis of EEG during attentional blink. *J Cog Neurosci,* 17:1969–1979.

Nasrallah FA, Tan J and Chuang KH. (2012). Pharmacological modulation of functional connectivity: alpha2-adrenergic receptor agonist alters synchrony but not neural activation. *Neuroimage,* 60 (1): 436–446.

Nelson LE, Guo TZ, Lu J, Saper CB, Franks NP and Maze M. (2002) The sedative component of anesthesia is mediated by GABA(A) receptors in an endogenous sleep pathway. *Nat Neurosci,* 5: 979–84.

Nghiem TAE, Tort-Colet N, Górski T, Ferrari U, Moghimyfiroozabad S, Goldman JS… Destexhe A. (2020). Cholinergic Switch between Two Types of Slow Waves in Cerebral Cortex. *Cerebral Cortex*, 30(6):3451–3466. https://doi.org/10.1093/cercor/bhz320

Ni Mhuircheartaigh R, Warnaby C, Rogers R, Jbabdi S, Tracey I. (2013) Slow-wave activity saturation and thalamocortical isolation during propofol anesthesia in humans. *Sci Transl Med,* 5: 208ra148.

Nicolelis MA, Baccala LA, Lin RC and Chapin JK. (1995). Sensorimotor encoding by synchronous neural ensemble activity at multiple levels of the somatosensory system. *Science*, 268: 1353–1358.

Niedermeyer E. (1999) A concept of consciousness. *Ital J Neurol Sci,* 20(1):7-15. doi:10.1007/s100720050004

Niell CM and Stryker MP. (2010). Modulation of visual responses by behavioral state in mouse visual cortex. *Neuron*, 65: 472–479.

Niesters M, Khalili-Mahani N, Martini C, Aarts L, van Gerven J, van Buchem MA, Dahan A and Rombouts S. (2012) Effect of subanesthetic ketamine on intrinsic functional brain connectivity: A placebo-controlled functional magnetic resonance imaging study in healthy male volunteers. *Anesthesiology,* 117:868–77.

Nir Y, Staba RJ, Andrillon T, Vyazovskiy VV, Cirelli C, Fried I, et al. (2011) Regional slow waves and spindles in human sleep. *Neuron*, 70(1): 153–169.

Nir Y, Vyazovskiy VV, Cirelli C, Banks MI and Tononi G. (2013) Auditory responses and stimulus-specific adaptation in rat auditory cortex are preserved across NREM and REM sleep. *Cereb Cortex,* 25(5):1362-1378. doi:10.1093/cercor/bht328.

O'Connor SM, Berg RW and Kleinfeld D. (2002). Coherent electrical activity between vibrissa sensory areas of cerebellum and neocortex is enhanced during free whisking. *J Neurophysiol*, 87: 2137–2148.

Ogilvie RD and Simons I. (1992). Falling asleep and waking up, a comparison of EEG spectra. In: Ogilvie R and Broughton R, editors. *Sleep, arousal and performance*. Boston: Birkähauser.

Ogilvie RD, Simons IA, Kuderian RH, MacDonald T and Rustenburg J. (1991). Behavioral, event-related potential (ERP), and EEG/FFT changes at sleep onset. *Psychophysiol*, 28: 54–64.

Ogilvie RD. (2001) The process of falling asleep. *Sleep Medicine Reviews*, 5(3): 247–270.

Oliver MD and Datta S. (2019). Electrophysiological Correlates of the Sleep–Wake Cycle. *The Behavioral, Molecular, Pharmacological, and Clinical Basis of the Sleep-Wake Cycle*. Yucatán: Academic Press Inc. 17-26. doi:10.1016/b978-0-12-816430-3.00002-6

Paasonen J, Stenroos P, Salo RA, Kiviniemi V and Gröhn O. (2018). Functional connectivity under six anesthesia protocols and the awake condition in rat brain. *NeuroImage,* 172: 9–20.

Pace-Schott EF and Hobson AJ. (2002) The neurobiology of sleep: genetics, cellular physiology and subcortical networks. *Nature reviews*, 3: 592–605.

Pal D, Hambrecht-Wiedbusch VS, Silverstein BH and Mashour GA. (2015). Electroencephalographic coherence and cortical acetylcholine during ketamine-induced unconsciousness. *Br. J. Anaesth*, 114: 979–989. doi: 10.1093/bja/aev095.

Pal D, Silverstein BH, Lee H and Mashour GA. (2016). Neural Correlates of Wakefulness, Sleep, and General Anesthesia: An Experimental Study in Rat. *Anesthesiology*, 125(5): 929–942.

Palanca BJ, Mitra A, Larson-Prior L, Snyder AZ, Avidan MS and Raichle ME. (2015). Resting-state functional magnetic resonance imaging correlates of sevoflurane-induced unconsciousness. *Anesthesiology,* 123: 346–356. doi: 10.1097/ALN.0000000000000731.

Palva S, Linkenkaer-Hansen K, Naatanen R, Palva M. (2005) Early neural correlates of conscious somatosensory perception. *J Neurosci*, 25:5248–5258.

Pavone KJ, Su L, Gao L, et al. Lack of Responsiveness during the Onset and Offset of Sevoflurane Anesthesia Is Associated with Decreased Awake-Alpha Oscillation Power. *Front Syst Neurosci,* 11:38. doi:10.3389/fnsys.2017.00038

Pawela CP, Biswal BB, Hudetz AG, Schulte ML, Li R, Jones SR, Cho YR, Matloub HS and Hyde JS. (2009). A protocol for use of medetomidine anesthesia in rats for extended studies using task-induced BOLD contrast and resting-state functional connectivity. *Neuroimage,* 46 (4): 1137–1147.

Paxinos G and Watson C. (2007). The Rat Brain in Stereotaxic Coordinates. Amsterdam: Academic Press.

Peltier SJ, Kerssens C, Hamann SB, Sebel PS, Byas-Smith M and Hu X. (2005) Functional connectivity changes with concentration of sevoflurane anesthesia. *Neuroreport,* 16: 285–8.

Peña JL, Pérez-Perera L, Bouvier M and Velluti RA. (1999) Sleep and wakefulness modulation of the neuronal firing in the auditory cortex of the guinea pig. *Brain Res.* 816(2):463-470. doi:10.1016/S0006-8993(98)01194-9.

Perez-Garci E, del-Rio-Portilla Y, Guevara MA, Arce C and Corsi-Cabrera M. (2001) Paradoxical sleep is characterized by uncoupled gamma activity between frontal and perceptual cortical regions. *Sleep,* 24: 118–26.

Peter-Derex L, Magnin M and Bastuji H. (2015). Heterogeneity of arousals in human sleep: A stereo-electroencephalographic study. *NeuroImage*, 123:229–44.

Pfaff D. (2005) Brain Arousal and Information Theory (*Harvard Univ. Press*, Cambridge, Massachusetts).

Pinault P. (2008). N-methyl-D-aspartate receptor antagonists ketamine and MK-801 induce wake-related aberrant gamma oscillations in the rat neocortex. *Biol. Psychiatry,* 63: 730–735.

Pivik RT and Harman K. (1995). A re-conceptualization off EEG alpha activity as an index of arousal during sleep: all alpha is not equal. *J Sleep Res*, 4:131–7.

Polack PO, Friedman J and Golshani P. (2013). Cellular mechanisms of brain state-dependent gain modulation in visual cortex. *Nature neuroscience*, 16:1331–1339.

Portas CM, Krakow K, Allen P, Josephs O, Armony JL and Frith CD. (2000). Auditory processing across the sleep-wake cycle: Simultaneous EEG and fMRI monitoring in humans. *Neuron*, 28(3), 991–999.

Poulet JF and Petersen CC. (2008). Internal brain state regulates membrane potential synchrony in barrel cortex of behaving mice. *Nature*, 454: 881–885.

Poulet JFA, Fernandez LMJ, Crochet S and Petersen CCH. (2012). Thalamic control of cortical states. Nature *Neuroscience,* 15:370–372. doi: 10.1038/nn.3035.

Prerau MJ, Brown RE, Bianchi MT, Ellenbogen JM and Purdon PL. (2017) Sleep neurophysiological dynamics through the lens of multitaper spectral analysis. *Physiology,* 32: 60–92.

Purdon PL et al. (2013) Electroencephalogram signatures of loss and recovery of consciousness from propofol. *Proc. Natl. Acad. Sci. USA*, 110: E1142–E1151.

Quiroz-Padilla MF, Guillazo-Blanch G, Vale-Martínez A, Martí-Nicolovius M. (2006) Excitotoxic lesions of the parafascicular nucleus produce deficits in a socially transmitted food preference. *Neurobiol Learn Mem*, 86(3):256-263. doi:10.1016/j.nlm.2006.03.007

Quiroz-Padilla MF, Guillazo-Blanch G, Vale-Martínez A, Torras-García M, Martí-Nicolovius M. (2007) Effects of parafascicular excitotoxic lesions on two-way active avoidance and odor-discrimination. *Neurobiol Learn Mem,* 88(2):198-207. doi:10.1016/j.nlm.2007.06.002

Quiroz-Padilla MF, Martí-Nicolovius M, Guillazo-Blanch G. (2010) Núcleos intralaminares posteriores del tálamo y procesos cognitivos [Posterior intralaminar nuclei of the thalamus and cognitive processes]. *Rev Neurol*, 51(4):217-225.

Raeva SN. (2006) The Role of the Parafascicular Complex (CM-Pf) of the Human Thalamus in the Neuronal Mechanisms of Selective Attention. *Neuroscience and Behavioral Physiology*, 36(3): 287–295.

Ramachandran R. (2015). Connectivity. *Curr Opin Anesthesiol*, 28(5): 498–504. https://doi.org/10.1097/ACO.0000000000000237.

Rampil IJ, Kim JS, Lenhardt R, Negishi C, Sessler DI. (1998) Bispectral EEG index during nitrous oxide administration. *Anesthesiology,* 89:671–677.

Ranft A, Golkowski D, Kiel T, Riedl V, Kohl P, Rohrer G, et al. (2016). Neural correlates of sevoflurane-induced unconsciousness identified by simultaneous functional magnetic resonance imaging and electroencephalography. *Anesthesiology,* 125: 861–872. doi: 10.1097/ALN.0000000000001322

Rechtschaffen A and Kales A. (1968). A Manual of Standardized Terminology, Techniques and Scoring System for Sleep Stages of Human Subjects. (*Brain Information Service/ Brain Research Institute*, University of California Los Angeles).

Redinbaugh MJ, Phillips JM, Kambi NA, et al. (2020) Thalamus Modulates Consciousness via Layer- Specific Control of Cortex Thalamus Modulates Consciousness via Layer-Specific Control of Cortex. *Neuron*, 0(0):1-10. doi:10.1016/j.neuron.2020.01.005

Rees G, Kreiman G and Koch C. (2002). Neural correlates of consciousness in humans. *Nat Rev Neurosci,* 3(4):261–70.

Reig R and Sanchez-Vives MV. (2007). Synaptic transmission and plasticity in an active cortical network. *PloS one,* 2(8), e670.

Reig R, Gallego R, Nowak LG and Sanchez-Vives MV. (2006) Impact of cortical network activity on short-term synaptic depression. *Cereb Cortex,* 16(5):688-695. doi:10.1093/cercor/bhj014

Reig R, Mattia M, Compte A, Belmonte C and Sanchez-Vives MV. (2010) Temperature modulation of slow and fast cortical rhythms. *J Neurophysiol,* 103:1253–1261.

Reig R, Zerlaut Y, Vergara R., Destexhe A and Sanchez-Vives MV. (2015). Gain modulation of synaptic inputs by network state in auditory cortex in vivo. *Journal of Neuroscience,* 35(6), 2689-2702.

Reimer J, Froudarakis E, Cadwell CR, Yatsenko D, Denfield GH and Tolias AS. (2014). Pupil fluctuations track fast switching of cortical states during quiet wakefulness. *Neuron,* 84:355–362.

Ribeiro S, Gervasoni D, Soares ES, Zhou Y, Lin SC, Pantoja J, Lavine M and Nicolelis MAL. (2004). Long-lasting novelty-induced neuronal reverberation during slow-save sleep in multiple forebrain areas. *PLoS Biol*, 2:126–137.

Rieder MK, Rahm B, Williams JD, Kaiser J. (2010). Human gamma-band activity and behavior. *Int J Psychophysiol*, 79:39–48.

Rivolta D, Heidegger T, Scheller B, Sauer A, Schaum M, Birkner K et al. (2015) Ketamine dysregulates the amplitude and connectivity of high-frequency oscillations in cortical-subcortical networks in humans: evidence from resting-state magnetoencephalography recordings. *Schizophr. Bull,* 41: 1105–1114.

Rodriguez E, George N, Lachaux JP, Martinerie J, Renault B and Varela FJ. (1999) Perception's shadow: long-distance synchronization of human brain activity. *Nature,* 397: 430–433.

Rosa RR, Bonnet MH and Warm JS. (1983) Recovery of performance during sleep following sleep deprivation. *Psychophysiology*, 20:152–159.

Roth M, Shaw J and Green J. (1956). The form, voltage distribution and physiological significance of the K-complex. *Electroencephalogr Clin Neurophysiol*, 8(3):385-402. doi:10.1016/0013-4694(56)90004-9.

Rovó Z, Ulbert I and Acsády L. (2012). Drivers of the primate thalamus. *J. Neurosci,* 32: 17894–17908.

Rudolph U and Antkowiak B. (2004) Molecular and neuronal substrates for general anaesthetics. *Nat Rev Neurosci,* 5(9): 709–720.

Ruiz-Mejias M, Ciria-Suarez L, Mattia M, Sanchez-Vives MV. (2011) Slow and fast rhythms generated in the cerebral cortex of the anesthetized mouse. *J Neurophysiol,* 106(6):2910-2921. doi:10.1152/jn.00440.2011

Ruiz-Mejias M, Martinez de Lagran M, Mattia M, et al. (2016) Overexpression of Dyrk1A, a Down Syndrome Candidate, Decreases Excitability and Impairs Gamma Oscillations in the Prefrontal Cortex. *J Neurosci*, 36(13):3648-3659. doi:10.1523/JNEUROSCI.2517-15.2016

Sakai T, Singh H, Mi WD, et al. (1999) The effect of ketamine on clinical endpoints of hypnosis and EEG variables during propofol infusion. *Acta Anaesthesiol Scand,* 43:212–6.

Sánchez-López, A., Silva-Pérez, M., and Escudero, M. (2018). Temporal dynamics of the transition period between nonrapid eye movement and rapid eye movement sleep in the rat. Sleep 41. doi: 10.1093/sleep/zsy121

Sanchez-Vives MV and Mattia M. (2014). Slow wave activity as the default mode of the cerebral cortex. *Arch. Ital. Biol,* 152: 147–155.

Sanchez-Vives MV and McCormick DA. (2000) Cellular and network mechanisms of rhythmic recurrent activity in neocortex. *Nat Neurosci,* 3(10):1027-1034. doi:10.1038/79848

Sanchez-Vives MV, Massimini M, Mattia M. (2017) Shaping the Default Activity Pattern of the Cortical Network. *Neuron,* 94(5):993-1001. doi:10.1016/j.neuron.2017.05.015

Sanders RD, Banks MI, Darracq M, Moran R, Sleigh J, Gosseries O, Bonhomme V, Brichant JF, Rosanova M, Raz A, Tononi G, Massimini M, Laureys S and Boly M. (2018a) Propofol-induced unresponsiveness is associated with impaired feedforward connectivity in cortical hierarchy. *Br J Anaesth,* 121:1084–1096.

Saper CB, Fuller PM, Pedersen NP, Lu J and Scammell TE. (2010) Sleep State Switching. *Neuron*, 68: 1023–1042.

Sarasso S, Boly M, Napolitani M, Gosseries O, Charland-Verville V, Casarotto S, Rosanova M, Casali AG, Brichant JF, Boveroux P, Rex S, Tononi G, Laureys S and Massimini M. (2015). Consciousness and complexity during unresponsiveness induced by propofol, xenon, and ketamine. *Curr. Biol*, 25: 3099–3105. http://dx.doi.org/10.1016/j.cub.2015.10.014.

Sarter M, Givens B and Bruno JP. (2001). The cognitive neuroscience of sustained attention: where top-down meets bottom-up. *Brain Res Brain Res Rev*, 35(2):146–60.

Sasaki K, Staunton HP and Dieckmann G. (1970) Characteristic features of augmenting and recruiting responses in the cerebral cortex. *Exp. Neurol.,* 26: 369–392.

Schabus M, Gruber G, Parapatics S, Sauter C, Klosch G, Anderer P, et al. (2004). Sleep spindles and their significance for declarative memory consolidation. *Sleep,* 27(8):1479–1485.

Schartner M, Seth A, Noirhomme Q, Boly M, Bruno MA, Laureys S and Barrett A. (2015). Complexity of multi-dimensional spontaneous EEG decreases during propofol induced general anaesthesia. *PLoS One*, 10: 1–21. http://dx.doi.org/10.1371/ journal.pone.0133532.

Scheidegger M, Walter M, Lehmann M, Metzger C, Grimm S, Boeker H, Boesiger P, Henning A, Seifritz E. (2012) Ketamine decreases resting state functional network connectivity in healthy subjects: Implications for antidepressant drug action. *PLoS One*, 7:e44799.

Schiff ND and Plum F. (2000) The role of arousal and "gating" systems in the neurology of impaired consciousness. *J Clin Neurophysiol,* 17(5):438-452. doi:10.1097/00004691-200009000-00002

Schiff ND et al. (2007) Behavioral improvements with thalamic stimulation after severe traumatic brain injury. *Nature,* 448: 600–603.

Schroeder KE, Irwin ZT, Gaidica M, Bentley JN, Patil PG, Mashour GA and Chestek CA. (2016). Disruption of corticocortical information transfer during ketamine anesthesia in the primate brain. *Neuroimage,* 134: 459–465. https://doi.org/10.1016/j.neuroimage.2016.04.039.

Schrouff J, Perlbarg V, Boly M, et al. (2011) Brain functional integration decreases during propofol-induced loss of consciousness. *Neuroimage,* 57: 198–205.

Schwender D, Klasing S, Madler C, Poppel E and Peter K. (1993). Mid-latency auditory evoked potentials during ketamine anaesthesia in humans. *Br. J. Anaesth,* 71: 629–632.

Scott G, Fagerholm ED, Mutoh XH, Leech R, Sharp DJ, Shew WL and Kno, XT. (2014). Voltage imaging of waking mouse cortex reveals emergence of critical neuronal dynamics. *J. Neurosci,* 34: 16611–16620. http://dx.doi.org/10.1523/ JNEUROSCI.3474-14.2014.

Shaw AD, Saxena N, Jackson LE, Hall JE, Singh KD and Muthukumaraswamy SD. (2015) Ketamine amplifies induced gamma frequency oscillations in the human cerebral cortex. *Eur Neuropsychopharmacol,* 25:1136-1146. doi:10.1016/j.euroneuro.2015.04.012

Sherman SM and Guillery RW. (2006). Exploring the thalamus and its role in cortical function (2nd ed.). *MIT Press.*

Shi W, Xianyu A, Han Z, Tang X, Li Z, Zhong H, Mao T, Huang K and Shi SH. (2017) Ontogenetic establishment of order-specific nuclear organization in the mammalian thalamus. *Nat Neurosci,* 20(4):516-528. doi: 10.1038/nn.4519.

Shin TJ, Cho D, Ham J, Choi DH, Kim S, Jeong S, Kim HI, Kim JG and Lee B. (2016). Changes in thalamo-frontal interaction under different levels of anesthesia in rats. *Neurosci. Lett,* 627: 18–23.

Shiromani PJ, Kilduff TS, Bloom FE and McCarley RW. (1992). Cholinergically induced REM sleep triggers Fos-like immunoreactivity in dorsolateral pontine regions associated with REM sleep. *Brain Res,* 580: 351–357.

Sikich N and Lerman J. (2004). Development and psychometric evaluation of the pediatric anesthesia emergence delirium scale. *Anesthesiology,* 100: 1138–1145.

Singer W & Gray CM. (1995). Visual feature integration and the temporal correlation hypothesis. *Annu. Rev. Neurosci.* 18: 555–586.

Singer W. (1995). Development and plasticity of cortical processing architectures. *Science,* 270:758–764.

Sinha AK, Smythe H, Zarcone VP, Barchas JD and Dement WC. (1972). Human sleep electroencephologram: a damped oscillatory phenomenon. *J Theor Biol,* 35:387–93.

Sleigh J, Harvey M, Voss L and Denny B. (2014) Ketamine, More mechanisms of action than just NMDA blockade. *Trends Anaesth Crit Care,* 4:76–81.

Sleigh JW, Andrzejowski J, Steyn-Ross A and Steyn-Ross M. (1999). The bispectral index: a measure of depth of sleep? *Anesth. Analg,* 88: 659–661.

Smith C and Peters KR. (2011) Sleep, memory, and molecular neurobiology. *Handb Clin Neurol,* 98: 259–272.

Smith C, Young J and Young W. (1980). Prolonged increases in paradoxical sleep during and after avoidance-task acquisition. *Sleep,* 3:67–81.

Solovey G, Alonso LM, Yanagawa T, Fujii N, Magnasco MO, Cecchi GA and Proekt A. (2015). Loss of consciousness is associated with stabilization of cortical activity. *J. Neurosci,* 35: 10866–10877. http://dx.doi.org/10.1523/ JNEUROSCI.4895-14.2015.

Sos-Hinojosa H, Guillazo-Blanch G, Vale-Martínez A, Nadal R, Morgado-Bernal I, and Martí-Nicolovius M. (2003) Parafascicular electrical stimulation attenuates nucleus basalis magnocellularis lesion-induced active avoidance retention deficit. Behavioural Brain Research, 144(1–2): 37–48.

Srinivasan R, Russell D, Edelman G and Tononi G. (1999) Increased synchronization of neuromagnetic responses during conscious perception. *J Neu- rosci,* 19:5435–5448.

Steinberg EA, Wafford KA, Brickley SG, Franks NP and Wisden W. (2015). The role of K_2p channels in anaesthesia and sleep. Pflugers Archiv: *European journal of physiology*, 467(5): 907–916. doi:10.1007/s00424-014-1654-4.

Steriade M and McCarley RW. (2005). Brain control of wakefulness and sleep. New York: Springer.

Steriade M and McCarley RW. (2005). Brainstem Control of Wakefulness and Sleep. New York: Plenum Press

Steriade M and Timofeev I. (2003) Neuronal plasticity in thalamocortical networks during sleep and waking oscillations. *Neuron,* 37:563–76.

Steriade M, Amzica F and Contreras D. (1996). Synchronization of fast (30–40 Hz) spontaneous cortical rhythms during brain activation. *J Neurosci*, 16:392–417.

Steriade M, Datta S, Paré D, Oakson G and Curro Dossi R. (1990). Neuronal activities in brain-stem cholinergic nuclei related to tonic activation processes in thalamocortical systems. J Neurosci, 10: 2541–59.

Steriade M, McCormick DA and Sejnowski TJ. (1993b) Thalamocortical oscillations in the sleeping and aroused brain. *Science* 262: 679–685.

Steriade M. (2000) Corticothalamic resonance, states of vigilance and mentation. *Neuroscience,* 101: 243–276.

Steriade M. (2001) Active neocortical processes during quiescent sleep. *Arch. Ital. Biol.* 139: 37–51.

Stickgold R, Hobson JA, Fosse R and Fosse M. (2001). Sleep, learning, and dreams: off-line memory reprocessing. *Science*, 294:1052–1057.

Stickgold R. (2005) Sleep-dependent memory consolidation. *Nature,* 437:1272–1278.

Strauss M, Sitt JD, King JR, et al. (2015) Disruption of hierarchical predictive coding during sleep. *Proc Natl Acad Sci U S A*, 112(11):E1353-E1362. doi:10.1073/pnas.1501026112.

Supp GG, Siegel M, Hipp JF and Engel AK. (2011) Cortical hypersynchrony predicts breakdown of sensory processing during loss of consciousness. *Curr Biol*, 21:1988–93. [PubMed: 22100063]

Tajima S, Yanagawa T, Fujii N and Toyoizumi T. (2015). Untangling brain-wide dynamics in consciousness by cross-embedding. *PLoS Comput. Biol,* 1–28. http://dx.doi.org/ 10.1371/journal.pcbi.1004537.

Tanaka H, Hayashi M and Hori T (1996). Statistical features of hypnagogic EEG measured by a new scoring system. *Sleep*, 19: 731–738.

Tassi P and Muzet A. (2001). Defining the states of consciousness. *Neuroscience and Biobehavioral Reviews*, 25: 175–191.

Timofeev I, Grenier F and Steriade M. (2001) Disfacilitation and active inhibition in the neocortex during the natural sleep-wake cycle: an intracellular study. *Proc. Natl Acad. Sci.* USA 98: 1924–1929.

Tinker JH, Sharbrough FW and Michenfelder JD. (1977) Anterior shift of the dominant EEG rhythm during anesthesia in the Java monkey: Correlation with anesthetic potency. *Anesthesiology,* 46:252–259.

Tononi G and Laureys S. (2008) The neurology of consciousness: an overview. In: Laureys S and Tononi G editors. *The Neurology of Consciousness: Cognitive Neuroscience and Neuropathology*, Elsevier Ltd.

Tononi G and Massimini M. (2008). Why does consciousness fade in early sleep? *Ann. N. Y. Acad. Sci,* 1129 (1): 330–334.

Tononi G and Sporns O. (2003). Measuring information integration. *BMC Neurosci,* 4:31.

Tononi G, Boly M, Massimini M, and Koch C. (2016). Integrated information theory: from consciousness to its physical substrate. *Nat. Rev. Neurosci,* 17: 450–461. doi: 10.1038/nrn.2016.44.

Tononi G, Edelman GM and Sporns O. (1998) Complexity and coherency: integrating information in the brain. *Trends in Cognitive Sciences*, 2 (12): 474-484.

Tort-Colet N, Capone C, Sanchez-Vives MV and Mattia M. (2019). Attractor competition enriches cortical dynamics during awakening from anesthesia. *BioRxiv,* 1–24. https://doi.org/10.1101/517102

Tsubokawa T, Yamamoto T, Katayama Y, et al. (1990) Deep-brain stimulation in a persistent vegetative state: follow-up results and criteria for selection of candidates. *Brain Inj*, 4:315–327.

Tu Y, Yu T, Fu XY, Xie P, Lu S, Huang XQ and Gong QY. (2011). Altered thalamocortical functional connectivity by propofol anesthesia in rats. *Pharmacology,* 88 (5–6): 322–326.

Tung A, Bergmann BM, Herrera S, Cao D and Mendelson WB. (2004) Recovery from sleep deprivation occurs during propofol anesthesia. *Anesthesiology,* 100: 1419–1426.

Uhlhaas PJ, Pipa G, Lima B, Melloni L, Neuenschwander S, Nikolic D, et al. (2009). Neural synchrony in cortical networks: history, concept and current status. *Front Integr Neurosci*, 3:17.

Ursin R and Sterman MB. (1981). A Manual for Standardized Scoring of Sleep and Waking States in the Adult Cat. Los Angeles, CA: *University of California.*

Vale-Martínez A, Guillazo-Blanch G., Aldavert-Vera L, Segura-Torres P and Martí-Nicolovius M. (1999). Intracranial self-stimulation in the parafascicular nucleus of the rat. *Brain Research Bulletin,* 48(4): 401–406.

Van Buren JM and Borke RC. (1972). Variations and Connections of the Human Thalamus. *Springer Berlin,* Heidelberg.

Van der Werf YD, Witter MP, Groenewegen HJ. (2002) The intralaminar and midline nuclei of the thalamus. Anatomical and functional evidence for participation in processes of arousal and awareness. *Brain Res Rev,* 39:107–140. [PubMed: 12423763]

Vanderwolf CH (1969) Hippocampal electrical activity and voluntary movement in the rat. *Electroencephalogr Clin Neurophysiol*, 26:407–418.

Varela F, Lachaux JP, Rodriguez E and Martinerie J. (2001). The brainweb: phase synchronization and large-scale integration. *Nat Rev Neurosci*, 2: 229–239.

Veselis RA et al. (1997). Midazolam changes cerebral blood flow in discrete brain regions: an H2 5O positron emission tomography study. *Anesthesiology*, 87:1106–1117.

Vijayan S, Ching S, Purdon PL, Brown EN and Kopell NJ. (2013) Thalamocortical mechanisms for the anteriorization of alpha rhythms during propofol-induced unconsciousness. *J Neurosci,* 33: 11070–11075.

Vinck M, Batista-Brito R, Knoblich U and Cardin JA. (2015). Arousal and locomotion make distinct contributions to cortical activity patterns and visual encoding. *Neuron*, 86:1–15.

Von Stein A, Sarnthein J. (2000). Different frequencies for different scales of cortical integration: from local gamma to long range alpha/theta synchronization. *Int. J. Psychophysiol.* 38:301-313.

Voss LJ, Ludbrook G, Grant C, Sleigh JW and Barnard JP. (2006) Cerebral cortical effects of desflurane in sheep: Comparison with isoflurane, sevoflurane and enflurane. *Acta Anaesthesiol Scand,* 50: 313–9.

Voss U, Holzmann R, Tuin I and Hobson JA. (2009) Lucid dreaming: a state of consciousness with features of both waking and non-lucid dreaming. *Sleep,* 32: 1191–200.

Vyazovskiy VV, Cui N, Rodriguez AV, Funk C, Cirelli C and Tononi G. (2014). The dynamics of cortical neuronal activity in the first minutes after spontaneous awakening in rats and mice. *Sleep*, 37:1337–47.

Vyazovskiy VV, Olcese U, Hanlon EC, Nir Y, Cirelli C and Tononi G. (2011). Local sleep in awake rats. *Nature*, 472: 443–447.

Vyazovskiy VV, Olcese U, Lazimy YM, Faraguna U, Esser SK, Williams JC, Cirelli C and Tononi G. (2009). Cortical firing and sleep homeostasis. *Neuron*, 63, 865–878.

Wang K, Steyn-Ross ML, Steyn-Ross DA, Wilson MT and Sleigh JW. (2014). EEG slow-wave coherence changes in propofol-induced general anesthesia: experiment and theory. *Front. Syst. Neurosci,* 8: 215.

Warltier DC, Lydic R and Baghdoyan HA. (2005) Sleep, Anesthesiology, and the Neurobiology of Arousal State Control Sleep Is Temporally Organized, Homeostatically Regulated, and Actively Generated by the Brain Any number of physiologic signs could. *Anesthesiology*, 103:1268–95.

Warnaby CE, Sleigh JW, Hight D, Jbabdi S, Tracey I (2017) Investigation of Slow-wave Activity Saturation during Surgical Anesthesia Reveals a Signature of Neural Inertia in Humans. *Anesthesiology*, 127: 645-657.

Wehrle R, Kaufmann C, Wetter TC, Holsboer F, Auer DP, Pollmacher T and Czisch M. (2007). Functional microstates within human REM sleep: first evidence from fMRI of a thalamocortical network specific for phasic REM periods. *Eur J Neurosci,* 25:863–871.

Weinberger NM, Velasco M and Lundsley DB. (1965) Effects of lesions upon thalamically induced electrocortical desynchronization and recruiting. *Electroenceph. Clin. Neurophysiol.*, 18: 369–377.

Welch PD. (1967) The use of fast Fourier transform for the estimation of power spectra: A method based on time averaging over short, modified periodograms. *IEEE Trans Audio Electroacoust,* AU-15(2):70–73. doi:10.1109/TAU.1967.1161901

White NS and Alkire MT. (2003) Impaired thalamocortical connectivity in humans during general-anesthetic-induced unconsciousness. *Neuroimage,* 19:402–411.

Williams KA, Magnuson M, Majeed W, LaConte SM, Peltier SJ, Hu X and Keilholz SD. (2010). Comparison of alpha-chloralose, medetomidine and isoflurane anesthesia for functional connectivity mapping in the rat. *Magn. Reson. Imag,* 28 (7): 995–1003.

Wilson DA, Hoptman MJ, Gerum SV and Guilfoyle DN. (2011). State-dependent functional connectivity of rat olfactory system assessed by fMRI. *Neurosci. Lett,* 497 (2): 69–73.

Wörgötter F, Suder K, Zhao Y, Kerscher N, Eysel UT and Funke K. (1998) State-dependent receptive-field restructuring in the visual cortex. *Nature,* 396(6707):165-168. doi:10.1038/24157.

Yamamoto T, Katayama Y, Kobayashi K, Oshima H, Fukaya C and Tsubokawa T. (2010) Deep brain stimulation for the treatment of vegetative state. *European Journal of Neuroscience,* 32: 1145–1151.

Yamamoto T, Kobayashi K, Kasai M, Oshima H, Fukaya C, Katayama Y. (2005) DBS therapy for the vegetative state and minimally conscious state. *Acta Neurochir Suppl,* 93:101–104.

Yamamura T, Fukuda M, Takeya H, et al. (1981) Fast oscillatory EEG activity induced by analgesic concentrations of nitrous oxide in man. *Anesth Analg,* 60:283–8.

Yang J, Chai YF, Gong CY, Li GH, Luo N, Luo NF and Liu J. (2009). Further proof that the spinal cord, and not the brain, mediates the immobility produced by inhaled anesthetics. *Anesthesiology,* 110:591–595.

Young GB (2000) The EEG in coma. *J Clin Neurophysiol,* 17(5):473–485.

Yuan R, Di X, Taylor PA, Gohel S, Tsai Y-H and Biswal BB. (2015). Functional topography of the thalamocortical system in human. *Brain Struct. Funct,* 221: 1971–1984. http://dx.doi.org/10.1007/s00429-015-1018-7

Zecharia AY, Nelson LE, Gent TC, Schumacher M, Jurd R, et al. (2009) The involvement of hypothalamic sleep pathways in general anesthesia: testing the hypothesis using the GABAA receptor beta3N265M knock-in mouse. *J Neurosci,* 29: 2177–2187.

Zhou J, Liu X, Song W, Yang Y, Zhao Z, Ling F… Li S-J. (2011). Specific and Nonspecific Thalamocortical Functional Connectivity in Normal and Vegetative States. *Conscious Cogn,* 20(2), 257–268.

Zhurakovskaya E, Paasonen J, Shatillo A, Lipponen A, Salo R, Aliev R, Tanila H and Grohn O. (2016) Global functional connectivity differences between sleep-like states in urethane anesthetized rats measured by fMRI. *PLoS One,* 11 (5), e0155343.